Properties of cosmic rays incident in the near-horizontal direction

S. S. Said

Plate 1

Frontispiece

The Durham Cosmic Ray Horizontal Spectrograph Mark II

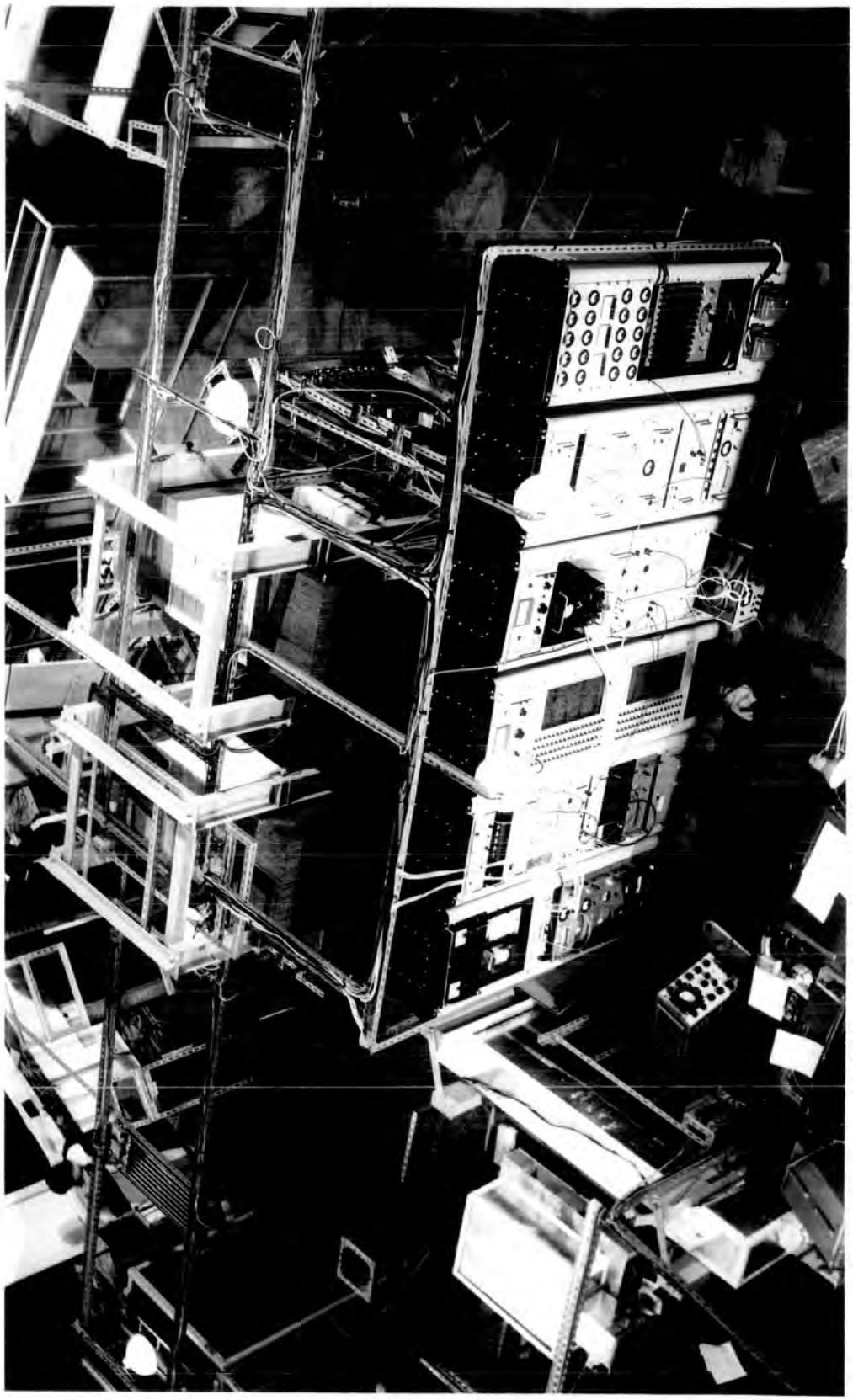

Properties of Cosmic Rays Incident in the Near-Horizontal Direction

by

S. S. Said, B.Sc.

A thesis submitted to the University of Durham, in support of an application for the degree of Doctor of Philosophy

November, 1966.

CONTENTS

		Page
ABSTRACT		i
PREFACE		iii
CHAPTER 1	Introduction	1
1.1	The cosmic radiation	1
1.2	The significance of studies of near-horizontal cosmic rays	3
1.3	The present work	5
CHAPTER 2	Previous studies in the near-horizontal direction	7
2.1	Introduction	7
2.2	Magnetic spectrograph method	9
2.2.1	Momentum spectrum of muons and the derivation of the K/π ratio	9
2.2.2	The muon charge ratio	12
2.3	Burst study method	13
CHAPTER 3	Durham Horizontal Spectrograph Mark II	16
3.1	Brief description of the instrument	16
3.1.1	General	16
3.1.2	The magnets	17
3.1.3	The flash tube trays	18
3.1.4	The Geiger Counter Trays	18
3.1.5	The Electronics	19
3.1.6	Alignment of the spectrograph	20
3.2	Data Analysis	21

		Page
3.2.1	General	21
3.2.2	Analysis of data	27
CHAPTER 4	Results on Muon Spectrum	31
4.1	Basic data	31
4.2	Derivation of the experimental momentum spectra	32
4.3	The predicted spectra at large zenith angles	35
4.3.1	Introduction	35
4.3.2	The measured vertical muon spectrum	37
4.3.3	Production spectrum of the parents of muons	39
4.3.4	The predicted muon spectra at large zenith angles	42
4.4	Derivation of the K/π ratio	42
4.5	Comparison with the results of other workers	45
4.5.1	K/π ratio determination from studies of inclined spectra	45
4.5.2	Comparison with K/π ratio determination by other indirect methods	47
4.5.3	Comparison with direct K/π ratio determination	49
4.5.4	Conclusions on the K/π ratio	52
CHAPTER 5	Results on the muon charge ratio	54
5.1	Muon charge ratio measurements	54
5.2	The basic data	55
5.3	The charge ratio at production	57
5.4	Comparison with other data	60
5.5	The best estimate of the μ^+/μ^- ratio	62

		Page
5.6	Brief summary of the interpretation of the μ^+/μ^- ratio	63
5.6.1	Introduction	63
5.6.2	Pionization model	65
5.6.3	Models with significant kaon production	66
5.6.4	Isobar models for particle production	68
5.6.5	The Peripheral Model	69
5.6.6	Conclusions	69
CHAPTER 6	Results on muon interactions	71
6.1	Introduction	71
6.2	Basic data	72
6.3	Variation of interaction probabilities with energy	73
6.4	Interpretation of the results in terms of muon interactions	75
6.4.1	Introduction	75
6.4.2	Probability of a muon producing single electrons in a flash tube tray	76
6.4.3	Probability of a muon producing single electrons in the iron magnet	78
6.4.4	Probability of a muon producing cascade showers in the iron magnet	79
6.4.5	Double electron cases	82
6.4.6	Conclusion	83
CHAPTER 7	Discussion and conclusions	84
7.1	Properties of high energy nuclear interactions	84

Page

7.2 Presence of non-muons in the near-horizontal beam 87

7.3 Further studies 88

ACKNOWLEDGEMENTS 90

REFERENCES 91

ABSTRACT

The Durham 'horizontal spectrograph' Mark II has been used to measure the momentum spectrum and the charge ratio of Cosmic-ray muons in the zenith angle range 82.5° - 90° to about 2000 GeV and the results are based on a sample of 3918 particles.

By comparing the measured spectra with those predicted from the measured vertical spectrum, for different values of the K/π ratio, a value of 0.42 ± 0.20 has been derived for the K/π ratio in the muon energy range at production, 100 - 2000 GeV, corresponding to primary energy range of $\sim 3.10^3$ - 10^5 GeV. When comparison is made with the K/π ratios determined by other indirect methods it is concluded that there is no evidence against a near-constant ratio over the wide primary energy range 10^2 - 10^6 covered by all methods and that the average value is 0.35 ± 0.20 over this energy range.

The present results confirm the results of other authors on the existence of an appreciable charge excess up to energies of at least a few hundred GeV. The present results suggest that at the largest zenith angles there is a maximum in the charge ratio in the energy region 50 - 100 GeV, a feature which does not confirm the minimum in the same energy region, but at somewhat smaller zenith angles, reported by some other workers. The reason for the appearance of the maximum is not known despite strenuous efforts to explain it.

At higher energies, one cannot say, due to the considerable errors in all the data, that there is disagreement between the present result and other data and neither an increase or decrease in the ratio is ruled out.

The interaction of the incident particles (hitherto assumed to be muons) has been studied from the point of view of identification of the particles. It is shown that the results can be interpreted in terms of the known electromagnetic interactions of muons and the conclusion arrived at is that there is no evidence for the existence of an appreciable flux of the so-called X - particles that could be contaminating the incident muon beam.

PREFACE

The work reported in this thesis was carried out while the author was a research student, under the supervision of Professor A. W. Wolfendale, in the Cosmic Ray Group in the Physics Department of the University of Durham.

The work describes measurements of the momentum spectrum and the charge ratio of cosmic ray muons incident in the near-horizontal direction, using the Durham horizontal spectrograph Mark II. It also contains an investigation of the interactions of the incident muons.

Together with a share in the work of constructing the spectrograph, the author was solely responsible for the optical side of the instrument, and the measurement of the magnetic field. With his colleagues he was also responsible for the operation of the spectrograph and the collection of data over a running period of 3884 hours, as well as the subsequent analysis and interpretation of these data.

The analysis and interpretation of the data on the muon interactions was the responsibility of the author.

Interim reports on the results of the momentum spectrum and the charge ratio of muons were presented in two papers, by the author and his colleagues, at the International Cosmic Ray Conference in London (1965).

CHAPTER 1

Introduction

1.1 The cosmic radiation

Since the first discoveries some sixty years ago, there has been a continuing interest in the cosmic radiation. Two main lines of approach have been apparent in cosmic ray physics. The first is the study of elementary particles in cosmic rays and the interaction of these particles at high energies. The second is the study of the geophysical and astrophysical aspects of cosmic rays; this study being related to the origin and properties of the primary radiation such as the energy spectrum, particle composition, directionality, time variation and the interaction with the earth's magnetic field.

The problem of the origin of the cosmic radiation is as yet far from a definite solution. That there was no significant diurnal variation in the number of cosmic rays registered at a given point on the globe pointed to the fact that the bulk of the radiation was not of solar origin. Also the time variations in intensity were found to be small, leading to the conclusion that the immediate source of the radiation is not within the solar system, but the correlation between certain large irregular fluctuations and the appearance of large solar flares has led to the idea that the sun is, in fact, responsible for at least a part of the low energy radiation. It is generally accepted that the more energetic primaries are of galactic

origin and those of the highest energies may well be of extra-galactic origin, but the solution of the problem of the origin must await further advances in knowledge, both of the cosmic ray flux itself and of astrophysical phenomena.

At energies in the region of some tens of GeV the primary radiation arrives almost isotropically and is composed of 85 - 88% protons, ~10% α- particles, 1 or 2% of nuclei with $Z > 2$ up to Fe^{26} and a small flux of electrons and γ - rays. Their energies range from about 10^{9} to 10^{20} eV, the lower limit depending on the geomagnetic latitude. The intensity of the primary nucleons is a rapidly varying function of their energy, with an integral spectrum given by the relation $N(>E_o) \propto E_o^{-1.6}$ for energies between 10^{12} - 10^{16} eV.

On entering the earth's atmosphere, the primary cosmic rays interact with the nuclei of the atmosphere producing secondary particles such as pions, kaons, nucleons and other baryons. Their number is attenuated exponentially in the atmosphere with an attenuation length of about 120 g cm^{-2}. Many of the charged pions decay to form muons which in the main, survive to ground level to form the hard component of the cosmic rays. Those muons which decay give rise to electrons which contribute to the soft component, but the majority of this component comes via the electron-photon cascades initiated by the decay of the neutral pions into photons. For high primary energies, the number of particles, mainly electrons, becomes very great and the event is known as an extensive air shower. A small fraction of the protons

and neutrons reach sea-level contributing to the hard component, but at this depth the flux is dominated by the secondary components, mainly muons and electrons.

Direct studies of the primary radiation is necessarily difficult since it involves the transport of elaborate apparatus to high altitudes. At low primary energies $E_o \lesssim 10^{14}$ eV, the fluxes are sufficient for localised interactions (e.g. at mountain and balloon altitudes) of primary nucleons to be studied using nuclear emulsion and ionization calorimeter. At higher energies, $E_o \gtrsim 10^{15}$ eV, localised interactions cannot be studied because of the very low particle fluxes, and instead the interactions are studied indirectly from observations on the secondary products of the interactions in extensive air showers. The indirect studies of the secondaries are also useful at the lower primary energies because when comparison ismade with similar direct studies in the same energy range, information can be obtained about the properties of the interactions. Furthermore, these indirect methods are capable of investigating quantities which cannot easily be measured by the direct methods, e.g. the charge composition.

1.2 The significance of studies of near-horizontal cosmic rays

Due to the fact that the thickness of the atmosphere in the near-horizontal direction, i.e. at large zenith angles, is some 36 times that in the vertical, consideration of interaction and decay lengths of cosmic ray particles shows that the only particles arriving in this

direction are muons.

Besides, when one is specifically interested in high energy muons, they are best studied in this direction. This arises from the different properties of the muon spectrum in this direction from that in the vertical direction.

At low energies, the enormously greater flux of particles in the vertical direction is a considerable complication in the measurements and analysis. In the near-horizontal direction, the relative intensity of particles is severely reduced with a resulting much higher median energy of muons in the flux (at 90^{o}, the median energy is ~ 80 GeV). This is due to the fact that in the near-horizontal, the path length traversed, and thus the energy loss of muons, is very much greater than in the vertical direction.

At high energies, i.e. greater than ~ 100 GeV, the overall intensity of muons in the near-horizontal direction is greater than in the vertical direction. The reason for this increase is that high energy pions (or kaons) travelling in this direction have a greater probability of decay into high energy muons than pions of similar energy travelling in the vertical direction where the atmosphere is comparatively dense.

Added to the above is the fact that, on account of energy losses in the atmosphere, the production energies in the near-horizontal direction are some tens of GeV higher than measured.

A particular significance of the spectrum of muons at large zenith angles is that if comparison is made with the vertical spectrum then conclusions can be drawn about the nature of the parents of the muons. In this way it is found that the muon spectra at large zenith angles are sensitive to the ratio of kaons to pions produced in high energy interactions, i.e. the K/π ratio and the sensitivity is greatest in the muon energy regio of 1000 GeV.

Normally, it is assumed that one is dealing with a pure beam of high energy muons incident at large zenith angles and a study of their interaction characteristics enables theoretical predictions to be checked. However, the argument can be turned round and, from studies of the interactions of the particles and assuming the validity of the theoretical predictions, an identification of the particles can be made.

The relatively high intensity of high energy muons, $\gtrsim$ 100, GeV at large zenith angles enables the determination of their charge ratio to be made, with better statistics, at these angles than at lower zenith angles. Such measurements are of great contemporary interest in view of the well-known problem of interpreting the high charge excess (MacKeown and Wolfendale 1966).

1.3. The present work

This work was mainly initiated to investigate the muon momentum spectrum and muon charge ratio at high energies, using the Durham

horizontal spectrograph Mark II and the two quantities have been determined in the zenith angular range 82.5° - 90° up to muon energies of $\sim$1000 GeV.

Another object of the present work was to examine the nature of the incident particles (hitherto assumed to be muons) from studies of their interactions in some of the components of the spectrograph namely, the flash tube trays and the solid iron magnets.

The present introduction is followed, in Chapter 2, by a brief review of the previous studies in the near-horizontal direction. Chapter 3 contains a description of the Mark II spectrograph and the method of analysis of the data. The results on the muon momentum spectrum and a derivation of the K/π ratio are given in Chapter 4, and Chapter 5 gives the results on the muon charge ratio. Studies of the incident particle interactions are dealt with in Chapter 6 from the point of view of their identification and an attempt is made to interpret the results. Finally, in Chapter 7, conclusions are drawn from the present work.

CHAPTER 2

Previous studies in the near-horizontal direction

2.1. Introduction

Two main methods have been used for studying high energy muons arriving in the near-horizontal direction, i.e. at large zenith angles.

(i) directly; using magnetic spectrographs and

(ii) indirectly; by studying the electromagnetic bursts produced by the muons.

Using magnetic spectrographs, one can measure the momentum spectrum and the charge composition of the incident muons, while the burst study method enables only the determination of the muon spectrum, but no information on the charge composition can be obtained.

In recent years three groups have used the first method. These are the Nagoya, Durham and Nottingham groups. All three groups applied solid iron magnets as the deflecting element.

At Nagoya, (Japan, Latitude 25° N), a spectrograph has been constructed (Kamiya et al. 1961) which consists of a solid iron magnet, four arrays of flash tubes and a coincidence set of two plastic scintillators. The particles were accepted at zenith angle of $78^{\circ} \pm 2^{\circ}$ and measurements on muon charge ratio were made at the four azimuths, namely east, west, south and north. The M.D.M (maximum detectable momentum) of the spectrograph was 170 GeV/C.

At Durham (Latitude 54° $47'$ N), Ashton and Wolfendale (1963) constructed the first version of the Durham 'horizontal spectrograph' (this was later to be modified, as will be seen later). This spectrograph consisted of solid iron magnet and three trays of Geiger Counters with the axis of the spectrograph pointing in the direction 55° $36'$ east of the geomagnetic north. Particles were accepted in the zenith angular range 81° $48'$ to 78° $28'$ i.e. at~80° and a measurement of the differential momentum spectrum over the momentum range 1.5 - 40 GeV/C was given by the authors cited above.

At Nottingham (Latitude 53° N), Judge and Nash (1965) made a measurement of the momentum spectrum of the muons arriving in the zenith angular range 83° - 90° using the Nottingham spectrograph. This consisted of a solid iron magnet, four trays of flash tubes and a four-fold Geiger Counter coincidence. The axis of the spectrograph was in the east-west direction and, as particles were accepted from both directions, no determination of the charges of the particles would be made. The M.D.M. of the spectrograph was ~ 28 GeV/C.

As will be seen later, the Durham group were interested in the determination and interpretation of both the momentum spectrum and the charge ratio of the incident muons, while the Nagoya group concentrated on the charge ratio, and the Nottingham group, due to the reason given above, made a measurement of the muon spectrum only.

Two recent experiments applying the indirect method of studying electromagnetic bursts produced by high energy muons arriving at large

zenith angles were reported. These are that of Ashton and Coats (1965) at Durham and that of Borog et al. (1965) at Moscow.

A brief review of the results obtained by the various experiments mentioned above will now be given.

2.2 Magnetic spectrograph method

2.2.1 Momentum spectrum of muons and the derivation of the K/π ratio

Prior to the work of Ashton and Wolfendale (1963), it was not clear that the inclined muon spectrum was, in fact, sensitive to the nature of the parents of the muons. The theoretical studies of Allen and Apostolakis (1961) had shown that the inclined spectrum should be comparatively insensitive to the mass of the parent particles. However, the later calculations of Ashton and Wolfendale (1963) disprove this fact.

Ashton and Wolfendale (1963), using the vertical spectrum given by Hayman and Wolfendale (1962[a]) deduced some sensitivity and these authors gave an estimate for the K/π ratio of 0.35 ± 0.23 over the muon energy range at production 30 - 50 GeV. Their calculations were first based on the assumption that the $K_{\mu 2}$ mode is the only decay mode of kaons, but an estimate of the contribution of the other modes ($K_{\pi 2}$, K_1^o) was included.

Mindful of increasing its resolution, the spectrograph of Ashton and Wolfendale has been modified (Pattison 1963) by introducing four

trays of flash tubes at the measuring levels for defining the trajectories of the particles. This change resulted in an M.D.M. of ~ 300 GeV/C. The spectrograph was reorientated to accept particles from a direction 7.8° east of geomagnetic north, and in this case the correction to be applied to the calculated spectrum, due to geomagnetic deflection of the particles, is very small (the correction to the charge ratio determination is bigger and will be discussed in Chapter 5). The reason why the axis of the spectrograph was not made exactly in the geomagnetic meridian is because of the presence of a massive building in this direction. This version of the Durham horizontal spectrograph is called Mark I spectrograph. Particles were accepted in the zenith angular range 77.5° - 90.0°. Preliminary results on the momentum spectrum and the K/π ratio have been given by Ashton et al. (1963a). These authors deduced an upper limit to the K/π ratio of 0.10 over a wide energy range at production, 20 - 500 GeV, taking all decay modes of kaons into consideration, but the final results using the Mark I spectrograph (Ashton et al. 1966), based on a greater number of particles and a later version of theoretical analysis, gave a higher upper limit of 0.40 to the K/π ratio over the same energy range.

It was clear that the effective use of this method for the determination of the K/π ratio is best shown at higher energies in the region of 1000 GeV where the sensitivity of the inclined spectra

to the K/π ratio is greatest (Chapter 4, fig. 4.3). Therefore, it was felt necessary to increase the M.D.M. of the Mark I spectrograph. This was achieved by increasing the longitudinal dimension of the spectrograph by a factor of ~ 2.5 and adding another solid iron magnet and a fifth tray of flash tubes. These changes increased the M.D.M. to ~ 2000 GeV/C. This version is called the Mark II spectrograph. The particles were accepted in the zenith angular range $82.5^{\circ} - 90.0^{\circ}$.

The present work gives the final results using this spectrograph (the instrument has since been dismantled). Preliminary results of the present work have been given by MacKeown et al.(1965)[a].

Another measurement, at low momenta, of the momentum spectrum of muons in the near horizontal direction is that of Judge and Nash (1965) ($\theta = 83^{\circ} - 90^{\circ}$). These authors gave an upper limit to the K/π ratio of 0.43, taking only $K_{\mu 2}$ mode into consideration, over the energy range at production 40 - 90 GeV. This value is not inconsistent with others but, in view of the approximate analysis, the result is not very useful.

As a conclusion, it seems difficult to obtain an accurate value of the K/π ratio from this method, but, since the sensitivity is greatest at very high energies (in the region of 1000 GeV) the aim, therefore, is to get good statistics in that region and indeed this was the main object of the present work. Besides, the results depend on the accuracy of the measured vertical spectrum from which the

inclined spectrum has been derived and, therefore, it is necessary to have an accurate vertical spectrum in that high energy region.

2.2.2 The muon charge ratio

The first study of the muon charge ratio at large zenith angles was reported by Kamiya et al. (1961). These authors gave preliminary results on the positive excess of muons, arriving at zenith angles of $78^{\circ} \pm 2^{\circ}$, using the Nagoya spectrograph. Their continuation of this work (Kamiya et al. 1963) indicated the expected East-West asymmetry of the sea-level muon positive excess which is essentially due to the deflection of the charged particles in the geomagnetic field. The positive excess as a function of muon energy at production was obtained in the energy range 5 - 200 GeV, and the authors found an appreciable charge excess in this energy range and their results were in agreement with the others.

Ashton et al. (1963[b]), using the Durham Mark I horizontal spectrograph, gave preliminary results on the muon charge ratio over energy range at production ~30 - 500 GeV in the zenith angular range $77.5^{\circ} - 90.0^{\circ}$. These authors concluded that their results together with those of the other workers indicate the existence of a minimum in the charge ratio at muon energies (at production) of about 50 GeV and at energies > 100 GeV, there is some indication of a continuous rise in the ratio, but the statistics were poor in this region. The authors also realised that better statistics were needed to enable further study

of the minimum and also the dependence of the charge ratio on muon energy at energies > 150 GeV. The experiment was then continued and the final results given by MacKeown (1965) showed only very slight evidence for a minimum in the energy region at production 50 - 100 GeV and the results still indicated a rise in the ratio at higher energies, but again the statistics were poor in this region.

Support for the existence of a minimum in the charge ratio came from the work of Kawaguchi et al. (1965), but the preliminary results using the Durham Mark II horizontal spectrograph (MacKeown et al. (1965b) gave no evidence for a minimum, but instead these results show a maximum in the same energy region.

As a conclusion, there seems to be an apparent inconsistency between these results on the charge ratio concerning the existence, or non-existence, of a minimum (or a maximum) in the ratio in the energy region 50 - 100 GeV. This point will be discussed in some detail in Chapter 5. Also, it seems necessary to get better statistics at higher energies > 100 GeV, and this was the main object of the present work.

2.3 Burst study method

As mentioned in § 2.1, two groups applied this method recently to investigate high energy muons arriving at large zenith angles namely, Ashton and Coats (1965) and Borog et al. (1965).

The purpose of the experiment of Ashton and Coats, using cosmic

ray muons incident in the near-horizontal direction, was two-fold (i) to obtain information on the details of muon electromagnetic interactions over the energy region where the muon spectrum is known ($E_\mu < 1000$ GeV) and (ii) at energy transfers corresponding to higher energies, to obtain some information on the shape of the high energy muon spectrum. A preliminary results have been reported by these authors for bursts produced in an iron absorber and only the first study has been done, while the second one is now in progress. It was concluded in this work that for energy transfers up to 10 GeV, where μ-e collision is most important, there was no significant divergence from the accepted theory. At large energy transfers (> 40 GeV) there was an indication that the theoretical bremsstrahlung cross-section is too large. In these calculations, the adopted energy spectrum of muons was that of Ashton et al. (1966). However, very recent measurements with increased statistical accuracy (Sept. 1966) have not substantiated the discrepancy. The measurements to date (Private Communication) do not indicate any deviation from the predicted behaviour of high energy muons (30 - 600 GeV) undergoing large energy transfers (5 - 200 GeV).

The argument can be turned round and, assuming that the muons behave as predicted theoretically, the energy spectrum of muons can be derived - the conclusion is then that the spectrum of Ashton et al. (1966) is correct.

Borog et al (1965) have studied the electron-photon bursts produced by cosmic ray muons using an ionization calorimeter, and have derived the integral spectrum of these bursts (of energies 200 - 2000 GeV) in the zenith angular range 55° - 90°. Borog et al. stated that since the muons of cosmic rays, owing to the character of the incident energy spectrum, transmit about 70% - 80% of their energy to γ quanta, the integral spectrum of the produced bursts can be converted to an integral spectrum of muons in the corresponding energy range, 300 - 3000 GeV. It was found by these authors that the best fit between the theory and experiment occurs when the integral spectrum of muons is represented by $I = I_0 E^{-\gamma}$ where $\gamma = 2.15 \pm 0.15$ and $I_0 = 10^{-5}$ cm^{-2} sec^{-1} sterad^{-1}, E being in units of 100 GeV.

This slope is a little greater than was predicted by Ashton et al. (1966) for large zenith angles but the discrepancy cannot be regarded as serious in view of the very wide zenith angular range used by Borog et al. (55° - 90°).

CHAPTER 3

Durham Horizontal Spectrograph Mark II

3.1 Brief description of the instrument

3.1.1 General

A schematic diagram of the spectrograph is shown in fig. 3.1, and an aerial photograph of the apparatus is shown in plate 1. It consists of six trays of Geiger Counters A to F, five trays of flash tubes and two identical solid iron magnets. The axis of the spectrograph is orientated at an angle of 7.8° east of the geomagnetic north, this being the most suitable position so as to avoid the effect of the thick sandstone wall of Durham Cathedral on the flux of the incident cosmic rays and to make the axis as close as possible to the geomagnetic meridiam. On the south side of the laboratory there is a hill corresponding to a path $\sim 3\times10^{4}$ g cm^{-2} at 82° and $\sim 2\times10^{5}$ g cm^{-2} at 90°, which strongly attenuates the flux from this direction. Furthermore, the Geiger Counter trays are arranged in such a way as to be strongly biased to particles arriving from the north. In other words, the spectrograph is accepting particles coming almost entirely from the north with only a very small probability that south-north particles will traverse the instrument.

The selction system consisted of four vertical trays of Geiger Counters A, B, C, and D which defined the trajectories of

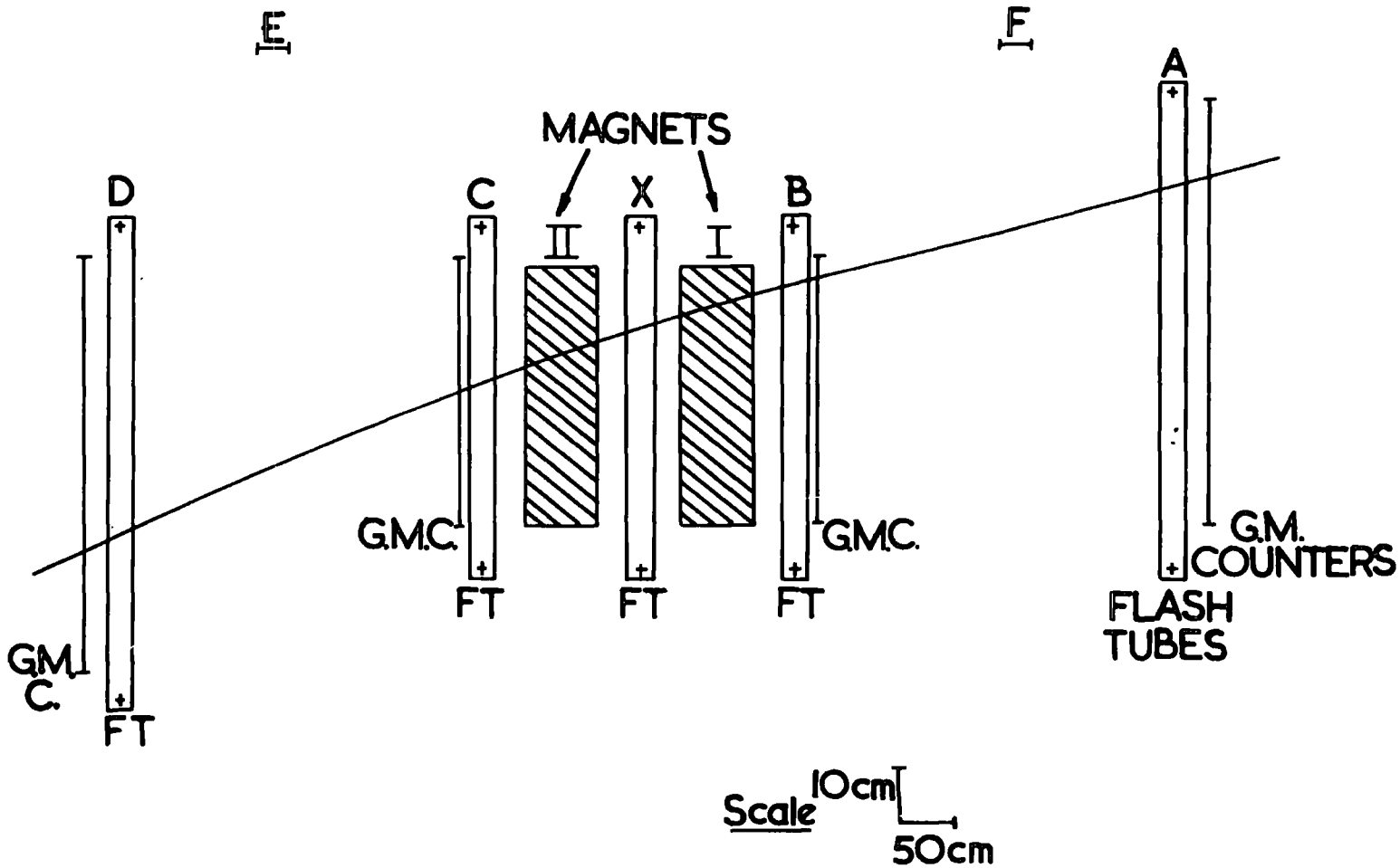

Fig. 3.1 A schematic diagram of the Mark II spectrograph.

accepted particles and two further counter trays E and F placed symmetrically over the instrument and connected in anti-coincidence to the others in order to reduce the frequency of extensive air showers triggering the instrument. The longitudinal dimension of the spectrograph was 10.3 meters.

3.1.2 The Magnets

The two magnets were almost identical and were positioned parallel to each other and one of them, Magnet I, was described in detail by O'Conner and Wolfendale (1960). The magnets are in the shape of large rectangular transformers, each of deflecting lengths of 63.5 cm. Each consisted of 50 iron laminations of thickness 0.5 inches. The laminations were mounted vertically in an iron framework and pressure of retaining bolts was applied to them to reduce the air gaps between them to a minimum. The exitation coils consisted of 250 turns of 14 SWG double cotton-covered wire on each deflecting limb. The total resistance of the coils was 5.70 ohms for Magnet I and 5.64 ohms for Magnet II. The current to the coils was supplied from the same mains rectifier through rheostats to enable the currents to be adjusted to equality and reversing switches were used for field reversals. The two fields were made equal to within 3% by obtaining near zero deflection in a fluxmeter when the windings of the search coils around the two magnets were in opposite directions. The Volume Uniformity of field was studied by O'Conner and Wolfendale (1960) and is uniform to $\sim$ 2%. Each magnet was

energised by a mean current of 13.6 amperes producing a mean induction of 15.58 K gauss. During the run, the directions of the fields were reversed daily to reduce the effect of any source of bias slowly varying with time.

3.1.3 The Flash Tube Trays

Each of the five trays contained eight columns of tubes (a column in trays A and D contained 41 tubes, and in trays B, X and C 29 tubes) with aluminium electrodes fitted in between them. The tubes were supported in slots milled in "Tufnol" rods and the vertical separation of adjacent slots was (1.905±0.002) cm, a unit to be referred to in the text as a 'tube spacing' and abbreviated to "t.s.". The horizontal separation between adjacent columns was 2.8 cm. The individual columns were staggered relative to each other, such that at least four tubes per tray would be traversed by a particle. In the majority of cases not less than six tubes were observed to flash in a tray along the path of a particle. The flash tubes, which were of the type described by Coxell (1961), were ~80 cm in length and 1.8 cm in external diameter, made of soda glass and contained "commercial" neon (98% Ne, 2% He, < 200 volumes per million A, O2, N2) to a pressure of 60 cm Hg.

3.1.4 The Geiger Counter Trays

Trays A and D had 27 counters each, B and C 17 each, and E and F 8 each. The counters were of the type 20th Century Electronics

'G60', of sensitive length 60 cm and internal diameter 3.35 cm. They were arranged in the four trays A, B, C and D in an overlapping manner to cover the gaps between them, and groups of four counters were connected to a quenching unit from which the output pulses were taken. A close-up photograph of flash tube tray B and Geiger Counter tray B, together with Magnet I, is shown in plate 2.

3.1.5 The Electronics

As mentioned in 3.1.1 the requirement for an event to be accepted was a four-fold coincidence pulse ABCD without a coincidence pulse from E and F. When this requirement was satisfied, a high voltage pulse was applied to the flash tube electrodes and a photograph of the flashed tubes was taken through a system of plane mirrors. At the same time a cycling system was triggered which illuminated a clock, flashed two fiducial bulbs on each flash tray, and illuminated a chart on which was displayed the series number of the film and the field direction. All of these were recorded on the same frame of the event. The cycling system also moved on the film in the camera after the occurence of the event.

The high voltage pulse was obtained as follows: A Thyratron was triggered by the output pulse from the anti-coincidence gate. This in turn triggered a high voltage unit, which consisted of a large hydrogen Thyratron and a pulse transformer. This unit in

Plate 2 Close-up of Geiger Counter tray B, flash tube tray B and magnet I

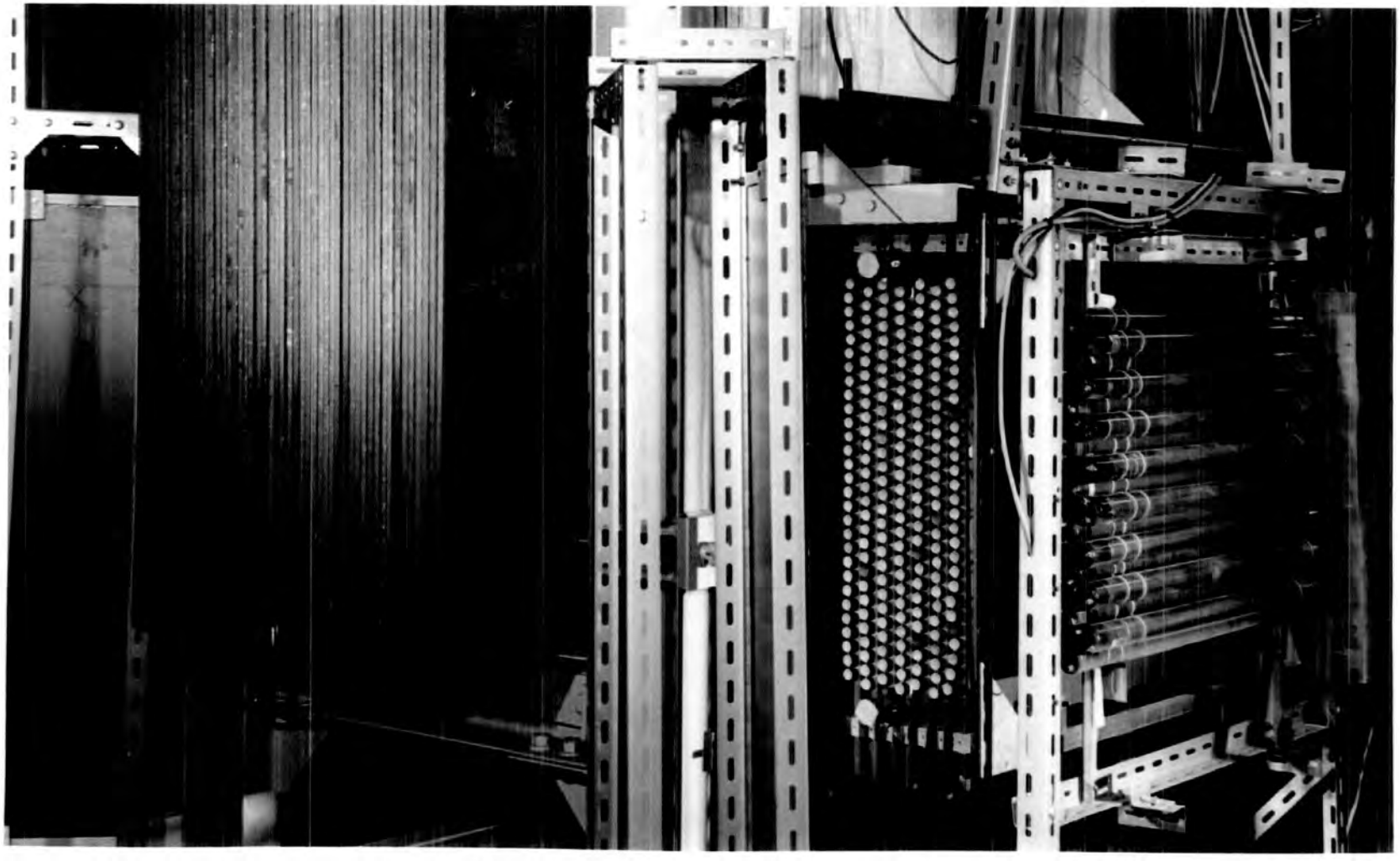

turn triggered four further units each of which consisted of a trigatron and a pulse transformer. The pulses from these units were delivered to the electrodes of the flash tube trays. The high voltage pulse reached the electrodes ~ 9 μ sec after the passage of the particle through the instrument and had a rise time of 0.8 μ sec to a maximum of 8 KV and a width of ~ 2.5 μ sec, producing a field across the flash tubes of 2.86 KV/cm. The arrangement of the electronics is shown in plate 3.

3.1.6 Alignment of the Spectrograph

The whole instrument was made symmetric about a plane midway between the magnets as shown in fig. 3.2. The flash tube trays B, X and C were supported on arms fixed to the pillars of the magnets framework and trays A and D were supported in frames firmly fixed to the floor of the laboratory. Each tray was fitted with adjusting screws to permit the movement of the tray in its frame in the three perpendicular directions during alignment. The trays were made horizontal by three methods; optically with a cathetometer and telescope, by a sensitive spirit level, and by using a uniform closed glass tube containing a small amount of mercury (effectively a large spirit level). The trays were then aligned in the longitudinal direction by fitting to each tray a plate, with a hole in it, at identical positions in the trays and then adjusting the position of the trays so that a tensioned cotton thread would pass through the

Plate 3 The Electronics

centre of the hole in each plate.

The degree of alignment in the vertical plane was also checked by measuring the separation of corresponding points on the trays, at the top and bottom. After the alignment of the instrument was finished the constants a_o, b_o, x_o, c_o, and d_o, together with ℓ_1, ℓ_2, ℓ_3 and ℓ_4, shown in fig. 3.2, were measured. The constants a_o, b_o, x_o, c_o and d_o are the distances from a horizontal reference level to a standard point in each tray. The centre of the lowest tube in the fourth column from the north was taken as the standard point in the tray, and as a reference horizontal level a free water surface was used; this was achieved by using large beakers of water connected to each other by a siphon and placed underneath each tray. The constants a_o, b_o, x_o, c_o and d_o were measured by a cathetometer on both east and west sides of the instrument, and the longitudinal constants ℓ_1, ℓ_2, ℓ_3 and ℓ_4 by an accurate steel tape, also on both sides. The adopted mean values of the constants (with reference to d_o taken as zero) of the instrument are given in table 3.1.

The Geiger Counter trays were aligned in a similar way with the axes of the tubes being parallel to the magnetic field direction.

3.2 Data Analysis

3.2.1 General

If a singly charged particle (e.g. a muon) of momentum P (eV/C) passes through a magnetic field of strength B (gauss) the total

Table 3.1

Adopted values of the geometrical constants

Dimension	cm	t.s
ℓ_1	334.5	175.59
ℓ_2	146.4	76.85
ℓ_3	146.4	76.85
ℓ_4	334.5	175.59
a_o	36.547	13.935
b_o	25.884	13.587
x_o	25.559	13.417
c_o	24.919	13.081
d_o	0	0

1 t.s. - 1.905 cm

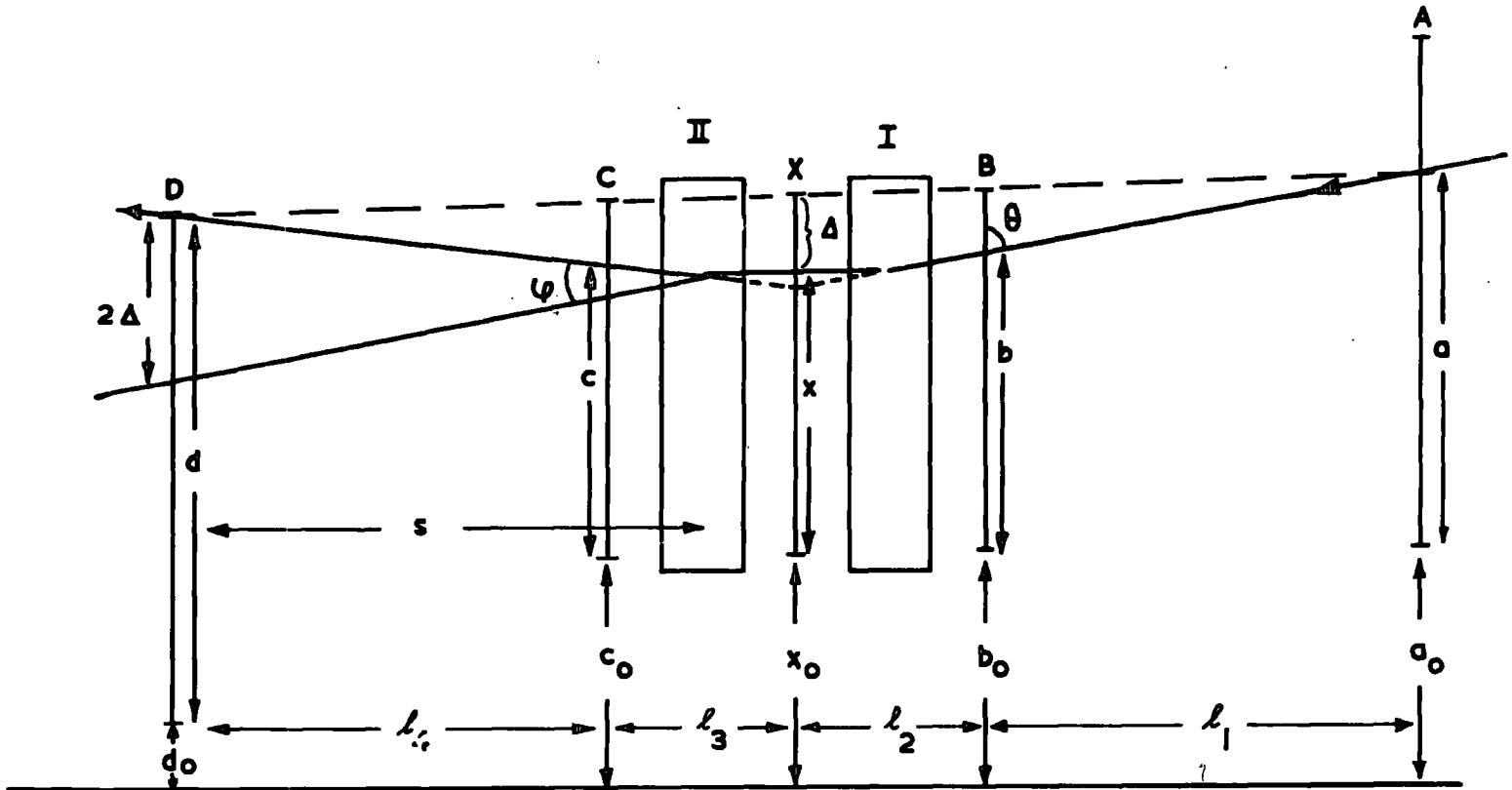

Fig. 3.2 The measured co-ordinates for the Mark II spectrograph.

angular deflection (radians) on traversing the field is given by $\varphi = 300 \int \frac{B\,dl}{P}$ where dl (cm) is the element of path perpendicular to the field, and if we ignore the energy loss in the magnet, we have

$$P = \frac{300}{\varphi} \int B\,dl \qquad (3.1)$$

When a solid iron magnet is used, the energy loss in the magnet becomes important at low energies; Ashton and Wolfendale (1963) found that the momentum of the muons on entering the magnet is given by

$$P = \alpha l \Big/ \left(1 - \exp - \left(\frac{\alpha \varphi}{300B}\right)\right)$$

instead of (3.1) where α is the mean momentum loss per unit of path length. In analysing the data relation (3.1) was used, and a small correction for the energy loss in the magnets was applied to the intensities.

As is seen from the above relations the determination of high momenta depends on the resolution of the angular deflection which is, in our case, limited by two factors:-

i) The finite size and efficiency of the flash tubes and the accuracy of their alignment, and

ii) the multiple Coulomb scattering experienced by the particle in traversing the instrument.

However, since the angular deflections considered are small it is more convenient to work with the linear deflection Δ and referring to

fig. 3.2 the relation between the two is given by

$$\varphi = \frac{2\Delta}{S}$$

Also from fig. 3.2

$$\Delta = \frac{a + d + a_o + d_o}{2} - x - x_o \qquad (3.2)$$

Since the magnetic field is uniform along the path of the particle, and since we have two magnets each of deflecting length ℓ relation (3.1) becomes

$$P = \frac{300\ B\ (2\ell)}{\varphi}$$

now, substituting for φ, its equivalent $\frac{2\Delta}{S}$ and inserting the numerical values of B, ℓ and S we get

$$P\Delta = 63.52 \text{ GeV/c t.s.} \qquad (3.3)$$

The discrepancy at the centre of the system also follows from the measured co-ordinates being given by

$$\epsilon = X_{ab} - X_{cd} \qquad (3.4)$$

where $X_{ab} = b - \frac{\ell_2}{\ell_1}(a-b) + (b_o - x_o) - \frac{\ell_2}{\ell_1}(a_o - b_o)$

and $X_{cd} = c - \frac{\ell_2}{\ell_1}(d - c) + (c_o - x_o) + \frac{\ell_2}{\ell_1} c_o$

are the intersections at the central plane expected from the measured co-ordinates.

This discrepancy is caused by:-

i) Error in the location of the track in the trays.

ii) Multiple scattering in traversing the instrument, and

iii) Energy loss in the magnets

Ashton and Wolfendale (1963) showed that in the case of one magnet the ratio of the r.m.s. scattering deflection $\langle\psi\rangle$ to the magnetic deflection φ is

$$\langle\psi\rangle/\varphi = 0.30$$

Ignoring energy loss, $\langle\psi\rangle$ is given by

$$\langle\psi\rangle = \frac{K}{\beta P\sqrt{2}} \sum t^{\frac{1}{2}}$$

where $\sum t$ is the total thickness of matter traversed in radiation lengths and β the relative velocity of the particle. Assuming scattering outside the magnetic field region to be small compared with that in the iron magnet, $t = l$, the length of the magnet, and since the magnetic deflection is proportioned to l, we will have

$$\langle\psi\rangle/\varphi \propto l^{-\frac{1}{2}} \quad , \text{for } \beta \to 1$$

This means for the case of two magnets

$$\langle\psi\rangle/\varphi = \frac{0.30}{\sqrt{2}} = 0.212 \qquad (3.5)$$

If the error in location is σ_i; assumed to be equal for all trays, then using (3.2) the error in the deflection Δ, σ_Δ will be given by $\sigma_\Delta = 1.225\ \sigma_i$. Similarly, using (3.4) and assuming that most of the contribution to ϵ comes from errors in track location, the error in

ϵ, σ_ϵ is given by $\sigma_\epsilon = 2.122\ \sigma_i$

From the two above relations we get

$$\sigma_\Delta = 0.575\ \sigma_\epsilon \tag{3.6}$$

If the value of σ_Δ is known, the quantity known as the maximum detectable momentum (m.d.m.) of the instrument can be found. This quantity is most usually defined as the momentum whose corresponding deflection Δ is equal to the most probable error in that deflection (probable error $= 0.675\ \sigma_\Delta$).

From (3.3), substituting $0.675\ \sigma_\Delta$ for Δ, it follows

$$P_{m.d.m.} = \frac{63.52}{0.675\ \sigma_\Delta}$$

Using (3.6), the m.d.m. can be expressed in terms of σ_ϵ the standard deviation of the distribution of the discrepancy ϵ, by

$$P_{m.d.m.} = \frac{63.52}{0.387\ \sigma_\epsilon} \tag{3.7}$$

It has been assumed, in the derivation of the m.d.m. that at high energies the contribution to ϵ from scattering is vanishingly small. The total standard deviation in ϵ is

$$\sigma_\epsilon^2 = \text{Const.}\ \Delta^2 + \sigma_o^2 \tag{3.8}$$

where the first term represents the contribution of the Coulomb scattering and the second represents the contribution of errors in track location. The first term will be very small at high momenta i.e. when $\Delta \to 0$, so our assumption is justified.

3.2.2 Analysis of data

The measured rates of events were as follows:-

$$\text{4-fold coincidence } (ABCD) = 27.8 \text{ hr}^{-1}$$

$$\text{6-fold coincidence } (ABC\overline{DEF}) = 4.5 \text{ hr}^{-1}$$

Despite the anti-coincidence requirement a significant fraction of the photographs showed weak extensive air showers and the rate of single-particle events observed on the film was only 1.03 hr^{-1}.

The photographs were analysed as follows: they were projected onto a board on which was marked the outline of all flash tubes in the instrument together with the pairs of fiducial marks for each tray. Also marked on the board were the numbers of tubes in the fourth column of flash tubes from the north in each tray. Each event was projected onto the board and the numbers of the tubes that flashed along the track of the particle in each tray were read off. The readings were then transferred to a device called the track simulator for an accurate measurement of the co-ordinates. This device, described in detail by Hayman (1962), consisted of an enlarged version of a section of a flash tube tray on which a scale was marked in units of tube spacings (t.s.) at the centre of the fourth column. In using this device the information available on the angle of incidence, angle after being deflected by the first magnet, and angle of emergence after being deflected by the second magnet of the tracks in the tray was incorporated.

A curser, with its angle found from the co-ordinates, was moved along the scale until an optimum path through the tubes was found, and its intersection with the scale was read off, giving the co-ordinate of the particle in each tray. This method of measurement will be referred to as 'initial measurement' method.

From the values of the co-ordinates found by this method, the computation was done as follows: using the three co-ordinates a, x and d, the deflection Δ, Zenith angle θ and the discrepancy ϵ were computed for all events and this method of computation will be referred to as the "three-point" method. For those particles of momenta greater than 100 GeV/c ($\Delta \leq 0.635$ t.s) a method of computation using a least square fit to the five co-ordinates a, b, x, c and d was applied and the method will be referred to as "five-point" method.

For greater accuracy, it was decided to remeasure the co-ordinates of those particles having momenta greater than 200 GeV/c by a more refined method. This is similar to the above, but considerations were also taken of the small differences between flash tube trays and the variation of the probability of a tube flashing with the point of the traversal of the particle, both inside and outside the tube together with a more enlarged version of flash tube section in each tray. This method of measurement will be referred to as "refined measurement". Finally, particles with large values of ϵ were reinvestigated

and then rejected if in the "three-point" method $\epsilon > \sqrt{(0.30)^2 + (0.15)^2 \Delta^2}$ or in the "five-point" method $\sum_{i=1}^{5} \delta a_i^2 > 0.045$ t.s.^{2} , where $\delta a_i = a_i - \bar{a}_i$ where $\bar{a}_i$ is the co-ordinate predicted by the least square fit and a_i is the observed co-ordinate. The particles rejected in the above way were corrected for in the calculation of the spectra as will be seen in the next chapter. In the analysis of photographs it was noticed that a number of particles have co-ordinates such that the incident angle appeared to be greater than 90°. Such events were interpreted as "south-north" particles and were rejected. The other particles having smaller zenith angle in trays C and D than in trays A and B were reconsidered. A probability function (which depends on the deflection Δ and the zenith angle from the north) for a particle to be a ["north-south"] has been calculated from the topography of the hill to the south of the laboratory. Then as a rejection criteria a particle will be rejected as being "south-north" if this probability is $\geq$ 2%.

Fig. 3.3a shows the distribution of ϵ for (3696) particles of all momenta where the co-ordinates were measured by the "initial method", while Fig. 3.3b shows the same distribution for the associated (465) particles with P > 200 GeV/c where the co-ordinates were measured by the "refined method". For the "initial method" we have $\langle \epsilon \rangle = (-0.010 \pm 0.003)$ t.s. and the standard deviation in ϵ, $\sigma_\epsilon = 0.213$ t.s. resulting, using equation (3.7), in an m.d.m.

$$P_{m.d.m.} = 770 \text{ GeV/c}$$

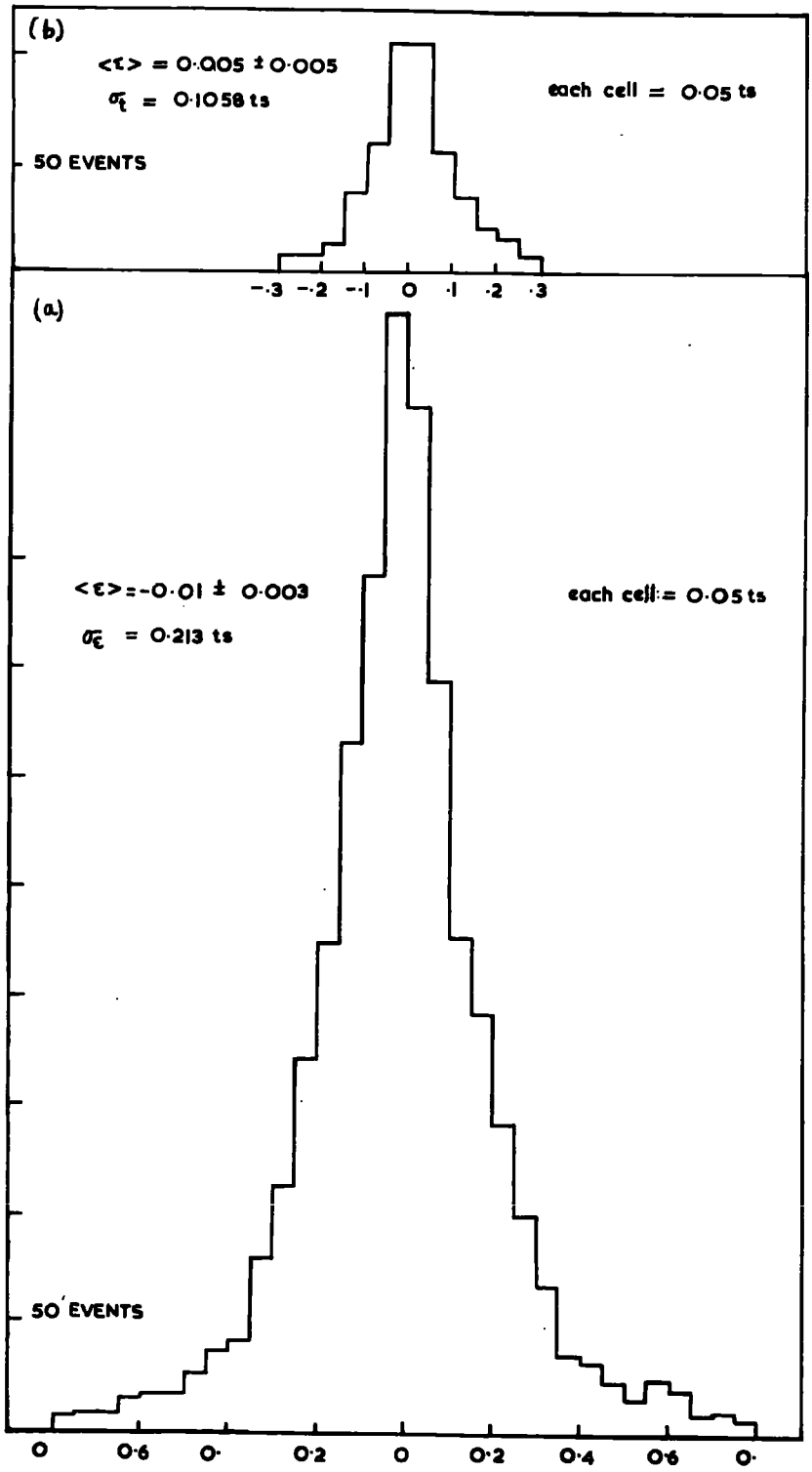

Fig. 3.3 The ϵ distribution (a) from the 'initial method', (b) from the 'refined method'.

For those analysed by the refined method we have $\langle \epsilon \rangle = (0.005 \pm 0.005)$ t.s and $\sigma_\epsilon = (0.1058)$ t.s. resulting in an m.d.m.

$$P_{m.d.m.} = 1550 \text{ GeV/c}$$

Also from σ_ϵ we find this error in track location in a tray

$$\sigma_i = \sigma_\epsilon / 2.122 = 0.950 \text{ mm}$$

There is also an improvement factor of 1.28 on the value of m.d.m. quoted above resulting from the fact that the momenta of these high energy particles were determined by a five-point least square fit to the co-ordinates while the discrepancy ϵ was computed from three co-ordinates only. Therefore, the m.d.m. will be

$$P_{m.d.m.} = 1984 \text{ GeV/c}$$

CHAPTER 4

Results on Muon Spectrum

4.1 Basic data

The basic data here refer to a total running time of 3883.8 hours (with daily reversal of the magnetic field direction) and the total number of accepted particles having momenta greater than 5.8 GeV/c in the zenith angular range $82.5^{\circ} - 90^{\circ}$ was (3761). The data were divided into cells of momentum, P, and zenith angle, θ, and are presented in table 4.1.

Table 4.1 Basic Data: The Momentum Distribution

P_μ s/ℓ (GeV/c)	$\langle P_\mu \rangle$ (GeV/c)	82.5-85.0°	85.0-87.5°	87.5-90°
5.8 - 9.8	7.5	104	120	28
9.8 - 20	14.2	109	297	142
20 - 31	25.3	62	286	147
31 - 51.3	39.5	66	398	182
51.3 - 73.8	61.4	33	236	152
73.8 - 215	121	55	550	371
215 - 500	290	9	157	144
500 - 1000	634	3	33	43
> 1000	1710	2	12	21

4.2 Derivation of the experimental momentum spectra

The method adopted to derive the momentum spectra of muons is to use trial muon spectra to predict the numbers of events to be expected in the various cells in the present experiment. The experimental spectra can then be obtained by multiplying the theoretical trial spectra at the mean energy point of each cell by the ratio of the observed to the predicted numbers in that cell. The trial spectra used in these calculations are those computed by Osborne (1966) from the vertical muon spectrum of Osborne et al. (1964) for the case of all pions as parents of the muons. A brief discussion of the calculations of the trial spectra will be given in the next section.

If the incident trial differential displacement spectra are represented by $N(\Delta',\theta)\,d\Delta'$ (The conversion from a momentum spectrum to displacement spectrum follows from the relation $P\Delta = 63.5$ GeV/c t.s), then the predicted numbers of events in a running time T in a displacement cell $\Delta_2 - \Delta_1$, and zenith angular cell $\theta_2 - \theta_1$ are given by the following expression:

$$N(\Delta_{1,2},\theta_{1,2}) = T\int_{\Delta_1}^{\Delta_2}\int_{\theta_1}^{\theta_2}\int_{-\infty}^{\infty} N(\Delta',\theta)F(\Delta',\theta)f(\Delta)\times(\Delta)Q(\Delta',\Delta)\,d\Delta'\,d\theta\,d\Delta \qquad (4.1)$$

$Q(\Delta',\Delta)$ is the probability that a particle of momentum corresponding to the displacement Δ' will be, due to scattering and errors in track location (noise), observed as having a displacement Δ. $Q(\Delta',\Delta)$ may be represented by a Gaussian distribution:

$$Q(\Delta',\Delta) = \frac{1}{\sigma(\Delta')\sqrt{2\pi}}\exp\left\{-\frac{(\Delta'-\Delta)^2}{2\sigma(\Delta')^2}\right\}$$

where, by (3.8), $\sigma'(\Delta') = \sqrt{\sigma_0^2 + K^2\Delta'^2}$. Expression (4.1) can now be written in the form:

$$N(\Delta_{1,2}, \theta_{1,2}) = T \int_{\Delta_1}^{\Delta_2} \int_{\theta_1}^{\theta_2} N(\Delta,\theta) F(\Delta,\theta) f(\Delta) \chi(\Delta) S(\Delta,\theta) d\theta\, d\Delta \quad (4.2)$$

where $S(\Delta,\theta) = \frac{1}{N(\Delta)} \int_{-\infty}^{\infty} Q(\Delta',\Delta)\, N(\Delta',\theta)\, d\Delta'$

$S(\Delta,\theta)$, which shows the effect of noise and scattering, has been computed by MacKeown (1965), using the above expression, for the present spectrograph with $\sigma_0 = 0.061$ t.s and $K = 0.212$ and the results are shown in fig. 4.1

The other functions stated in expression (4.2) are the following: $F(\Delta,\theta)$ is the spectrograph 'acceptance' function and may be expressed in the form $F(\Delta,\theta) = \eta_p \eta_D\, G(\Delta,\theta)\, A(\Delta,\theta)$ where η_p is the probability that the whole 'instrument' is not paralysed through having been triggered by a previous particle and is equal to 0.992; η_D is the probability that none of the four Geiger Counters traversed by a particle is insensitive; $G(\Delta,\theta)$ is the Geiger tray efficiency which depends on the arrangement of the Geiger Counters in a tray and was found to be independent of both Δ and θ for the present arrangement to very good accuracy, $\eta_D\, G(\Delta,\theta)$ is found to be equal to 0.924; $A(\Delta,\theta)$ is the geometrical differential aperture in units of cm^2 sterad deg^{-1}. Assuming that all the deflections occur in the central planes of the magnets, expressions for $A(\Delta,\theta)$ have been derived by MacKeown (1965) and typical values (averaged for upward and downward deflections) are given in table 4.2.

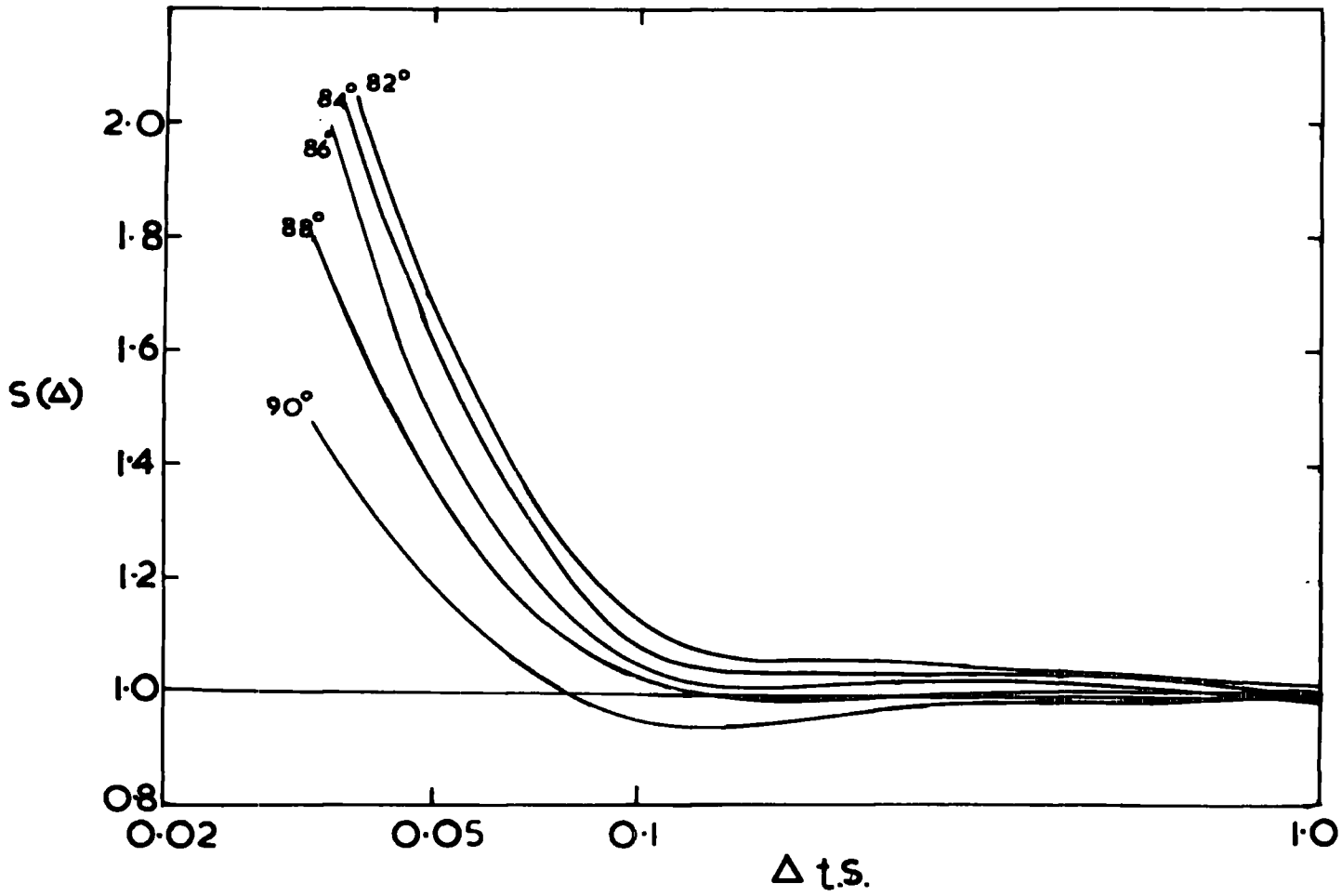

Fig. 4.1 The scattering function S (Δ) for the Mark II spectrograph, after MacKeown (1965).

Table 4.2

Geometrical differential aperture $A(\Delta,\theta)$ (cm^2 sterad. deg^{-1})

Δ(t.s.) \ θ°	82°	84°	86°	88°	90°
0.0	0	0	1.52	2.23	2.95
0.5	0	0	1.52	2.23	2.85
1.0	0	0	1.51	2.23	2.75
5.0	0	0.37	1.10	2.14	1.98
10.0	0	0.61	1.10	0.50	0.80
20.0	0.1	0.42	0	0	0

$f(\Delta)$ is the probability that a particle is not lost through large angle scattering. $X(\Delta)$ is the probability that a particle is not lost through producing a knock-on shower in traversing the instrument, sufficiently large to render the event unanalysable. From the number of particles rejected due to large scattering, by the rejection criteria imposed on the value of the discrepancy ϵ given in the previous chapter, values of the function $f(\Delta)$ have been obtained. The function $X(\Delta)$ has been obtained after finding, approximately, the momentum of those particles rejected because of producing knock-on showers. Typical values of $f(\Delta)$ and $X(\Delta)$ are given in table 4.3.

Table 4.3 Non-loss factors as a function of displacement

Δ(t.s)	0.05	0.10	0.50	1.0	5.0
$f(\Delta)$	0.990	0.990	0.988	0.985	0.972
$X(\Delta)$	0.975	0.978	0.984	0.987	0.993

At low energies, the predicted numbers have been corrected for the energy loss in the magnets. Furthermore a small correction factor, due to geomagnetic deflection in the atmosphere, has been derived, using the measurements on the charge ratio, and applied to the predicted intensities. The experimental momentum spectra are compared with the predicted ones, assuming only pions as parents of muons, in fig. 4.2; the agreement between the two is good, indicating that the propagation model is good to this accuracy. By comparison with the vertical spectrum in fig. 4.2, the expected softening of the spectrum with zenith angle is seen and the relative increase of the intensity of high energy particles over the vertical flux is observed. The dotted curves represent the predicted intensities before applying the correction due to scattering in the atmosphere.

4.3 The predicted spectra at large zenith angles

4.3.1 Introduction

The problem of deriving the momentum spectra of muons at large zenith angles ($\theta \gtrsim 80^{o}$) has been undertaken by a number of authors, notably Jackeman (1956), Smith and Duller (1959), Allen and Apostolakis (1961), Zatsepin and Kuzmin (1961), Sheldon and Duller (1962), Ashton and Wolfendale (1963), Maeda (1964) and Judge and Nash (1965). The calculations briefly described here were done by Osborne (1966) and details are given by the author cited above. One of the refinements made in these calculations is that for the case

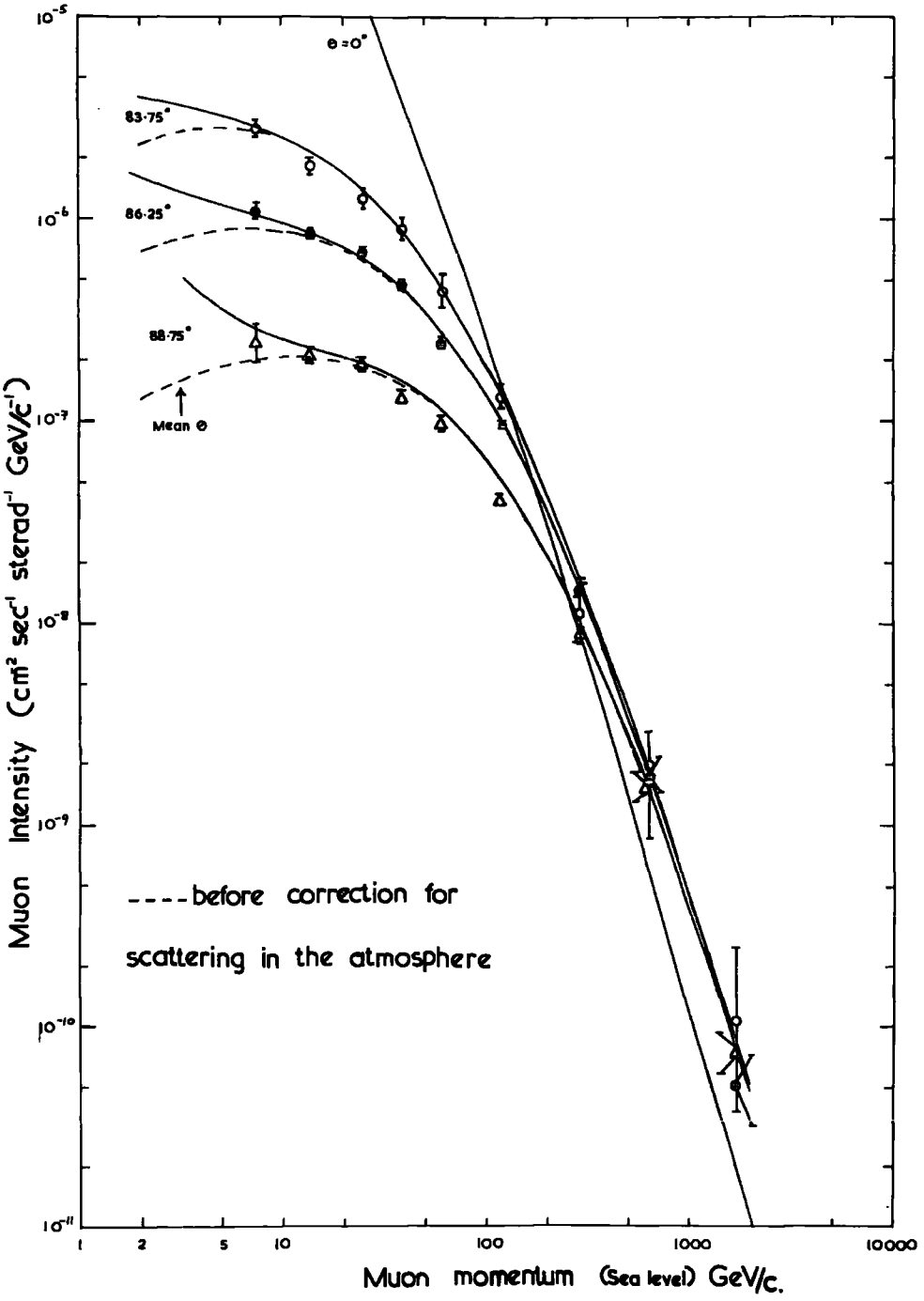

Fig. 4.2 Comparison of the measured momentum spectra at large zenith angles with the predicted ones after Osborne (1966).

where kaons are considered as possible parents of the muons, all decay modes of kaons with branching ratios greater than 1% were taken into account instead of simply the prominent $K_{\mu 2}$. The result differs considerably from that of taking only the $K_{\mu 2}$ mode.

The procedure adopted follows that outlined by Ashton and Wolfendale (1963) and is to start with the measured vertical muon spectrum at ground level and from it to calculate the production spectra of the parent particles (pions or kaons). The production spectra are then used to predict the muon spectrum at large zenith angles.

Another refinement made in these calculations is related to the parent production spectra. Previous workers have assumed that the production spectra can be expressed exactly as a power law. Here, as a first approximation, a power law spectrum has been assumed initially and then relaxed to fit the measured sea-level muon spectrum exactly.

Certain approximations have been made in the calculations. The effects of these approximations are small in themselves but their justification lies in the fact that, having obtained the parent production spectrum in this way, the muon spectrum at sea-level at large zenith angles is calculated from that production spectrum under the same approximations.

Calculations have been made for the extreme cases of all pions and all kaons as parents as well as for admixture of both. The

calculations assume rectilinear propagation of cosmic rays in the atmosphere. Two effects cause the deviation of the trajectory of a particle from a straight line and they must be considered; firstly the effect of the geomagnetic deflection of the particle in the Earth's magnetic field, and secondly the effect of the coulomb scattering of the particle on air nuclei. The geomagnetic effect depends on the location and orientation of the detecting instrument. In the present experiment the axis of the spectrograph was almost in the geomagnetic meridian (7.8^{o} east of geomagnetic north) and the effect of the geomagnetic deflection on the total intensity (of positive and negative particles together) is small. The effect of geomagnetic deflection on the charge ratio is more serious and will be discussed in the next chapter. The effect of scattering on the intensities can be quite large and it has been re-calculated by a Monte Carlo method, the results differing significantly from the previous approximate calculations.

4.3.2 The measured vertical muon spectrum

For energies up to 1000 GeV the vertical muon spectrum has been obtained using magnetic spectrographs. At higher energies three main indirect methods have been used; by measuring the variation of the muon intensity with depth underground and then using the theoretical energy loss relation to predict the integral spectrum at sea-level; by measuring the spectrum of electron

bursts produced by the muons in ionization chambers and scintillators and relating this spectrum to the muon energy spectrum; and finally by measuring the γ - cascade spectra at various heights in the atmosphere and relating them to the muon spectrum at sea-level.

The vertical muon spectrum adopted is that given by Osborne et al.(1964) (referred to as the OPW spectrum). This spectrum has been derived from direct spectrograph measurements at low momentum ($\leq$ 200 GeV/c)and from the underground depth - intensity curve at high momenta up to 7000 GeV/c. The other two methods were not used for the following reasons. In the burst experiment the quantity that is measured is not the vertical intensity but the omnidirectional flux over a solid angle of almost 2π steradians. To convert the latter to the vertical intensity the angular distribution of the muons must be assumed. This depends, at large zenith angles, on the K/π ratio, the quantity that is not in fact known, and the experimental results are weighted towards large zenith angles; in the Higashi et al (1964) experiment for example 75% of the bursts are produced by muons with zenith angles greater than 70^{o}. The objection against using the γ-cascade measurements was that to obtain the muon spectrum from these measurements it is necessary again to know the K/π ratio. A short discussion of the details of the derivation of the OPW spectrum has been given by Osborne (1966).

4.3.3 Production spectrum of the parents of muons

(a) Pion production spectrum

In order to derive the pion production spectrum that gives rise to the measured vertical spectrum, if all muons originate in pion decay, it has been assumed that the charged pion spectrum has the form $F_{\pi^{\pm}}(E_\pi) = AE_\pi^{-\gamma}$ and a general expression (which includes the variables A and γ) for the muon spectrum at sea-level is obtained. The values of A and γ are then varied to get a best fit between the expected and measured spectra.

The calculation starts from the general expression, given by Maeda (1960), for the number of pions, travelling vertically with energy E_π at depth X in the atmosphere as

$$N_\pi(E_\pi, X) = \int_0^X \exp\left[-\int_{X'}^{X}\left(\frac{B_\pi}{E_\pi'' X''} + \frac{1}{L_\pi}\right) dX'' - \int_0^{X'} \frac{dX''}{L_n}\right] \frac{F_\pi(E_\pi)}{L_c}\, dX' \qquad (4.3)$$

where L_π is the absorption mean free path of pions; L_n is the absorption mean free path of nucleons; L_c is the collision mean free path of cosmic ray primaries; and $B_\pi = \frac{m_\pi c}{\tau_\pi} \frac{x''}{\rho(x'')}$

The first term in square brackets represents the decrease in intensity due pion decay and absorption and the second represents the decrease of pion producing particles.

In order to get the muon spectrum at sea-level from expression (4.3) certain approximations and assumptions are necessary (to make the evaluation of the integral easier), the most important being that the primary nucleons (protons) and secondary pions

(or Kaons) are absorbed in the atmosphere with the same absorption lengths i.e. $L_\pi = L_n$ and both are equal to 120 g cm^{-2}. A value of 120 g cm^{-2} assigned for L_n comes from a variety of summaries (e.g. Sitte 1961, Perkins 1961, Brooke et al. 1964a), and a value of 120 g cm^{-2} was assumed for L_π, since many studies have shown that at high energies ($\gtrsim$ 100 GeV) the nuclear active component as a whole ($P + n + \pi$) has an attenuation length of 120 g cm^{-2} and the pion attenuation length must, therefore, be the same. At lower energies there is some evidence (Brook et al. (1964b)) that the attenuation length of pions is greater than 120 g cm^{-2}, the workers cited above inferred $L_\pi \simeq 150$ g cm^{-2} for $E_\pi \lesssim 30$ GeV, and the effect of taking $L_\pi > 120$ g cm^{-2} will be to reduce somewhat the predicted intensities at large zenith angles at low momenta (Maeda 1964). L_c is also taken as 120 g cm^{-2}.

In these calculations the spread in energy of muons arising from the decay of the parent particles has been allowed for accurately. From the comparison between the predicted and measured spectra it is found that a constant value of γ will not give a good fit over the entire energy range and the pion production spectrum giving the best fit is found to be

$$F_{\pi^\pm}(E_\pi) = 7.16\ 10^{-2}\ E_\pi^{-1.93}\ \text{cm}^{-2}\ \text{sec}^{-1}\ \text{sterad}^{-1}\text{GeV}^{-1} \quad \text{for } E_\pi \lesssim 3.5 \text{ GeV}$$

$$F_{\pi^\pm}(E_\pi) = 1.76\ 10^{-1}\ E_\pi^{-2.65}\text{cm}^{-2}\ \text{sec}^{-1}\ \text{sterad}^{-1}\ \text{Gev}^{-1} \quad \text{for } 3.5 \lesssim E_\pi \lesssim 2000 \text{ GeV} \qquad (4.4)$$

Using this pion spectrum the muon sea-level spectrum has been calculated and compared with the OPW spectrum in order to obtain the

relaxation factor.

(b) pion and Kaon production spectrum

An admixture of kaons in the flux of parent mesons that give rise to muons at sea-level has been assumed. As a first approximation the ratio of charged and neutral kaons to charged and neutral pions of a given energy at production has been taken to be independent of energy. This ratio, $N(K^{\pm o})/N(\pi^{\pm o})$, was denoted by R.

If the production spectrum of all kaons and pions is of the form $F_{K\pi}(E) = CE^{-\gamma}$, then, assuming charge independence in the production of pions, the production spectrum of charged pions is $F_{\pi^{\pm}}(E) = \frac{2}{3}\frac{C}{R+1}E^{-\gamma}$. Furthermore it is assumed that the production spectrum of charged kaons is the same as that for neutral kaons i.e. $F_{K^{\pm}}(E) = F_{K^o\,\bar{K}^o}(E)$ and both equal to $\frac{c}{2}\frac{R}{R+1}E^{-\gamma}$. In a similar way to the case of pions as the only parents of muons, the above production spectra have been used to give the muon sea-level spectrum for various admixtures of kaons and pions. For K/π ratio set equal to 0.4, the production spectrum of pions and kaons is found to be

$$F_{\pi K}(E) = 0.335E^{-2.70} \quad \text{cm}^{-2}\ \text{sec}^{-1}\ \text{sterad}^{-1}\ \text{GeV}^{-1} \qquad (4.5)$$

For K/π ratio set equal to 0.2 it is found that the production spectrum above will still give sufficiently close agreement between the calculated and the OPW spectrum, but the relaxing factor will

be different from that for $K/\pi = 0.4$

4.3.4 The predicted muon spectra at large zenith angles

(a) Muon spectra from pion parents

Starting again with the general expression for the number of pions with energy E_π at depth X expression (4.3) becomes, for pions at a local zenith angle $\theta^*(X)$:

$$N_\pi(E_\pi, X, \theta^*) = \int_0^X \exp\left[-\int_{X'}^{X} \left(\frac{B_\pi(X'')}{E_\pi'' X''} + \frac{1}{L_\pi}\right) \frac{dX''}{\cos\theta^*(X'')} - \int_0^{X'} \frac{dX''}{L_n \cos\theta^*(X'')}\right] \frac{F(E_\pi'')}{L_c \cos\theta^*(X')} dX' \quad (4.6)$$

Using the same approximation as before and using the pion production spectrum given by (4.4) the intensities of muons at sea-level at large senith angle have been calculated.

(b) Muon spectra from pion and kaon parents

The expressions for the intensity of muons produced by a mixture of kaons and pions for the vertical direction have been modified to large zenith angular directions and by using the production spectrum given by (4.5), the muon spectra at these angles for admixtures of kaons and pions have been obtained. The predicted differential muon sea-level spectra at zenith angles 80° and 90° for assumptions (i) that all muons come from pions and (ii) the K/π ratio is 40% are given in table 4.4, compared with the vertical spectrum ('OPW' spectrum).

4.4 Derivation of the K/π ratio

Having calculated the expected muon energy spectrum at large

Table 4.4 Predicted differential muon sea-level spectra at zenith angles 80° and 90° for (i) $K/\pi = 0$ and (ii) $K/\pi = 0.4$, compared with the vertical 'O.P.W.' spectrum. (The numbers represent the intensities in $cm^{-2}\ sec^{-1}\ sterad^{-1}\ GeV/C^{-1}$

P_μ S/L GeV/C	$\theta = 0^\circ$ (O.P.W) Spectrum	$\theta = 80^\circ$		$\theta = 90^\circ$	
		$K/\pi = 0$	$K/\pi = 0.4$	$K/\pi = 0$	$K/\pi = 0.4$
5	$3.96\ 10^{-4}$	$9.71\ 10^{-6}$	$9.71\ 10^{-6}$	$2.22\ 10^{-7}$	$2.12\ 10^{-7}$
10	$1.07\ 10^{-4}$	$7.13\ 10^{-6}$	$7.10\ 10^{-6}$	$1.52\ 10^{-7}$	$1.45\ 10^{-7}$
20	$2.20\ 10^{-5}$	$3.85\ 10^{-6}$	$3.83\ 10^{-6}$	$1.07\ 10^{-7}$	$1.01\ 10^{-7}$
50	$1.94\ 10^{-6}$	$9.89\ 10^{-7}$	$9.73\ 10^{-7}$	$6.85\ 10^{-8}$	$6.20\ 10^{-8}$
100	$2.50\ 10^{-7}$	$2.44\ 10^{-7}$	$2.36\ 10^{-7}$	$3.69\ 10^{-8}$	$3.40\ 10^{-8}$
200	$2.97\ 10^{-8}$	$4.77\ 10^{-8}$	$4.50\ 10^{-7}$	$1.47\ 10^{-8}$	$1.34\ 10^{-8}$
500	$1.46\ 10^{-9}$	$3.71\ 10^{-9}$	$3.36\ 10^{-9}$	$2.17\ 10^{-9}$	$1.88\ 10^{-9}$
1000	$1.15\ 10^{-10}$	$3.79\ 10^{-10}$	$3.36\ 10^{-10}$	$3.25\ 10^{-10}$	$2.75\ 10^{-10}$

zenith angles as a function of the K/π ratio, it should be possible, by comparing the calculated and measured spectra, to derive a value for this ratio. The range of muon energy at sea-level for which the K/π ratio could be estimated from the present experiment is 10 - 2000 GeV. Using the C.K.P. model (Cocconi et al. 1961), which gives the relation between mean primary energy E_o and energy of pions produced by the primary E_π as $\overline{E}_o = 5.8\ E_\pi^{1.27}$, the above sea-level muon energy range will correspond to a primary energy range of 10^3 - 10^5 GeV. In fig. 4.2 the general agreement of the measured and predicted spectra enables their combination to be carried out in an attempt to derive the K/π ratio. The events have been grouped together and the ratio of their numbers to that expected for pions as the only parents of muons is plotted in fig. 4.3 Also shown in the figure are the expected curves for $K/\pi = 0.2$, 0.4 and all kaons. For comparison the case of $K_{\mu 2}$ as the only decay mode of kaons is also shown. This simplifaction was used in some previous analyses e.g. Judge and Nash (1965) but it is apparent that taking all the kaon decay modes into consideration reduces the sensitivity of the inclined muon spectrum to the K/π ratio.

The vertical error flags on the experimental points represent statistical errors in the observed numbers only. The predicted numbers are also uncertain on account of the errors in the vertical muon spectrum from which they were derived. The effect of including

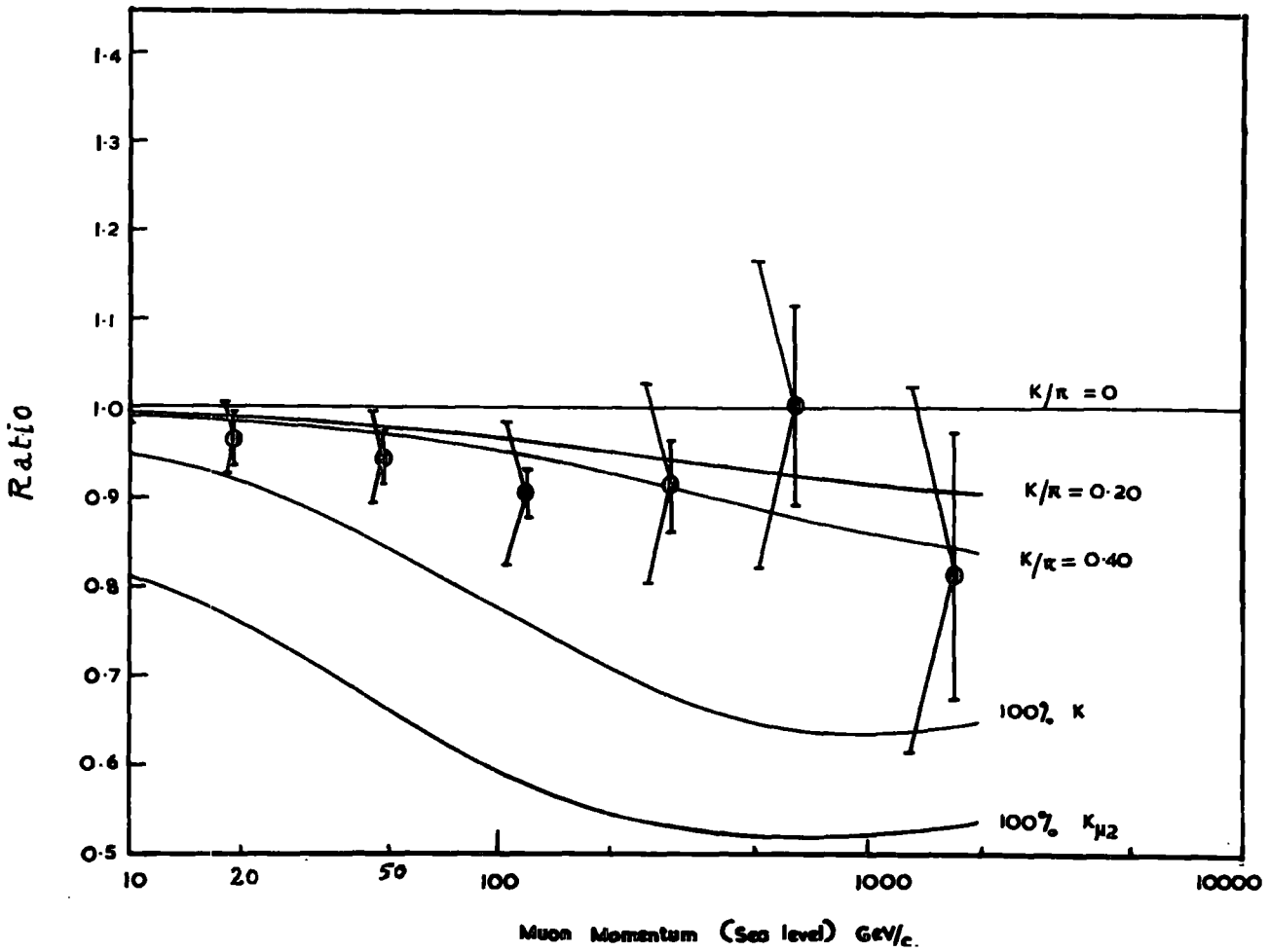

Fig. 4.3 Comparison of measured and predicted intensities with those for pions as the only parents.

these uncertainties is shown in the inclined error flags.

It is clear that the derivation of the K/π ratio from fig. 4.3 is difficult. Because of the low sensitivity of the inclined spectra to the K/π ratio at low energies an estimate of the K/π ratio was obtained for the high energy region, taken as 70 - 2000 GeV, besides an estimate for the whole energy region of interest i.e. 10 - 2000 GW. The two estimates are

$K/\pi = 0.42 \pm 0.20$ for $70 \leq E_\mu (S/L) \leq 2000$ GeV

$K/\pi = 0.56 \pm 0.17$ for $10 \leq E_\mu (S/L) \leq 2000$ GeV

The first estimate which corresponds to primary energy region of 2.8×10^3 - 10^5 GeV was considered as more realistic than the second since it corresponds to a region of high sensitivity and it will be referred to when comparison is made with the results of other workers.

4.5 Comparison with the results of other workers

4.5.1 K/π ratio determination from studies of inclined spectra

Previous attempts to determine the K/π ratio using this method have been made by Ashton and Wolfendale (1963), Judge and Nash (1965) and Ashton et al. (1966) and preliminary results of the present work have been given by MacKeown et al. (1965a) and later by MacKeown (1965). The values of the K/π ratio in the zenith angular range and muon energy range at production considered by these authors are given in table 4.5 compared with the results from the present work.

Table 4.5 Comparison of the K/π ratio from present work with previous determinations using inclined spectra method.

Authors	θ°	E_{μ}(Prod.)GeV	K/π
Ashton & Wolfendale(1963)	80°	30 - 50	0.35 ± 0.23
Judge and Nash (1965) (only $K_{\mu 2}$ mode)	$83\text{-}90^{\circ}$	40 - 90	≤ 0.43
Ashton et al. (1966)	$77.5\text{-}90^{\circ}$	20 - 500	≤ 0.40
MacKeown et al.(1965)	$82.5\text{-}90^{\circ}$	40 - 2000	≤ 0.40
MacKeown (1965)			
Present work	$82.5\text{-}90^{\circ}$	100 - 2000	0.42 ± 0.20
" "	" "	40 - 2000	0.56 ± 0.17

It can be seen from the table that the present result of the K/π ratio is higher than that given in the preliminary ones. It was found, after giving the preliminary results, that a correction factor of 0.94 which had been applied to the total running time of the preliminary data was not in fact correct. That factor was correcting for the blank frames that appeared on the films and which were thought to have been caused accidently. Later it was found that the blanks were caused by small pulses not big enough to trigger the high voltage unit and after amplifying these pulses the blanks disappeared and instead weak shower events were seen. Therefore the correction factor was wrongly applied to the preliminary data and the preliminary results must not be taken as

correct. The difference between the K/π ratio derived from these two data seems to be due mainly to this correction factor applied to the preliminary data and not applied in the present final data.

The present results again give higher upper limit to the K/π ratio than that given by Ashton et al. (1966) using the Durham horizontal spectrograph Mark I for a narrower muon energy range but the two results are not inconsistent with each other taking into consideration the large statistical errors of both results and the low sensitivity of the spectra to the K/π ratio at low energies.

As far as the other two estimates of the K/π ratio given in table 4.5 which correspond to very much lower muon energy ranges than the present work, there seems to be no inconsistency between them and the present work.

4.5.2 Comparison with K/π ratio determination by other indirect methods

The present measurement corresponds to primary energy range $\sim 3 \cdot 10^3$ - 10^5 GeV. At higher primary energies, measurements of electromagnetic cascades at various heights in the atmosphere allow an estimate to be made of the K/π ratio. Osborne and Wolfendale (1964) combined all the available measurements of the energy spectra of electromagnetic cascades in the cosmic radiation to calculate the K/π ratio for mean primary energies in the region 2×10^4 - 6×10^5 GeV under the assumptions that the energy

spectra of the kaons and pions produced in nuclear interactions have the same form, that π^+, π^- and π^0 mesons are produced in equal numbers and that the number of charged and neutral kaons produced are equal. The procedure used by the authors cited above was the following. Under the hypothesis that the γ-e cascades in the atmosphere results only from the decay of neutral pions, then the production spectrum of these pions can be calculated, and, with the assumption of charge independence, the production spectrum of muons from pions may be derived. Alternatively, if it is assumed that the neutral pions and muons are produced in the decay of kaons the same flux of γ quanta implies a different production spectrum of muons. The two predicted muon production spectra may then be compared with that obtained from the known sea-level muon flux and values of the K/π ratio can be obtained which give a predicted muon production spectrum equal to the observed one. The sea-level vertical muon spectrum used was the OPW spectrum (Osborne et al. 1964) but later Pattison (1965) derived a new value for the spectrum from new underground measurements and concluded that the OPW spectrum underestimates the intensity at depths of the order of 2000 m.w.e. corresponding to an underestimate in the K/π ratio by perhaps 10 - 20% in the primary energy range 6×10^4 - $\sim 2 \times 10^5$ GeV. The results given by Osborne and Wolfendale (1964) were increased by the above factor and the modified results are shown in fig. 4.4. Also shown is the result of the present work for comparison.

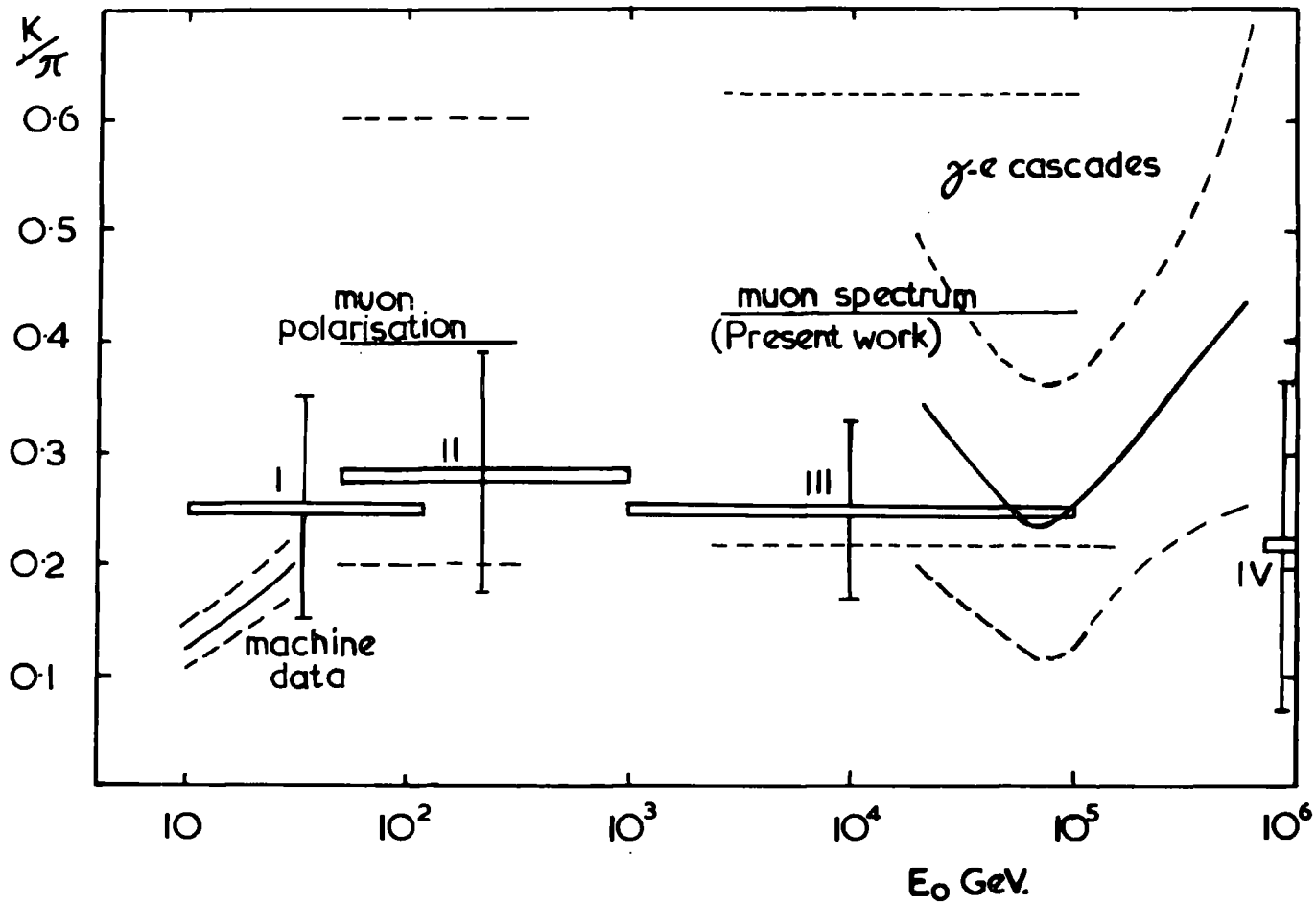

Fig. 4.4 Summary of the variation of the K/π ratio with mean Primary energy, after Osborne and Wolfendale (1964), including the present work I - IV, Perkins (1961), γ- e cascades modified by Pattison (1965)

In the lower primary energy range, 50 - 300 GeV, the K/π ratio may be deduced from measurements of the muon polarization at sea-level. The relative proportions of muons coming from pions and kaons can be determined because muons of a given energy at sea-level come from different energy ranges of parents in the two cases, which leads to a difference in the predicted polarization. Osborne (1964) has summarized the measurements up to November 1963 and further results have been given by Asatiani et al (1964). The statistical errors are large, but, combining the results together, under the assumption that the K/π ratio is constant over the energy range considered, the estimated ratio was $40 \pm 20\%$ and is shown in fig. 4.4.

It can be seen from fig. 4.4 that there is rough consistency between the present work and these two other indirect methods over the wide energy range covered by all three methods.

4.5.3 Comparison with direct K/π ratio determination

The results given by the indirect methods mentioned above refer to the ratio of the production spectra of kaons and pions averaged over all interactions of the primary particles. This is the same as the ratio of kaons to pions produced in individual nuclear interactions only if the effective mean energies of the two types of mesons are the same. Assuming this to be the case, the result of the present work and the other two indirect methods

can be compared with those obtained by the direct methods.

Below 30 GeV primary energy the K/π ratio for proton - light nucleus interactions has been measured in machine experiments and it was found that there is a slow increase with increasing primary energy. The mean energy of the kaons appears to be slightly greater than that of the pions. Summarized machine data are shown in fig. 4.4

Perkins (1961) has made a summary of direct measurements of non-pion production in nuclear collisions from the study of individual interactions in multiplate cloud chambers and nuclear emulsions. By counting the number of neutral pions, identified by their decay, and assuming charge symmetry in the production of pions, the proportion of non-pions amongst all charged particles is found. The results are plotted in fig. 4.4. Below 1000 GeV (points I and II) the data come from cloud chamber experiments and at higher energies (points III and IV) they refer to measurements on jets in emulsions. As indicated above the ratios refer not only to kaons but to all created particles heavier than pions and the ratios shown are therefore somewhat overestimates of the K/π ratio.

It can be seen from fig. 4.4 that the present result is consistent, within statistical errors, with result III of these direct measurements which corresponds to nearly the same primary

energy range.

Particles produced in high energy interactions that move in the extreme backward direction in the c.m.s. have sufficiently low laboratory energies that their mass may be deduced from measurements of grain density and scattering in nuclear emulsions. Most models of nucleon-nucleon collisions imply forward-backward symmetry in the c.m.s. both in particle composition and angular distribution. If this is so, measurements on the backward cone particles having low laboratory energy may be applied to the high laboratory energy forward cone. Kim (1964) examined 22 jets produced, in nuclear emulsions exposed at high altitude, by protons, neutrons and alpha particles with energies between 200 and 1.5×10^4 GeV. He found that for c.m.s. angles greater than 175°, of the secondaries, nine were identified as kaons and seven as pions and the ratio of their c.m.s. momenta was 1.7. If forward-backward symmetry is assumed, then the high kaon momenta will result in a value of the K/π ratio greater than 300%. This value is inconsistent with the present work and the results of the other methods that are shown in fig. 4.4. If the observation of higher mean energies of kaons is correct, the discrepancy may be due to a fault in the assumption of forward-backward symmetry in the c.m.s. for the particular interactions in which these particles were produced. Alternatively, the grain density measurements of Kim may be inaccurate.

4.5.4 Conclusions on the K/π ratio

It can be seen from fig. 4.4 that the present result on the K/π ratio is consistent with the other two indirect methods (muon polarization and γ-ray cascades) within statistical errors. What can be said from combining the three methods is that there is no evidence against a near-constant K/π ratio over the wide primary energy range 10^2 - 10^6 GeV covered by these indirect studies and that the average value is 0.35 ± 0.20 over this energy range.

Provided that the majority of the non-pions produced in individual nuclear interactions are kaons the general agreement, shown in fig. 4.4, between the indirect and direct method suggests, as indicated by Osborne (1966), that there is no indication of the effective mean energies of kaons and pions from individual interactions being appreciably different in the range of primary energies from 10 GeV to 10^5 GeV.

We have seen that, using the method of the present work i.e. from studies of inclined spectra, it was not possible to make an accurate determination of the K/π ratio owing mainly to two factors: uncertainty in the correction factor due to noise and scattering, which is very sensitive to both the shape of the spectrum $N(\Delta,\theta)$ and to the functional dependence of σ_Δ on deflection, and the uncertainties in the vertical muon spectrum (~24% at E_μ (sea-level) = 40 GeV and ~ 12% at E_μ (sea-level) = 300 GeV) from which the predicted spectra at large zenith angles were derived.

It is apparent that the effective use of this method for studying the K/π ratio must await an accurate measurement of the inclined muon intensity in the region of 1000 GeV/c, where the sensitivity to the K/π ratio is greatest, coupled with an improved determination of the vertical intensity in this same region.

CHAPTER 5

Results on the muon charge ratio

5.1 Muon charge ratio measurements

The most general and direct method of measuring the μ^+/μ^- ratio is the magnetic deflection method which is used in the present work. Several other methods have been used mostly at low energies, e.g. (i) the relative muon decay rates in different materials, Conversi (1949), Morewitz and Shamos (1953), and (ii) the deflection of the electrons from muon decay, Nereson (1948).

Although the magnetic deflection method is the simplest to identify the charge of the particle the results are, in general, subject to bias and ambiguities. There are three kinds of sources of bias (i) geometrical acceptance sources (ii) time dependent instrumental sources and (iii) bias arising from methods of analysis. Since the spectrograph in the present work contained no restrictive selection devices for choosing the particle to be registered, bias due to geometrical arrangement of the detecting trays can be eliminated by accepting results from equal running times on each field direction. The former is true only if there are no time varying sources of instrumental bias, and these, if they exist, can be minimised by reversing the field frequently; in the present work the field being reversed daily. No serious source of bias from the method of analysis is expected. Because the μ^+/μ^- ratio is varying

only slowly with energy small systematic errors in the determination of the energy of the particles will not be important. However, in the region of maximum detectable momentum, serious errors may occur due to scattering and errors in track location, because of the probability of a particle being detected as of opposite sign, and the overspill of the much more numerous low energy particles due to scattering.

5.2 The basic data

Preliminary results of the present work have been given by MacKeown et al. (1965b) and later by MacKeown (1965). The basic data presented here are the final data obtained using the Durham Horizontal spectrograph (Mark II) over the range of zenith angles 82.5° - 90° and refer to a total running time of 3883.8 hours (1886.3 hours on H^{+} and 1997.5 hours on H^{-}), The total number of accepted particles (positive and negative) over the range of zenith angles 82.5° - 90° was 3918. The basic data are presented in table 5.1. Also given in the table is the observed ratio, denoted by R_o , corrected for the small differences between the running times on the two field directions. The quoted errors on the values of R_o correspond to one standard deviation. The data were subdivided by field direction, and it was found that the ratios obtained were symmetrical, indicating that there was no serious source of bias.

Table 5.1 Basic data - muon charge ratio

E_μ (S/L) GeV	$\langle E_\mu S/L \rangle$ GeV	$\langle E_{\mu\,prod} \rangle$ GeV	$g(E_\mu)$	μ^+	μ^-	R_o	R_i	R_p
< 5	~3	29	*	58	61	$1.007 \pm .190$	$1.007 \pm .190$	—
5-15	8.8	43	1.185	286	297	$1.007 \pm .080$	$1.007 \pm .080$	$1.193 \pm .095$
15-30	21	64	1.100	408	297	$1.399 \pm .110$	$1.399 \pm .110$	$1.539 \pm .121$
30-50	38	87	1.063	373	282	$1.335 \pm .110$	$1.335 \pm .110$	$1.419 \pm .117$
50-100	70	124	1.040	425	372	$1.149 \pm .083$	$1.149 \pm .083$	$1.195 \pm .086$
100-220	139	204	1	352	290	$1.215 \pm .098$	$1.215 \pm .098$	$1.215 \pm .098$
220-500	296	360	1	172	129	$1.335 \pm .157$	$1.335 \pm .157$	$1.335 \pm .157$
> 500	1090	1200	1	57	59	$.967 \pm .180$	$.96^{+.27}_{-.25}$	$.96^{+.27}_{-.25}$

* Because the distribution in height of production is uncertain the appropriate correction factor for geomagnetic deflection is not available.

5.3 The charge ratio at production

Since, from the point of view of its interpretation the quantity of interest is the charge ratio at production, we must consider the corrections to be applied to the charge ratio at sea-level to get back to this quantity. The observed data must first be corrected for noise and scattering, and for contamination to derive the charge ratio in the incident flux (this is denoted by R_i in table 5.1). This quantity must then be corrected for the effect of geomagnetic deflection in the atmosphere and then transferred to energy at production to find the charge ratio of the muons at production, R_p. In the following, these three correction factors will be considered briefly.

(i) Contamination of the muon flux

Since solid iron magnets were used in the present work there was no contamination of the detected muon flux by the strongly interacting protons and pions because they will be absorbed by the iron.

(ii) Noise and scattering

Due to noise alone particles of the highest momenta may be detected as being of opposite sign; this has the effect of masking any charge excess in the flux. Since solid iron magnets were used in the present work another effect due to multiple coulomb scattering will occur and since this scattering increases with decreasing momentum, propagation of the charge excess at low momenta to high momenta occurs, which masks its true energy dependence. The effect of scattering was

neglected since up to the m.d.m. the effect is not very large. For noise alone it was assumed that the charge ratio varies very slowly with energy and that the mean value of the exponent of the muon momentum spectrum is 2 i.e. $N(P)\ dP \sim P^{-2}\ dP$ at large zenith angles (in the vertical direction the exponent is nearer 3 i.e. $N(P)\ dP \sim P^{-3}\ dP$). Then assuming that the noise is distributed according to a Gaussian distribution, it has been shown by MacKeown (1965) that the ratio in the incident flux, R_i, is related to the observed ratio R_o as follows:

$$R_i(\Delta) = \frac{(R_o+1)\ \mathrm{erf}\ (q) + (R_o - 1)}{(R_o+1)\ \mathrm{erf}\ (q) - (R - 1)}$$

where $q = \frac{\Delta}{\sigma_o\sqrt{2}}$, σ_o is the error in Δ due to track location errors and $\mathrm{erf}\ (q) = \frac{2}{\sqrt{\pi}}\int_0^q e^{-t^2} dt$

The calculated values of $R_i\ (E_\mu)$ are given in table 5.1.

(iii) Geomagnetic deflection

Because the axis of the spectrograph is at angle 7.8° east of the geomagnetic meridian, the charge excess in the incident flux at a given sea-level energy is not simply related to the excess at a given energy at production because of the opposite deflection of the two charges in traversing the atmosphere, the effect which gives rise to the well-known East-West asymmetry. Assuming that the charge ratio is energy independent and that pions are the only parents of muons, the relation between the incident ratio $R_i\ (E_\mu)$ and that at production

$R_p\ (E_\mu)$ can be written as

$$R_i\ (E_\mu) = (E_+^* / E_-^*)^{-\eta}\ \frac{S^+\ D^+}{S^-\ D^-}\ R_p\ (E_\mu^*)$$

where η is the exponent of the differential pion spectrum assumed to be a power law, the asterisk signifies energy at production and E_+, E_-, S^+, S^- and D^+, D^- are the energies, survival probabilities and (Parent's pions) decay probabilities of the two charged states respectively.

Assuming that all muons are produced at a unique depth of 120 g cm^{-2} along the path, and taking $\eta = 2.64$, the methods of Okuda (1963) and Kamiya (1964, Private Communication) were used by MacKeown (1965) to evaluate the quantities $S^\pm$ and $E\pm$ using the relevant geomagnetic data for Durham. The appropriate correction factors for geomagnetic deflection $g\ (E_\mu)$, weighted by energy and zenith angle are presented in table 5.1 together with the mean energy at production calculated using the energy loss expression of Hayman et al. (1963) and the final ratios at production. Because the assumption of a unique level of production is too crude and R_p is more rapidly varying with energy, the appropriate correction factor for the lowest energy cell, i.e. $E_\mu \leq 5$ GeV is not available.

The final ratio at production, as a function of energy at production, is shown in fig. 5.1. The most noticeable feature is the appearance of a maximum in the energy region 50 - 100 GeV; this will be discussed in some detail in the next section. There is also an indication that the ratio falls to unity above 1000 GeV, although

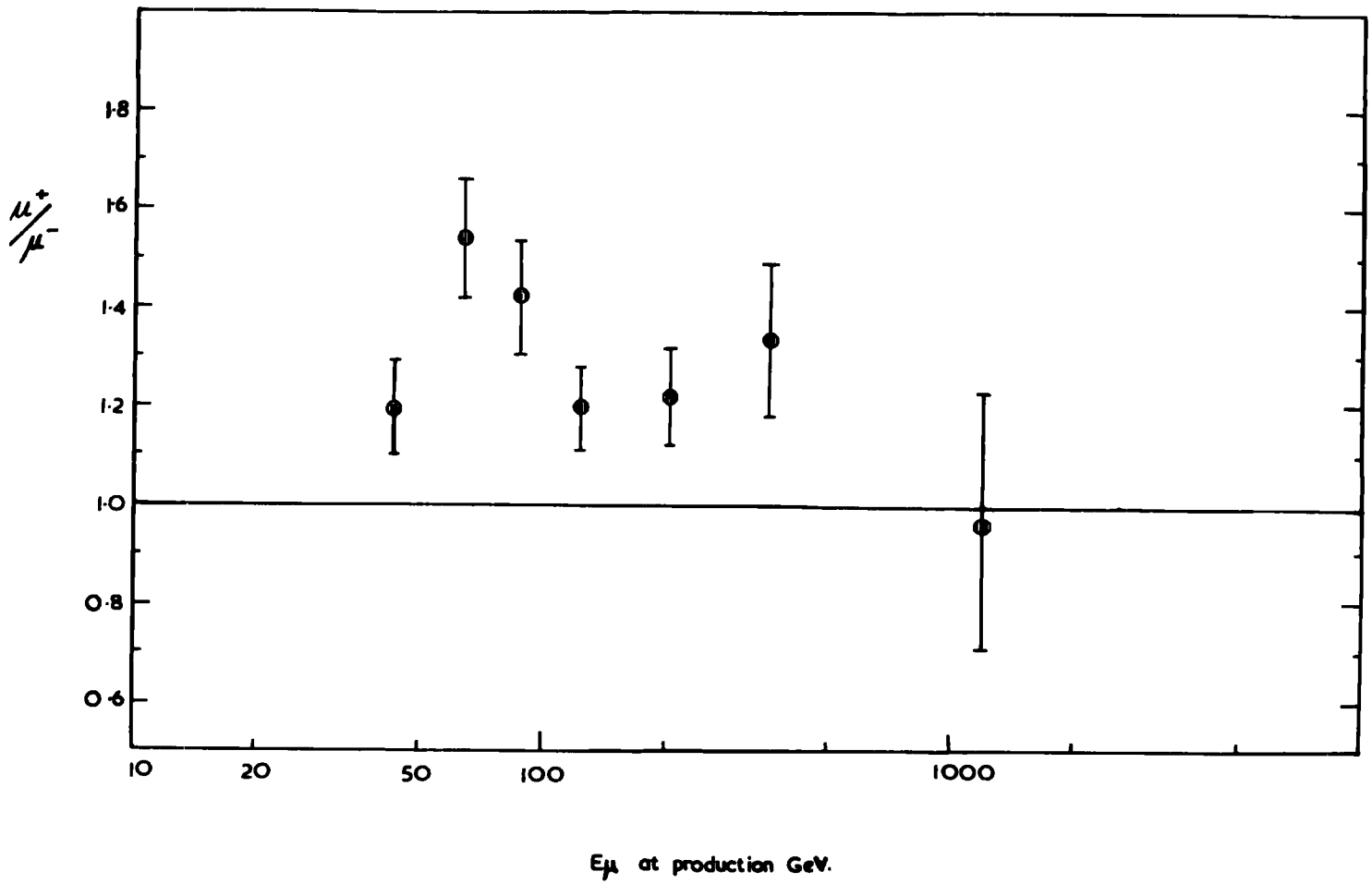

Fig. 5.1 The corrected charge ratio as a function of energy at production

the statistics are poor in this region.

5.4 Comparison with other data

The results of the present work are compared in fig. 5.2 with a collection of most of the previously published results on the muon charge ratio surveyed by MacKeown (1965) (see references for a list of the relevent authors). Some of the previous results at large zenith angles, Ashton et al.(1963b), and Kawaguchi et al. (1965) indicated the existence of a minimum in the charge ratio in the energy region 50 - 100 GeV. Apparently, the present result and the preliminary ones given by MacKeown et al. (1965b) and later by MacKeown (1965), in showing a maximum in the same energy region i.e. 50 - 100 GeV, are certainly not consistent with regard to existence of a minimum in this region reported by the workers cited above.

It was thought that the appearance of the maximum in the present result is a zenith angle effect, i.e. the maximum will be pronounced when θ increases, since most of the data in the present work come from the extreme zenith angular range, namely $85^{\circ} - 90^{\circ}$, while in the other results for large zenith angle, Kawaguchi et al.(1965) ($\theta = 78^{\circ}$) and MacKeown et al.(1963b) ($\theta = 77.5^{\circ} - 90^{\circ}$, MK1 experiment), most of the data come from lower angular range $\theta < 85^{\circ}$. This fact is also clear when all data for $75 \leq \theta \leq 90$ are combined (as will be mentioned in the next section) then the maximum disappears and a rather constant ratio appears in that energy region as shown in fig. 5.3, where the combination (including the present result) is compared with the present result.

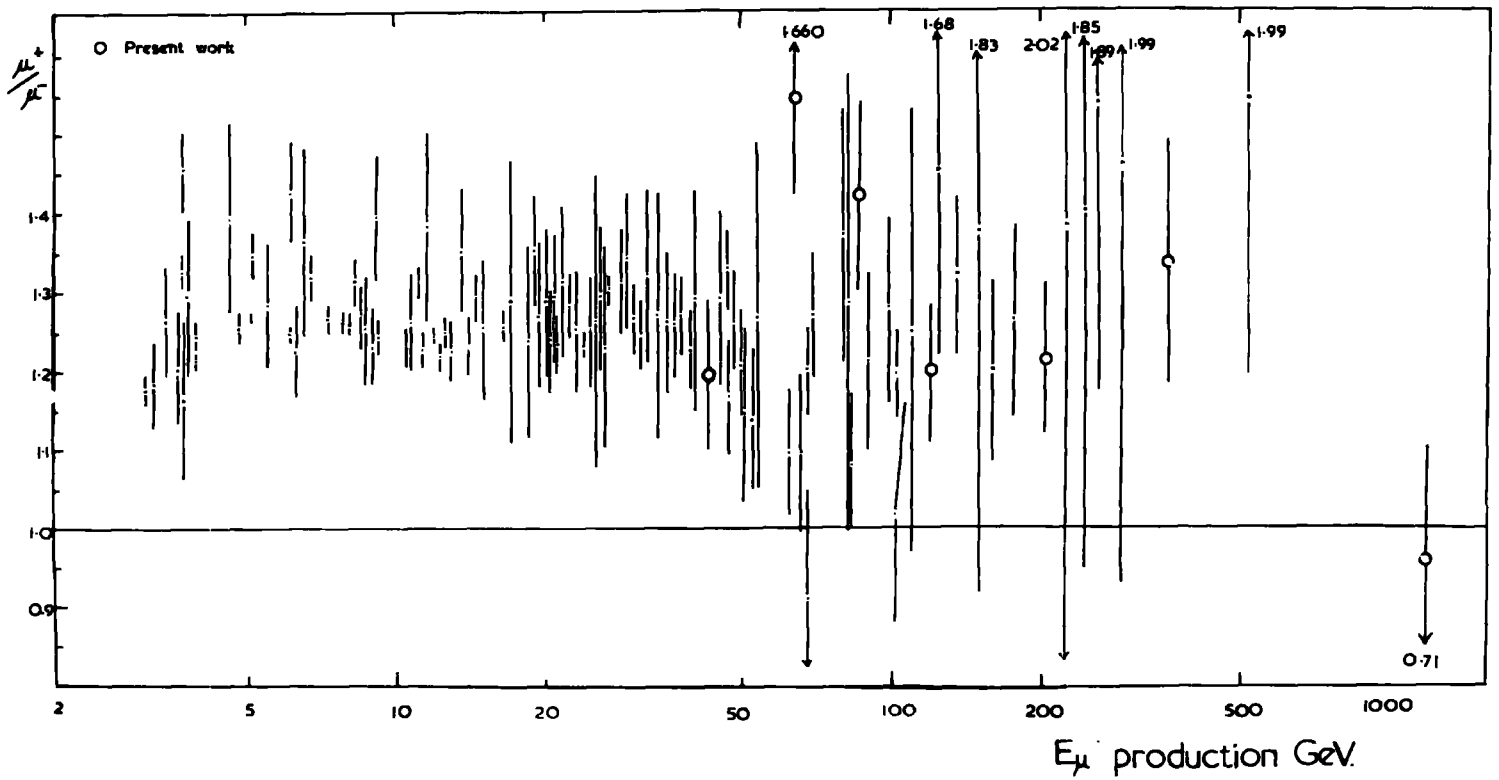

Fig. 5.2 Comparison of the present work with the World survey on the charge ratio after MacKeown (1965).

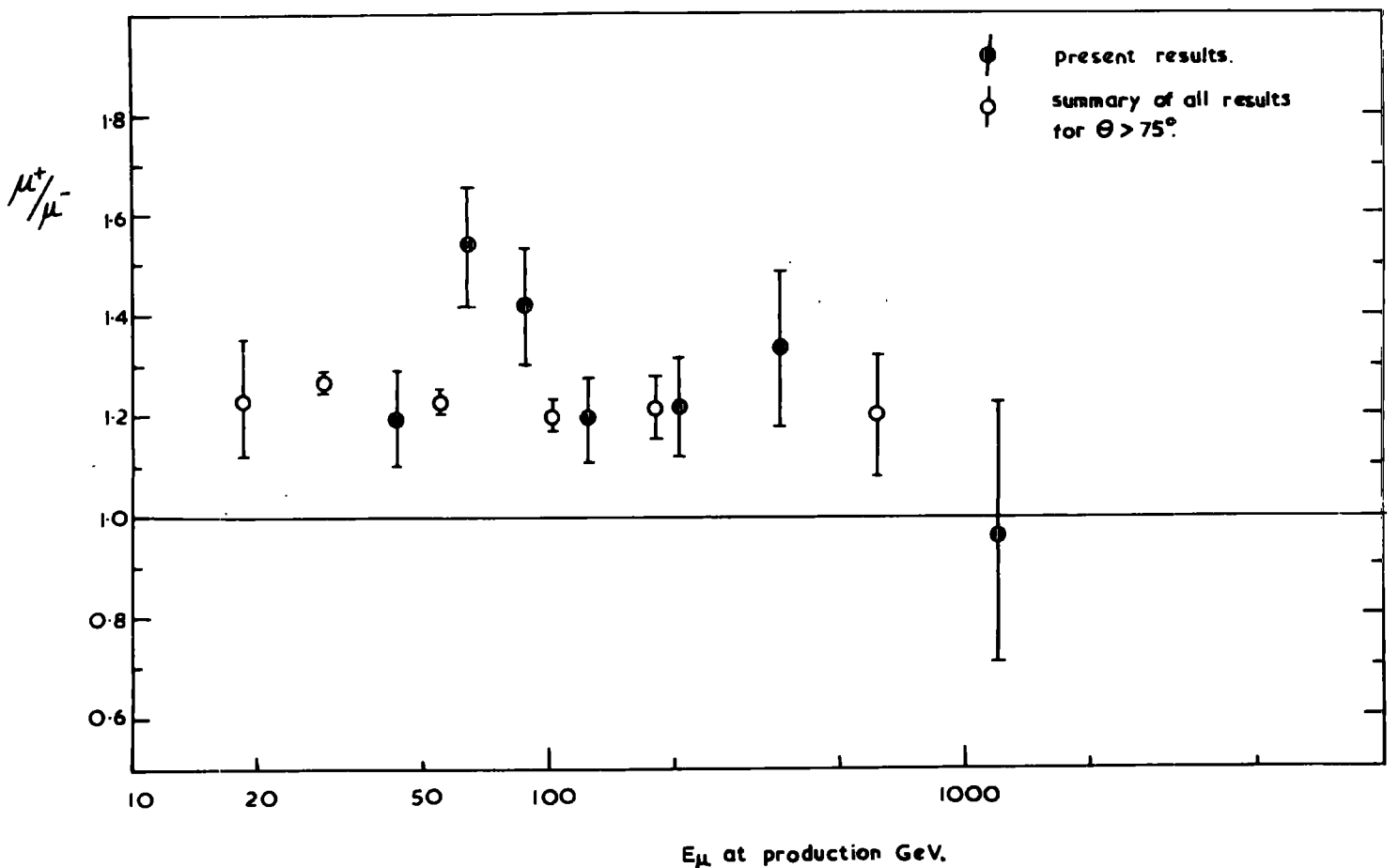

Fig. 5.3 Comparison of the present work with the summary of all results for $\theta > 75^{\circ}$

This is so because the data in this combination for $85^\circ \leq \theta \leq 90^\circ$ are statistically much weaker than for $75^\circ \leq \theta \leq 85^\circ$, with the latter showing no pronounced maximum but rather constant, or a minimum instead in some of the data. Therefore, the apparent discrepancy shown in fig. 5.3 between the present result and the summary should not be taken as it stands for the same reason given above.

As a further check on the zenith angle effect of the appearance of the maximum, all available data for large zenith angle measurements ($77.5^\circ \leq \theta \leq 90^\circ$) have been grouped into zenith angular cells of 2.5° i.e. $77.5^\circ - 80^\circ$, $80^\circ - 82.5^\circ$ etc., and it was found, as shown in fig. 5.4, that there is slight evidence for a maximum for the cell $77.5^\circ - 80^\circ$ while the maximum is not apparent for the cells $80^\circ - 82.5^\circ$ and $82.5^\circ - 85^\circ$ — this may be due to statistics, but it becomes increasingly pronounced in the extreme two cells, having a value of ~ 1.5 for $85^\circ \leq \theta \leq 87.5$ and ~ 1.6 for $87.5^\circ \leq \theta \leq 90^\circ$. All these maxima correspond to the same muon energy at sea-level but to different energies at production because of the different paths that the muon will traverse for the different zenith angular cells.

The reason for the appearance of the maximum is not known despite strenuous efforts to explain it.

At high energies, $E_\mu \geq 100$ GeV, due to the considerable error in all available data one cannot say that there is disagreement between the various results.

What can be said, from fig. 5.2, is that, taken all together, the data are not very suggestive of a pronounced minimum or a maximum

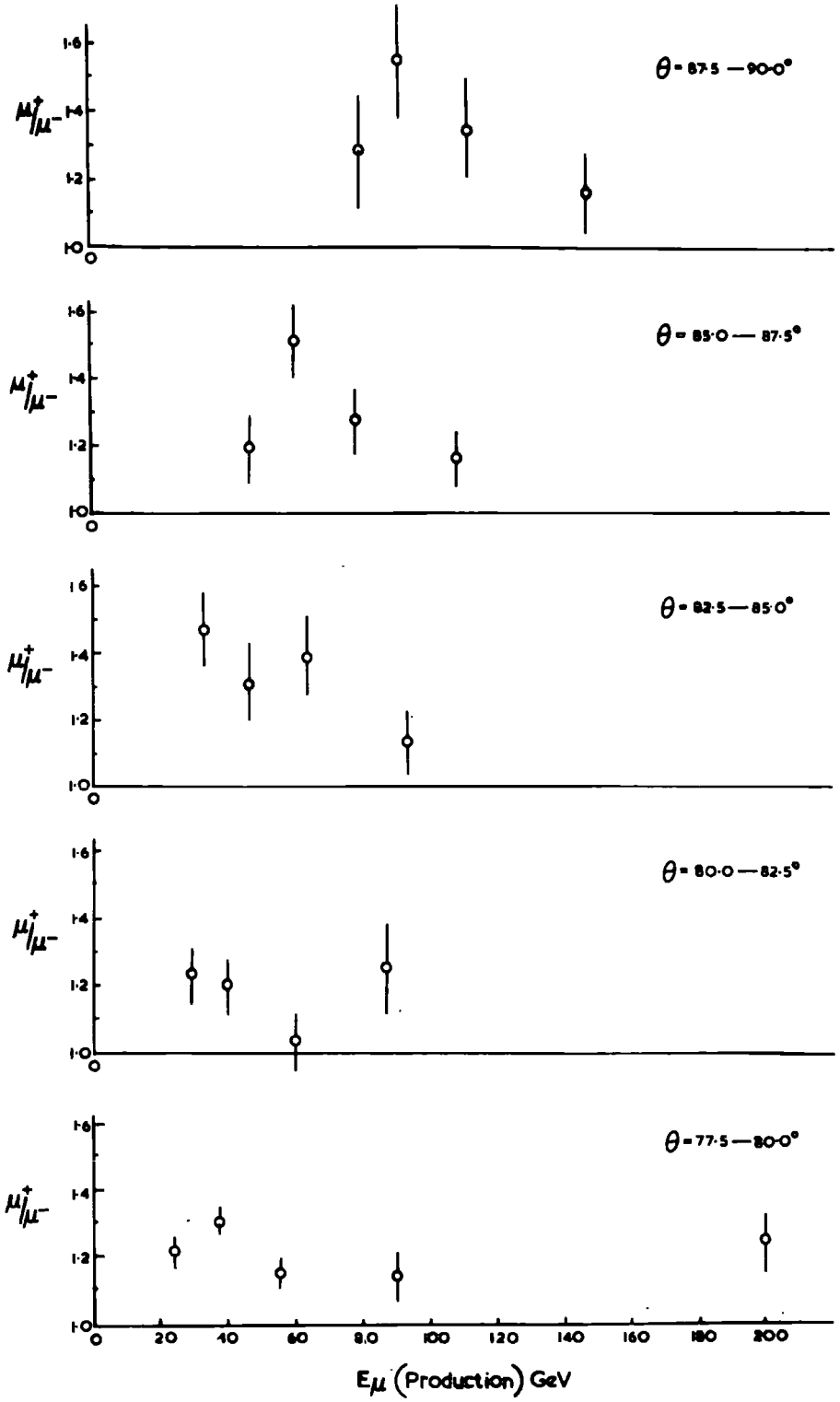

Fig. 5.4 The charge ratio maximum as a function of zenith angle.

in the charge ratio in the region 50 - 100 GeV for the whole angular range taken together, but that there appears to be fine structure which appears with increasing zenith angle.

5.5 The best estimate of the μ^+/μ^- ratio

In order to get a better picture of the energy dependence of the μ^+/μ^- ratio, the World Survey data of fig. 5.2 have been combined by MacKeown (1965) into energy cells at production. Bearing in mind the question of kaon production, i.e. to see if there is any dependence on zenith angle, the data have been further combined into two zenith angular ranges, namely, $\theta < 75^\circ$ and $\theta > 75^\circ$; the former cell consisting almost entirely of measurements near the vertical. In the other cell, $\theta > 75^\circ$, MacKeown (1965) included the preliminary results of the present work using the Mark II spectrograph, and later in the present work, the final results using this spectrograph have been used instead. In these combinations, as a consistency condition, it was demanded that all accepted points lie within three standard deviations from the mean in a cell, and as a result three points at low energies have been excluded from the summary. The points within each cell were combined by weighting each according to the inverse square on the quoted error i.e.

$$\langle R \rangle = \frac{\sum_i R_i/\sigma_i^2}{\sum_i 1/\sigma_i^2} \pm \left(\sum_i 1/\sigma_i^2\right)^{-\frac{1}{2}}$$

A point in the lowest energy cell for $\theta < 75^\circ$ by Filosofo et al. (1954)

has been plotted separately, indicated by F, because the quoted error on it was much smaller than on the other points in the cell. The chosen cells and the resulting means for the two zenith angular ranges are given in table 5.2 and the resulting points, as a function of the weighted mean energies at production are shown in fig. 5.5

It can be seen from fig. 5.5 that while low energy points are best established near the vertical, the high energy region is almost totally dependent on studies at large zenith angles. The dotted points in the range $\theta > 75^{\circ}$ represent the results given by MacKeown (1965) including the preliminary results using the Mark II spectrograph data , while the solid points represent the final summary for this range including the final results using the spectrograph data given in the present work. It can be seen that there is very little change in the summary and, therefore, the interpretations of the charge ratio examined, in detail, by the author cited above will still be valid. . .

The summary shows that the charge ratio remains remarkably constant over a very wide energy region $\sim 3 - 500$ GeV, and in the next section a brief discussion of the interpretation of this result will be given.

5.6 Brief summary of the interpretation of the μ^+/μ^- ratio

5.6.1 Introduction

The problem of interpretation has been examined in detail by

Table 5.2 The muon charge ratio as a function of zenith angle

E_μ prod. GeV	$\theta > 75^\circ$ No.of points	$\theta > 75^\circ$ $\langle E_\mu \text{ prod} \rangle$ GeV	$\theta > 75^\circ$ $R(\theta > 75^\circ)$	$\theta < 75^\circ$ No.of points	$\theta < 75^\circ$ $\langle E_\mu \text{ prod} \rangle$ GeV	$\theta < 75^\circ$ $R(\theta < 75^\circ)$	$\frac{R(\theta > 75^\circ)}{R(\theta < 75^\circ)}$
< 3				9*	2.72	$1.170 \pm .009$	
3-5				10	3.90	$1.215 \pm .007$	
5-10				21	5.78	$1.264 \pm .003$	
10-20	1	18.5	$1.235 \pm .120$	22	12.4	$1.250 \pm .006$	$.988 \pm .096$
20-40	9	29.1	$1.270 \pm .023$	21	26.4	$1.260 \pm .006$	$1.008 \pm .020$
40-80	8	55.0	$1.230 \pm .026$	8	54.9	$1.193 \pm .039$	$1.031 \pm .038$
80-160	6	102	$1.201 \pm .032$	7	101	$1.249 \pm .069$	$.961 \pm .059$
>160	7	213	$1.200 \pm .056$	3	244	$1.417 \pm .187$	$.847 \pm .118$
160-320	4	182	$1.216 \pm .061$				
>320	3	620	$1.200 \pm .120$				

* A point in this cell by Filosofo et al. (1954) (E_μ prod. = 2.90 GeV, $R = 1.212 \pm .001$) has been plotted separately because the quoted error on it is very much smaller than on any other point in the cell.

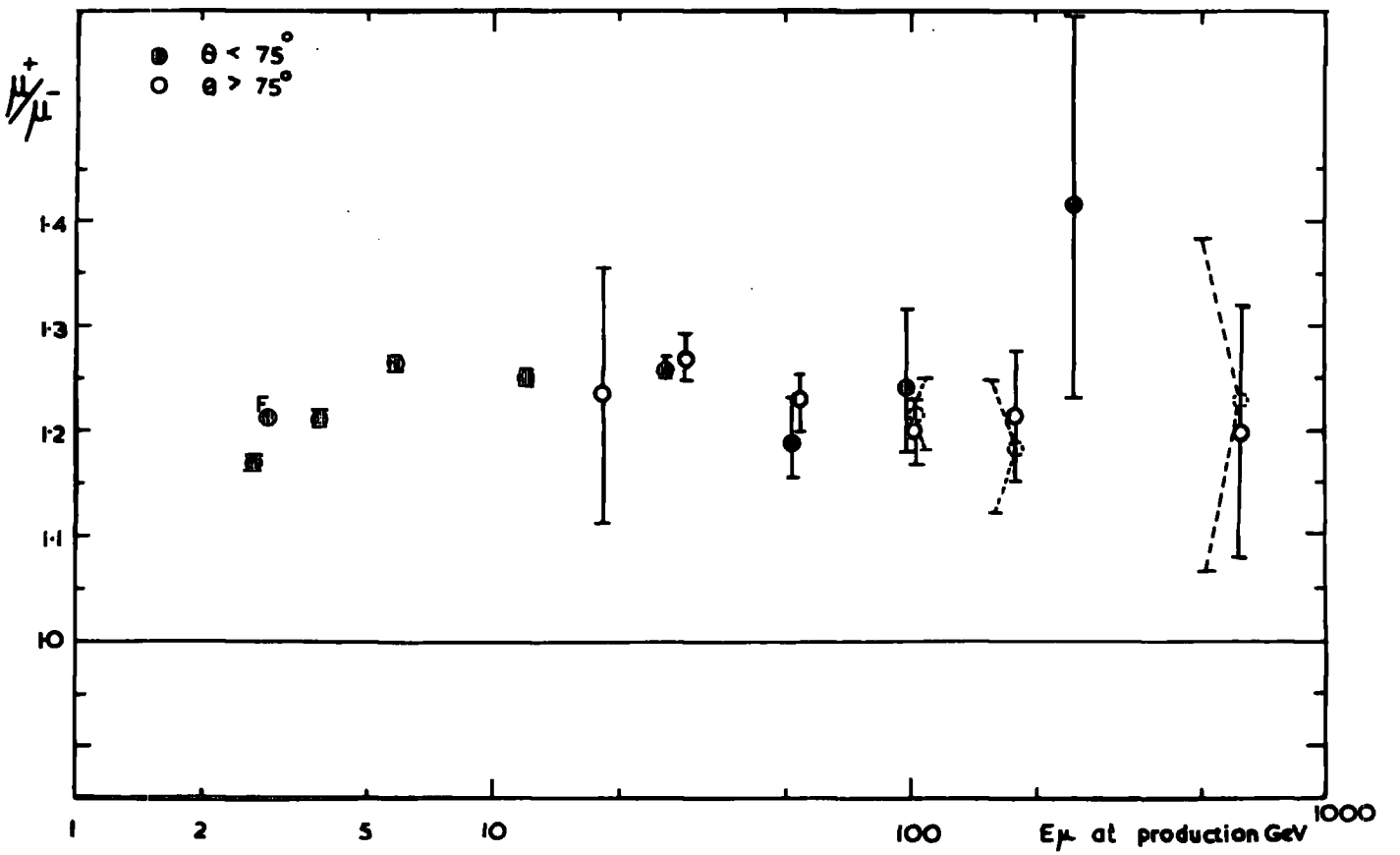

Fig. 5.5 A summary of all experimental data on the charge ratio divided by zenith angle, after MacKeown (1965), including the present work.

MacKeown (1965) and the present summary is based on the work of this author. The interpretation of the observed charge ratio requires a knowledge of three factors, (i) the properties of the primary radiation, i.e. its charge and particle composition and energy spectrum, (ii) the parameters which characterise the propagation in the atmosphere of the primary and secondary components, and (iii) the dynamical properties of the collisions between the primaries and air nuclei in the primary energy region of interest 10^{11} - 10^{14} eV. Since factors (i) and (ii) are reasonably well known, the interpretation of the charge ratio depends on our knowledge of the characteristics of high energy interactions in the energy region of interest. The predictions of the various models of particle production on the muon charge ratio will be discussed briefly in the following sections.

5.6.2 Pionization model

For the simplest case of this model of unique inelasticity and multiplicity at a given energy and taking pion multiplicity as varying as $E_o^{\frac{1}{4}}$, the resulting charge ratio, computed by MacKeown (1965), was found to be too small as shown by curve (a) in fig. 5.6.

It is known that fluctuation in multiplicity of produced pions may have a significant effect on the calculated ratio, provided the multiplicity and inelasticity are not positively correlated. MacKeown (1965) showed that the existing data on multiplicity are reasonably fitted by Polya distribution, though this distribution slightly

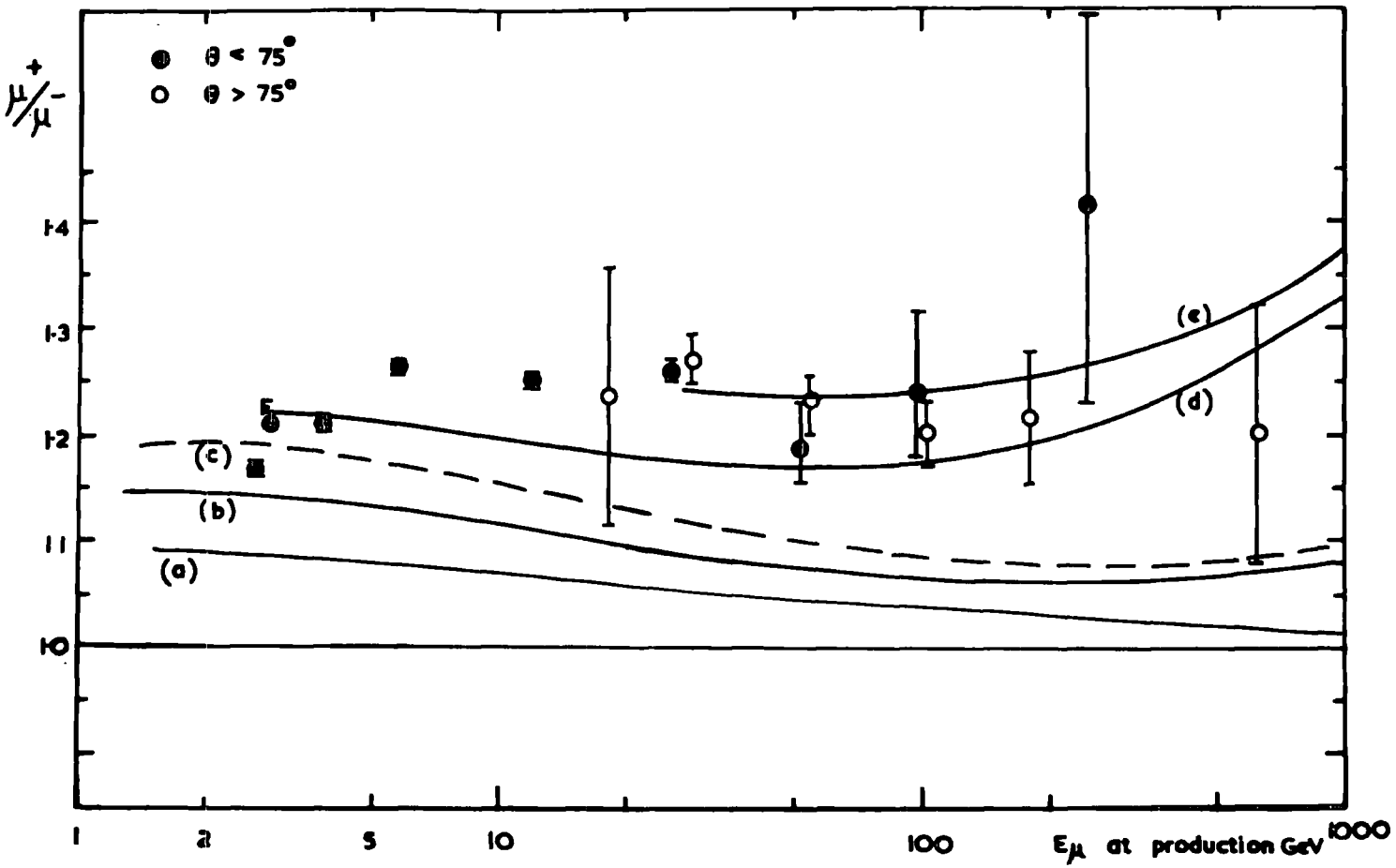

Fig. 5.6 Comparison of the observed charge ratio with the predictions (MacKeown 1965). (a) pionization with no fluctuations; (b) pionization with fluctuations; (c) upper limit to pionization; (d) pionization and kaons: $K^+/K^- = 4$, $K/\pi = 0.2$; (e) as (d) with $K/\pi = 0.5$.

underestimates the very low (and important) cases of $n_{\pi^{\pm}} = 1$ and 2. As a distribution in the inelasticity, the expression of Brooke et al. (1964a) has been adopted with $\langle K \rangle = 0.31$, and for the pion energy spectrum, an expression has been used which, when combined with the multiplicity and inelasticity distributions, results in the average exponential distribution derived by Cocconi et al. (1961), and known as the C.K.P. distribution. The resulting charge ratio computed in this way is shown as curve (b) in fig. 5.6.

As an upper limit on the ratio to be expected from this model the most favourable values of the parameters consistent with experimental data were used viz inelasticity $\langle K \rangle = 0.41$, exponent $\gamma = 2.8$ and exponent of the multiplicity law $\alpha = 0.24$, and the result is shown as curve (c) in fig. 5.6. It can be seen that the pionization model alone cannot explain the observed charge ratio.

It should be noted that more extreme fluctuation models have been considered by other authors, notably Grigorov and Shestoperov (1963, 1964) and these would give charge ratios in better agreement with experiment but, as yet, there is no experimental support for such models.

5.6.3 Models with significant kaon production

The effect of kaons on the charge ratio will be appreciable if their charge excess at production is large because those decay modes which give rise to muons directly play an important role at high

energies where pions are being preferentially removed by interactions. Assuming that the kaon production spectrum is parallel to the pion production spectrum, $K^+/K^- = 4$ independent of the nature of the primary nucleon and $F(K^{\pm}) = F(K^0 \overline{K^0})$, the excess from muons from kaon decay has been computed by MacKeown and added into the results obtained in § 5.6.2. The resulting value of μ^+/μ^- ratio at $\theta = 0^\circ$ for K/π ratio of 0.2 and 0.5 are shown as curves (d) and (e) in fig. 5.6 and it can be seen that under the above assumptions, a K/π ratio of about 0.5 would be needed to explain the observed charge ratio. This value of the K/π ratio is, at high momenta, consistent with the present work (Chapter 4), which gives a value for this ratio of 0.42 ± 0.20 for muon momenta at production of ≥ 100 GeV/C.

In principle it should be possible by examining the charge ratio as a function of zenith angle to distinguish between kaon and pion production. Thus, if there is a contribution to the charge excess from kaons having a large charge excess at production, the relative strength of muons from pion decay in diluting this excess will be greater at large zenith angles than at the vertical because of the higher energy at which pion interaction begins to compete with pion decay at these angles. The predicted ratio of the value of the charge ratio at a zenith angle of 80° to that of 0°, as a function of muon energy at production, is shown in fig. 5.7 for the values of K/π ratio of 0.2, 0.5 and 1. If the charge ratio is due to pion production alone, its

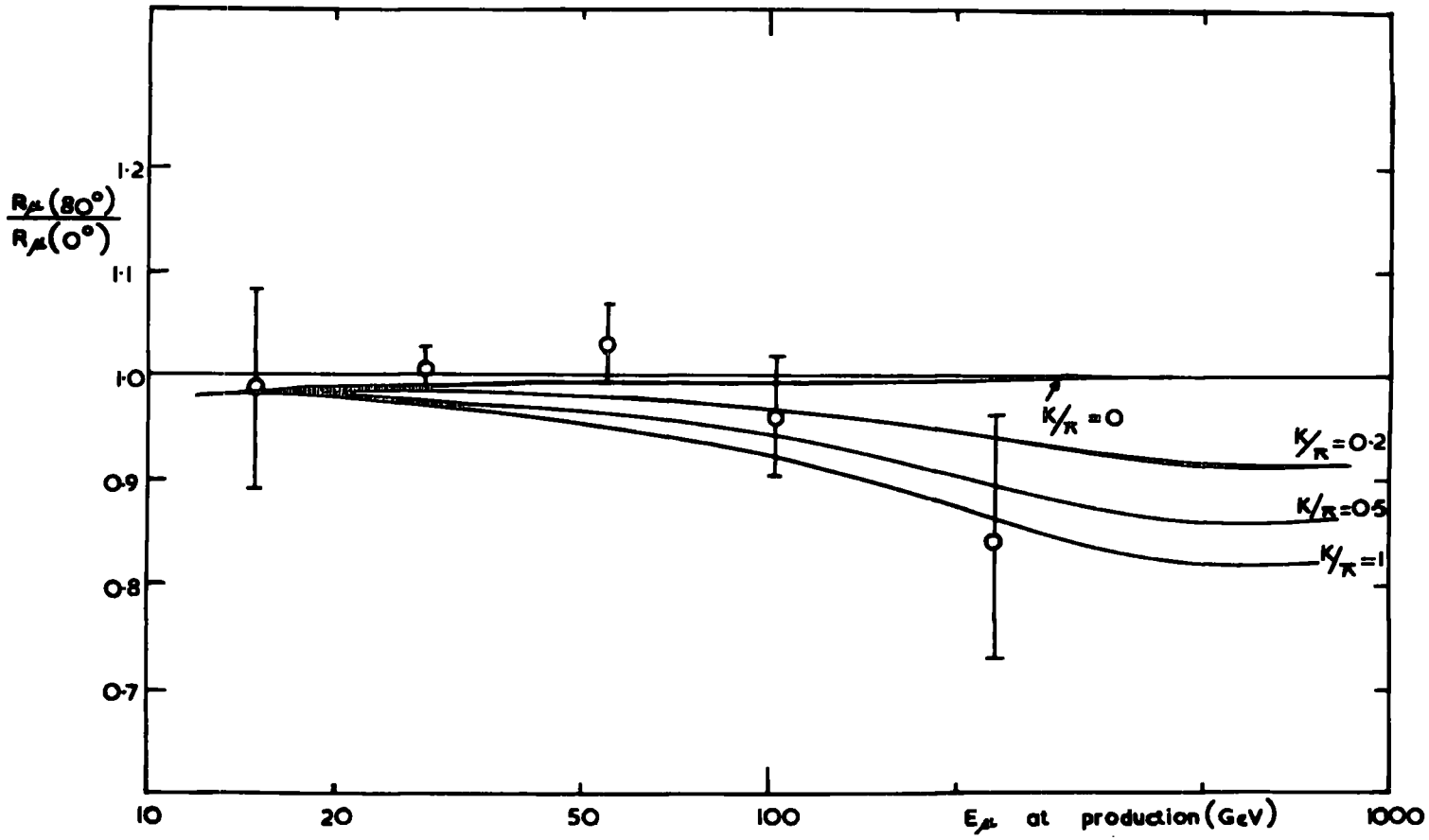

Fig. 5.7 The charge ratio at $\theta = 80^\circ$ relative to that at $\theta = 0^\circ$ for various K/π ratios, after MacKeown (1965); the experimental points refer to the ratios for $\theta > 75^\circ$ and $\theta < 75^\circ$ given in table 5.2

variation with zenith angles is negligible as shown in fig. 5.5, case $K/\pi = 0$. It is seen that some sensitivity to the K/π is predicted. Also shown in the figures are the experimental values for the ratio of $\mu^+/\mu^-(\theta > 75)$ to that of $\mu^+/\mu^-(\theta < 75)$ as given in table 5.2. These two zenith angular ranges correspond approximately to the theoretical conditions. A comparison shows that the results are at least not inconsistent with an explanation of the muon ratio in terms of kaon production and, in so far as the experimental result at the highest energy is depressed somewhat, there is some slight evidence favouring kaon rather than pion production.

5.6.4 Isobar models for particle production

The excitation of nucleon isobars will have a significant effect on the muon charge ratio and particular cases having been treated by Ramana Murthy (1963), and Pal and Peters (1964). MacKeown (1965) has computed the charge ratio expected assuming the excitation of the $T = \frac{1}{2}$ isobars $N^*(1515)$ and $N^*(1685)$ with a constant cross-section of 3 mb in the forward cone and including the dilution from pionization as calculated in §. 5.6.2 and his result is shown as curve (a) in fig. 5.8; the dashed portion of this curve representing the effect of including a $K\Lambda$ mode for the 1685 MeV state with a branching ratio of 10%. If instead of a constant cross-section an energy dependent one varying as $1/\log E$ is used, a better fit to the points results as shown by curve (b) in fig. 5.8.

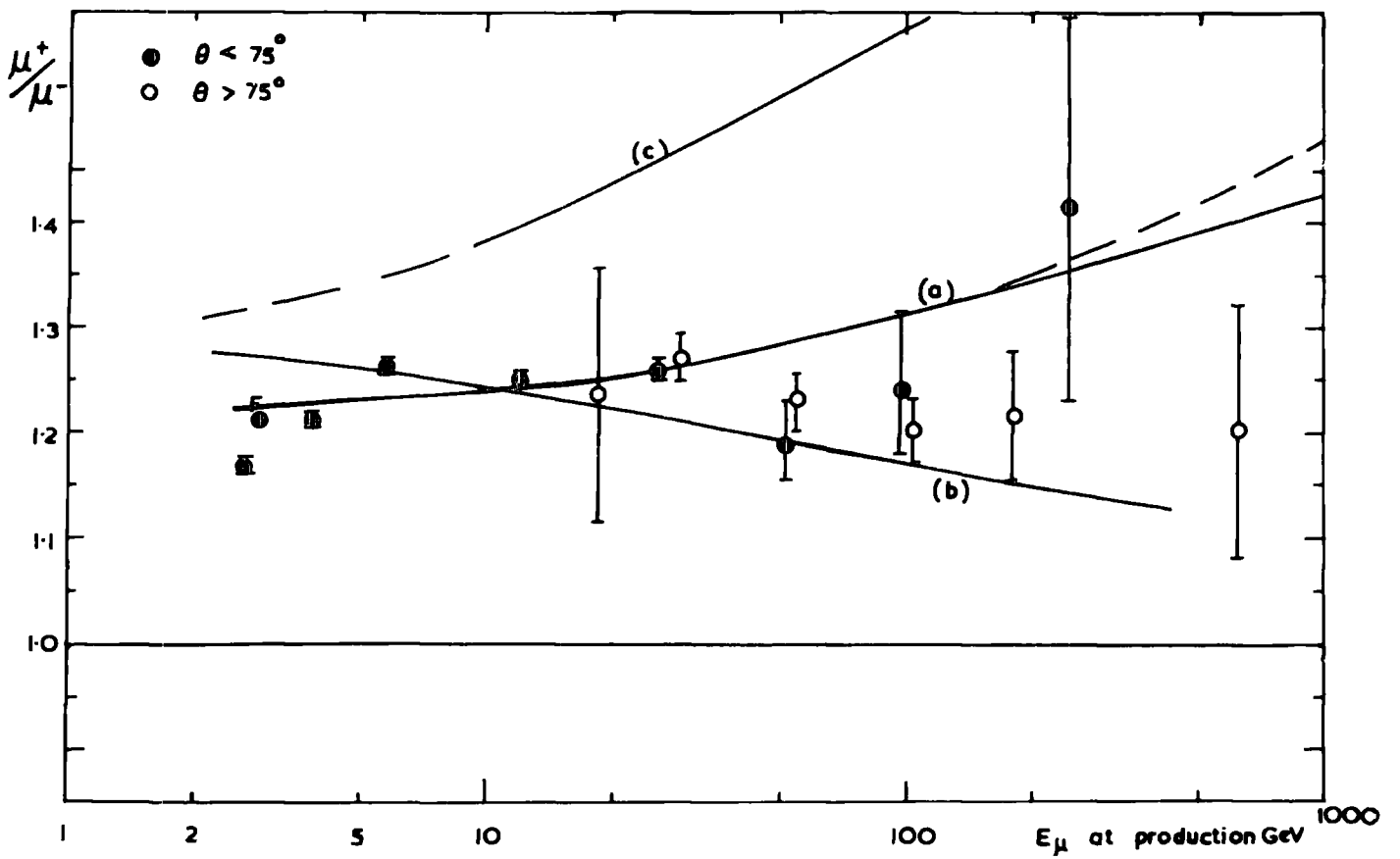

Fig. 5.8 Comparison of the observed charge ratio with the predictions (MacKeown 1965). (a) isobar production σ_i constant, 3mb, including pionization; (b) as (a) but $\sigma_i \propto (\log E_0)^{-1}$; (c) O.P.E. model.

5.6.5 The Peripheral Model

A particular version of this model is the one pion exchange (O.P.E.) model where single pion production is effected by the diffraction of a pion of the cloud of the incident nucleon at the target nucleon. Crossland and Fowler (1965) have followed up the earlier calculations of Narayan (1964) and have also found cross-section in the region of 2 mb for the production of single charged pion taking more than 20% of the energy. Such a cross-section would appear to give too high a charge ratio as shown by curve (c) in fig. 5.8. Further analysis of this process is required.

5.6.6 Conclusions

As mentioned before, the inclusion of the present result on the charge ratio did not change the summary given by MacKeown (1965) and the conclusion is that the ratio is constant (~1.20 - 1.25) over a very wide energy interval. In interpreting this behaviour it has been shown that pionization alone is insufficient but that models involving significant kaon or isobar production can provide the explanation. Kaon production (or isobar production is which kaon production is important in the ensuing de-excitation) appears to be slightly more probable. In addition to examining the zenith angle dependence in more detail, studies of the muon charge ratio in extensive air showers should also give information about the role of kaons due to the fact that if kaons are mainly responsible for the charge excess of single muons then the muon in E.A.S. should show also a charge

excess, but if pions are responsible the excess should be very small.

CHAPTER 6

Results on muon interactions

6.1 Introduction

One of the objects of the present work was to examine the nature of the particles (which we have hitherto assumed to be muons) under examination at large angles. This chapter deals with studies of particle interactions from the point of view of identification of the particles.

In the process of analysing the photographs of single muon events for the purpose of momentum measurements of muons (Chapter 3), cases in which the muon produces what is presumably an electron in one or more of the five flash tube trays or in either or both iron magnets were noted. Similarly, cascade showers were observed to be initiated in the magnets.

Having in mind the suggestion made by Vernov et al (1965) that the results they obtained could indicate the possibility of the existence of the so-called X - particles which have greater penetrating power than ordinary nuclear-active particles but less than muons, it was decided to analyse the events showing particle interaction to check on the possibility of the near-horizontal muon beam being contaminated by these so-called X - particles. Such a study is possible because the great mass of the atmosphere in the near-horizontal direction will absorb

almost all the ordinary nuclear-active (π and P) and in addition the two iron magnets used in the present experiment will filter the remaining very low flux of these particle. But if there is an appreciable flux of X - particles mixed with the muon beam, they will produce a type of interaction in the components of the spectrograph which is different from that of the muon interactions. Therefore, the purpose of the analysis is to try to interpret the results in terms of the known muon interactions and in the case of finding an anomaly in the results, to examine the possibility of interpreting it in terms of X - particles.

6.2 Basic data

The interaction events were grouped into five categories according to what was observed, as follows:

1) Single electron produced in any one of the five flash tube trays.
2) Double electron produced in any two of the five flash tube trays.
3) Single electron produced in either of the two iron magnets.
4) Double electrons produced in both magnet.
5) Cascade showers produced in either of the two magnets.

the five categories are illustrated in fig. 6.1, where A, B, X, C and D are the five flash tube trays and I and II are the two magnets.

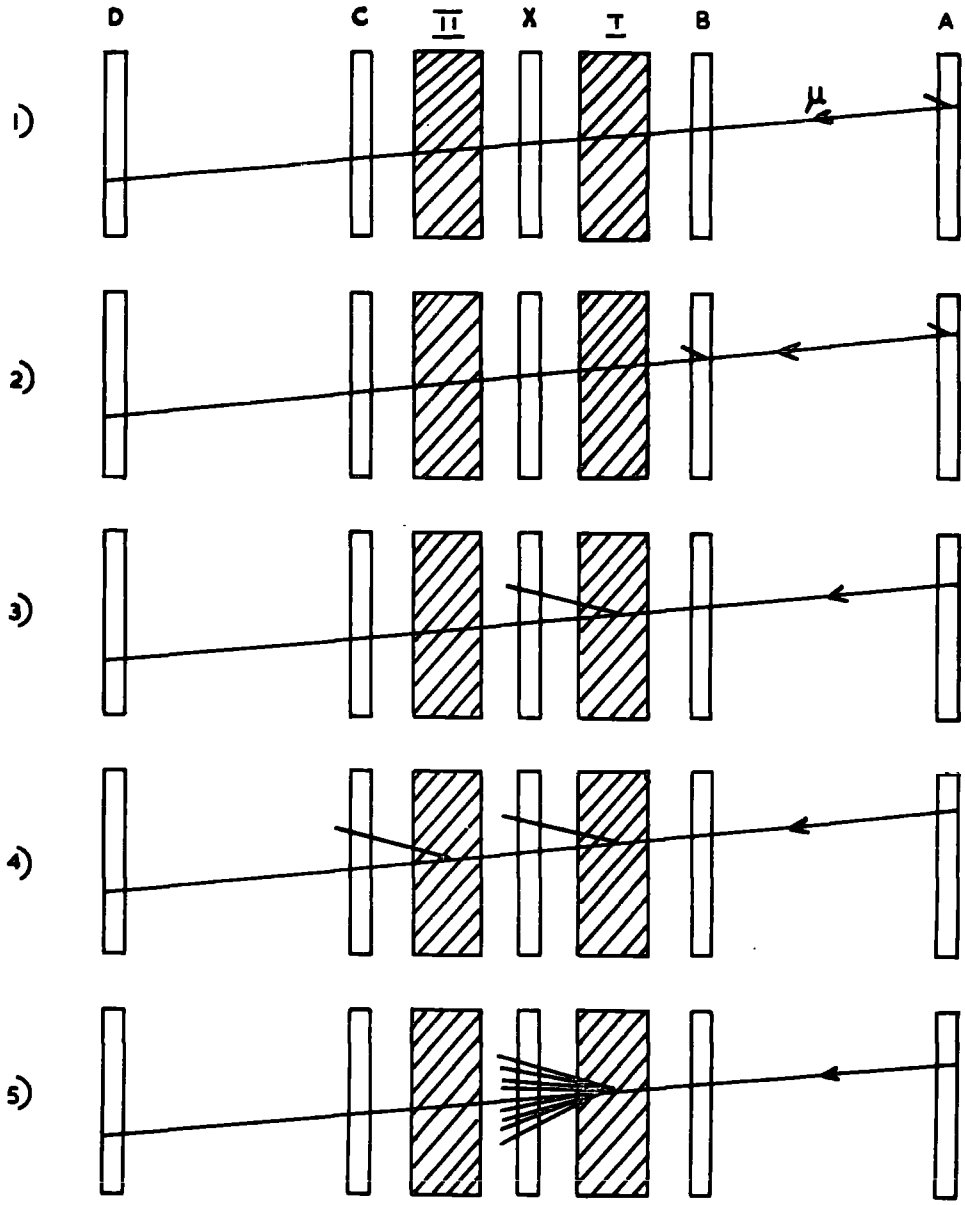

Fig. 6.1 An illustration of the interaction categories.

A track was considered as due to an electron when it was composed of two successive flashed tubes corresponding to an energy loss of ~ 3 MeV. A case was considered as a shower when the number of electrons produced in the shower was two or more. An electron produced in the magnet means a track that is seen in the flash tube tray which succeeds the magnet (e.g. tray X that succeeds Magnet I) and appears to originate in the magnet, while an electron produced in a tray simply means a track that is seen in the tray and originates within the boundary of that tray. The case of cascade showers produced in the magnet is similar to that of a single electron produced in the magnet, but instead of seeing one track in the case of single electrons one sees a number of tracks.

6.3 Variation of interaction probabilities with energy

The events of the various categories were grouped into muon energy cells and the interaction probabilities, i.e. the ratio of the number of particles that produce the interaction in a certain energy cell to the total number of particles in that cell, were obtained for the various categories. The results of categories 1) to 4) are given in table 6.1a, while those of category 5) are given in table 6.1b because of different energy cells used for this category from the others. The results of the five categories are shown in figures 6.2, 6.3, 6.4, 6.5 and 6.6 respectively.

Table 6.1a The probabilities % of a muon producing 1) single electrons in a tray, 2) double electrons in any two of the five trays, 3) single electrons in one magnet and 4) double electrons in both magnets

E_μ GeV	$\langle E_\mu \rangle$ GeV	1)	2)	3)	4)
< 9.8	5.7	$3.68 \pm .41$	$1.49^{+.90}_{-.60}$	$5.27 \pm .80$	$.22^{+.57}_{-.18}$
9.8–31	19.4	$3.54 \pm .26$	$.86^{+.40}_{-.27}$	$5.25 \pm .50$	$.29^{+.28}_{-.15}$
31–73.8	49	$3.50 \pm .26$	$1.13^{+.48}_{-.31}$	$7.02 \pm .57$	$.66^{+.35}_{-.24}$
73.8–215	118	$4.08 \pm .29$	$1.34^{+.50}_{-.35}$	$7.30 \pm .61$	$.82^{+.40}_{-.28}$
> 215	360	$4.08 \pm .45$	$1.42^{+.85}_{-.55}$	$7.79 \pm .96$	$.47^{+.60}_{-.31}$

Table 6.1b Probability % of a muon producing a cascade showers in one magnet (category 5)

E_μ GeV	$\langle E_\mu \rangle$ GeV	5)
< 9.8	5.7	$1.12^{+.50}_{-.35}$
9.8–20	14.2	$2.01^{+.55}_{-.45}$
20 – 31	25.3	$3.40^{+.70}_{-.60}$
31–51.3	39.8	$2.38^{+.54}_{-.36}$
51.3–73.8	62.8	$3.32^{+.77}_{-.65}$
73.8–215	118	$4.62 \pm .48$
215–500	282	9.40 ± 1.30
>500	700	$13.6^{+3.1}_{-2.7}$

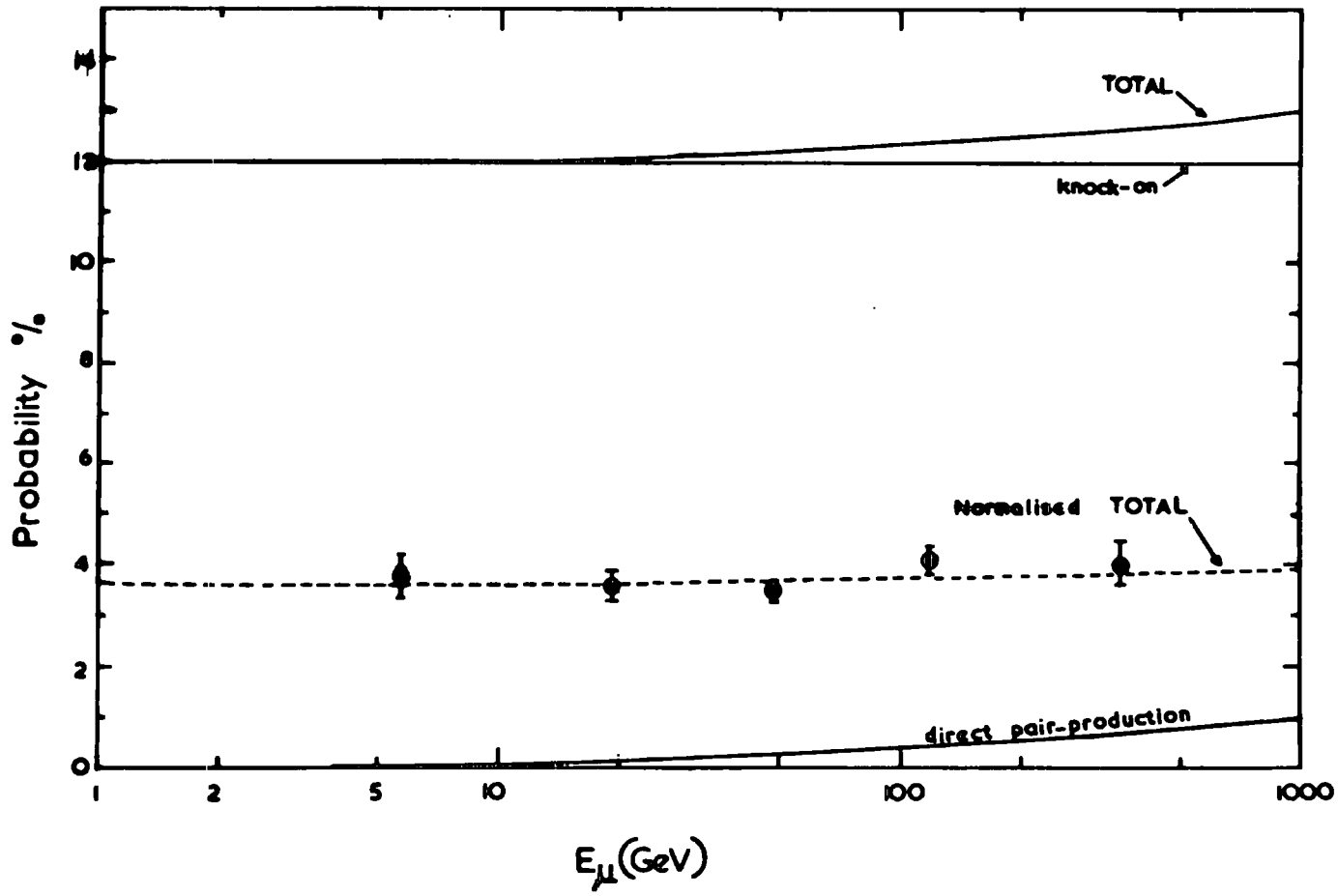

Fig. 6.2 Probability of a muon producing single electrons in a flash tube tray.

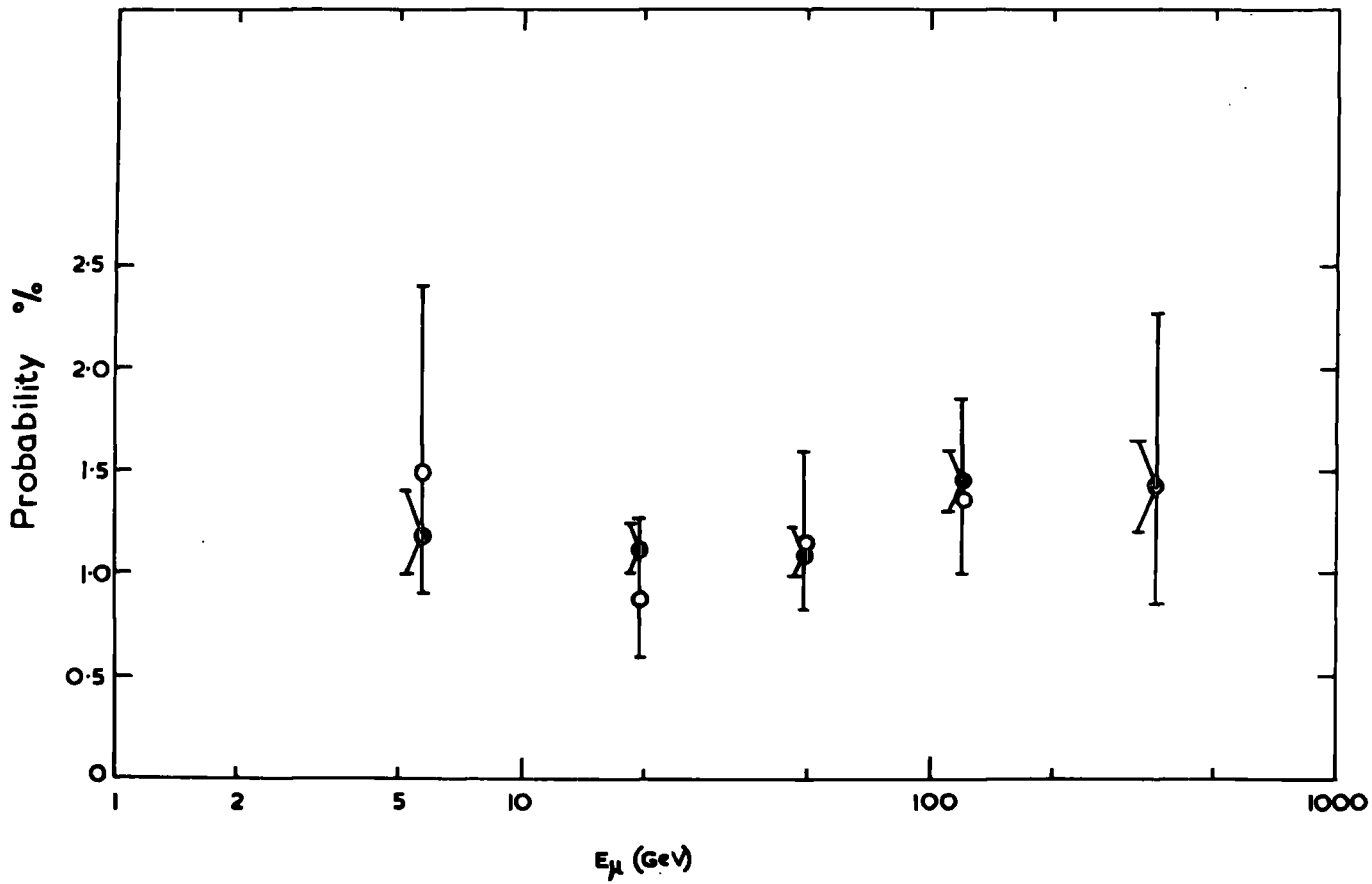

Fig. 6.3 Probability of a muon producing double electrons in any two of the flash tube trays; open circles: observed; closed circles: calculated from probability of producing single electrons in one tray.

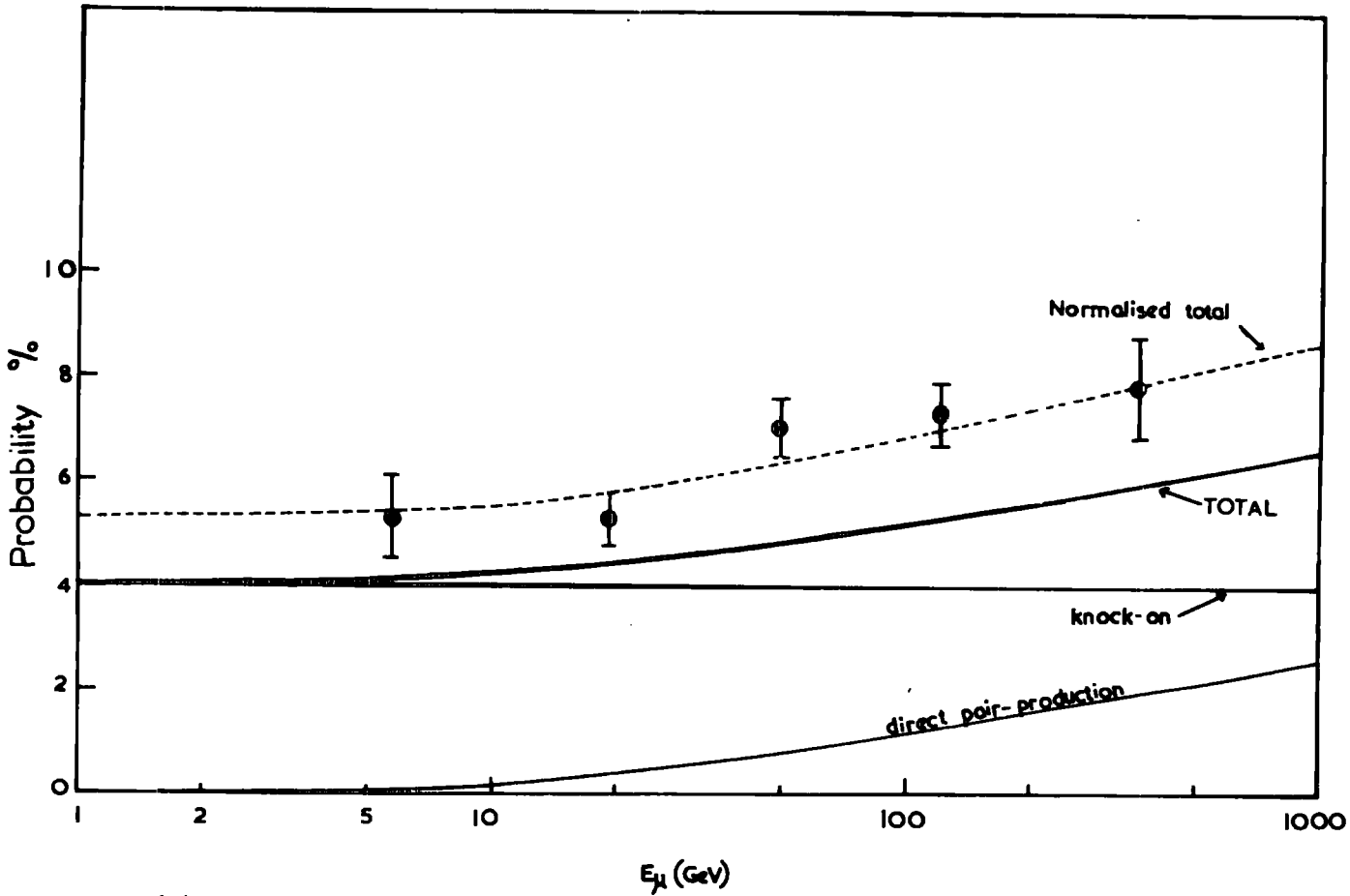

Fig. 6.4 Probability of a muon producing single electrons in the iron magnet.

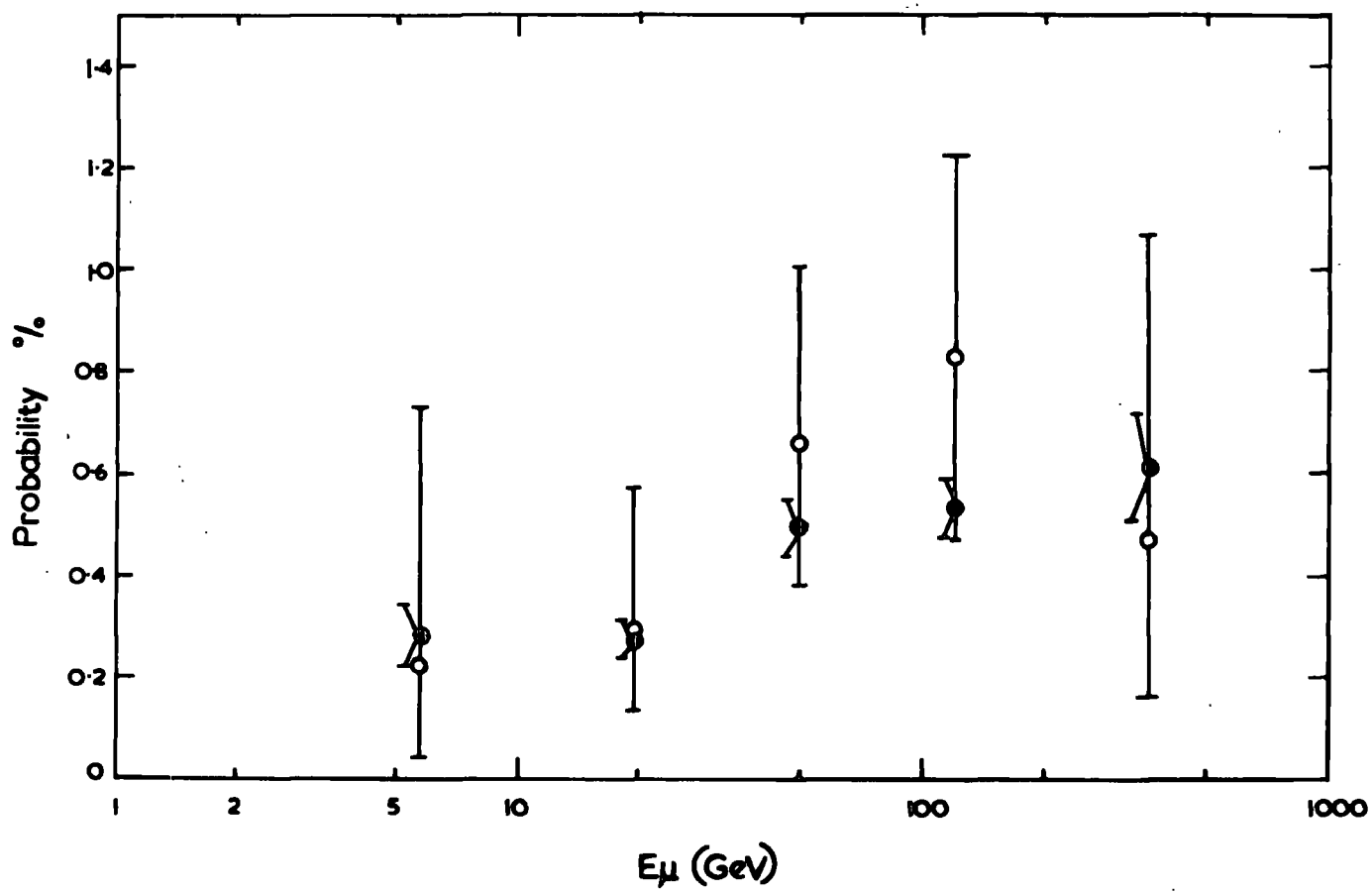

Fig. 6.5 Probability of a muon producing double electrons in both magnets; open circles: observed; closed circles: calculated from probability of producing single electrons in one magnet.

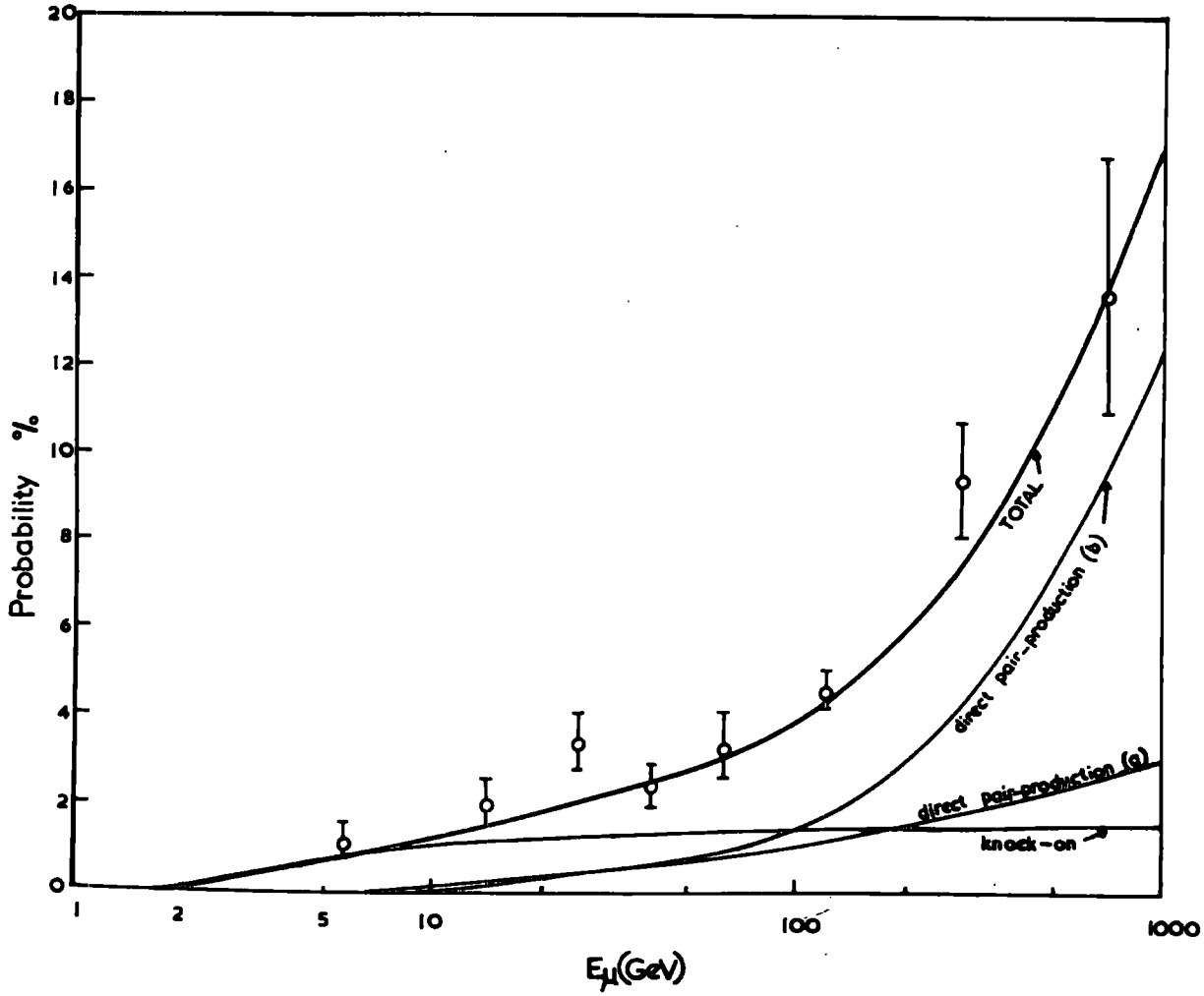

Fig. 6.6 Probability of a muon producing cascade showers in the iron magnet.

It can be seen that the probability of producing an electron in a tray is rather constant or varies very little with energy (fig. 6.2), that of producing an electron in the magnet increases slowly with energy (fig. 6.4) while that of producing a cascade shower in the magnet increases very rapidly with energy (fig. 6.6). In the next section an attempt is made to interpret these results in terms of the known electromagnetic interactions of muons.

6.4 Interpretation of the results in terms of muon interactions

6.4.1 Introduction

As is well known, the electromagnetic interactions of muon, and in fact of all charged particles, are of four types, namely i) the knock-on process in which the muon knocks an electron from the target atom, ii) bremsstrahlung which is the radiation emitted when the muon is accelerated in the coulomb field of the target nucleus, iii) direct pair-production which is similar to the bremsstrahlung except that an electron-position pair is produced rather than a photon and iv) the 'nuclear' interaction between the photons of the virtual photon cloud surrounding the muon and the target nucleus. Since, however, the cross-section of the last process is small compared with the other three processes for muon energies below 1000 GeV, this process was not considered in the present work. For the other three probabilities use was made of the results of Rogers (1965) who computed these probabilities using the theoretical expressions given by Bhabha (1938) for the

knock-on processes, by Christy and Kusaka (1941) for bremsstrahlung and by Murota et al. (1956) for the direct pair-production. Typical probability curves for these three processes, as a function of energy transfer, are shown in figures 6.7 and 6.8 (after Rogers (1965) for muon energies of 10 and 100 GeV. For the direct pair-production, the case where a minimum energy given to each electron of the produced pair of 2 MeV, was taken in the present calculations.

To calculate the probability of a muon producing a cascade shower in the iron magnet, use was made of the standard shower curves for iron obtained by Rogers (1965) from the experimental curves of Backenstoss et al. (1963). These shower curves, which include the incident muon, are shown in fig. 6.9 (after Rogers 1965) for incident electron energies of 1, 2, 3, 4 and 5 GeV.

The probabilities of the various categories have been calculated as follows.

6.4.2 Probability of a muon producing single electrons in a flash tube tray

Here we are dealing with the case of single electrons produced in a flash tube tray that is mainly composed of eight layers of glass tubes of wall thickness of 1 mm each and nine aluminium sheets (electrods), 1 mm in thickness, in between the tubes. This corresponds to a target of thickness of 6.75 g cm^{-2}.

A case was considered as an electron produced by muon interactions inside the tray when it caused the flashing of at least two

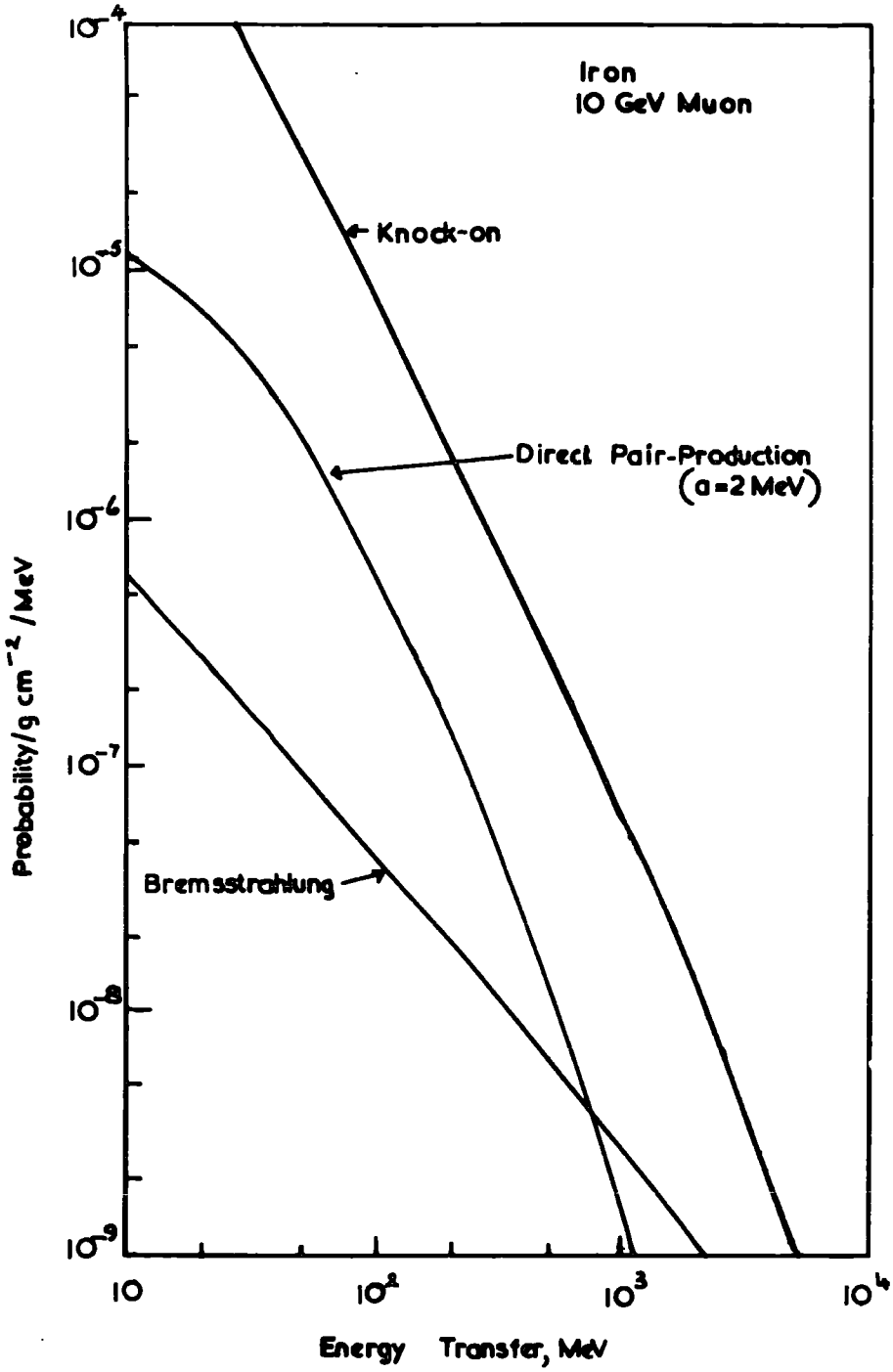

Fig. 6.7 Differential energy transfer curve for 10 GeV muons in iron, after Rogers (1965).

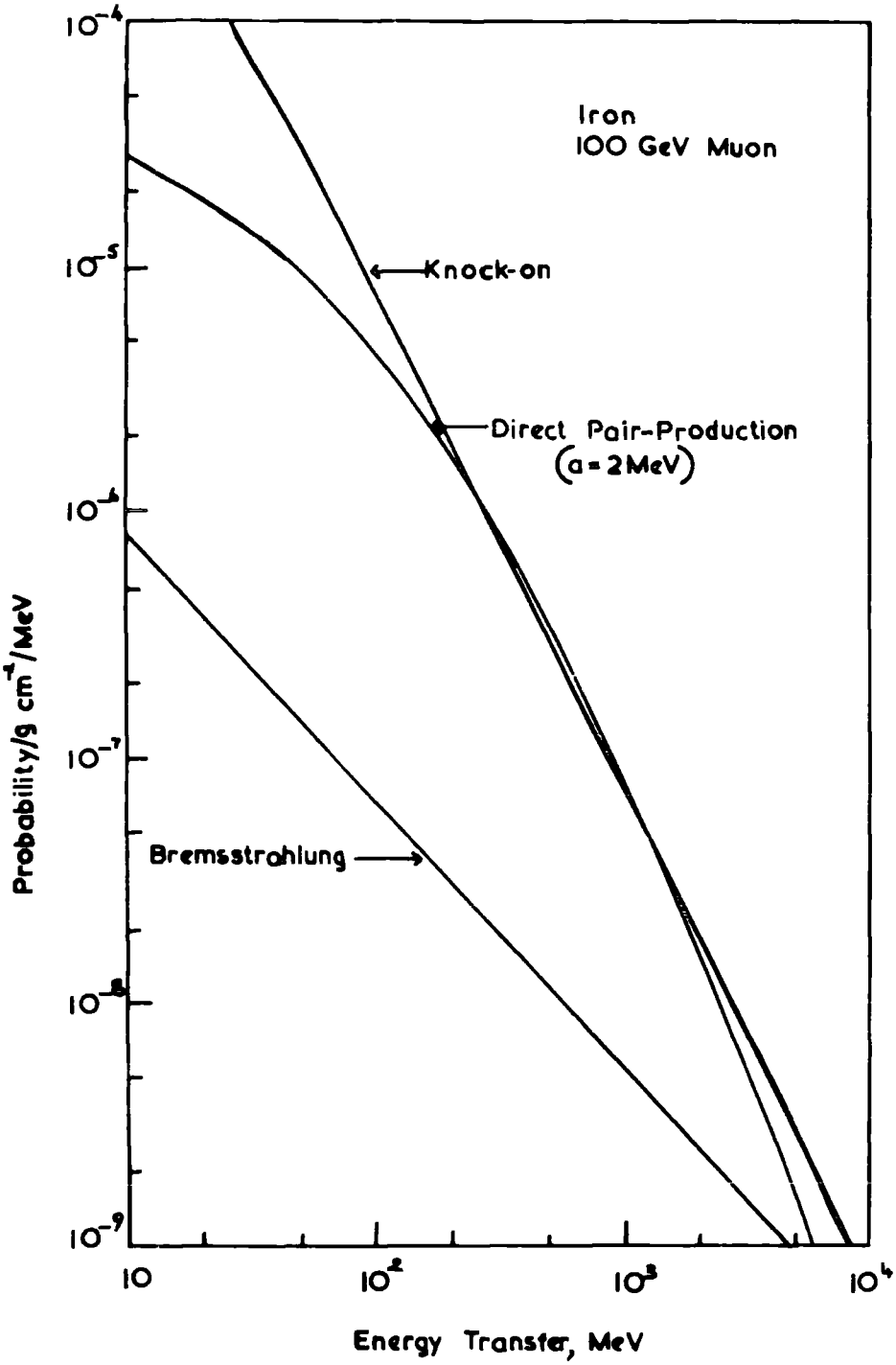

Fig. 6.8 Differential energy transfer curve for 100 GeV muons in iron, after Rogers (1965).

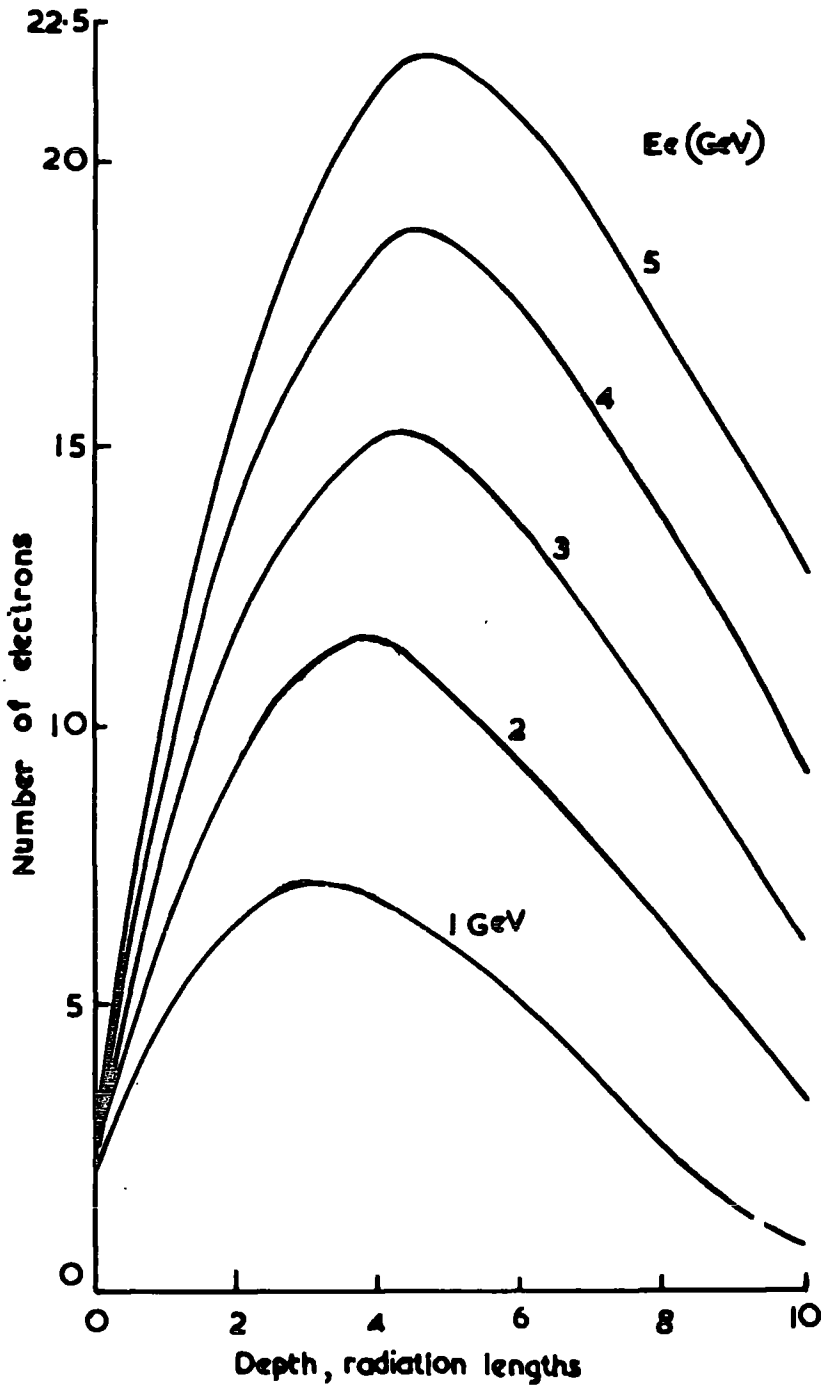

Fig. 6.9 Standard shower curves obtained from the experimental curves of Bachenstoss et al. (1963), after Rogers (1965).

adjacent tubes corresponding to a minimum energy recorded for the produced electrons of ~ 3 MeV. This limitation results in an effective target thickness of ~ 6/8th of the thickness of the tray, since electrons produced in the last 2/8th of the thickness of the tray were not recorded applying the above selection criteria. No limit on the maximum energy that the produced electrons can have, has been used.

The contributions from the knock-on and direct pair-production processes to the probability in question were then obtained by multiplying the probability values /g cm^{-2}/MeV for these processes (which are similar to the probabilities given in figures 6.7 and 6.8 for iron, but using the appropriate values of Z and A for the materials of the tray i.e. glass and aluminium) by the effective target thickness and then integrating the result with respect to the energy transfer between the limits 3 MeV and infinity for the knock-on process and 6 MeV and infinity for the direct pair-production assuming equal energies for the two electrons in the pair and that, on average, only one of the electrons from this process is observed. The resulting contributions are shown in fig. 6.2. The contribution from bremsstrahlung process was found to be negligible compared with the other two processes.

It can be seen that the predicted probability is much higher than the observed one and a normalization factor of 0.30 is needed

to get a fit with the experimental results. This difference is thought to be due to the fact that those produced electrons with very narrow projected angle with respect to the direction of the muon cannot be differentiated and will, therefore, be missed in the analysis. It is difficult to infer the number of these which are missed in this way, but the normalised result seems to fit very well the experimental points in showing that the probability is nearly constant. It is thus concluded that the experimental results are not inconsistent with those expected in terms of muon interactions.

6.4.3 Probability of a muon producing single electrons in the iron magnet.

The thickness of the magnet is 63.5 cm corresponding to 35.3 radiation lengths, but as an approximation it was assumed that the electrons that emerge from the magnet are produced within the last radiation length while those produced in the rest of the magnet are absorbed in it (the fact that the effective target thickness is not exactly equal to one radiation length will be removed later by normalisation). Thus, the contributions of the three processes, knock-on, bremsstrahlung and direct pair-production to the probability in question were obtained by simply multiplying the probability curves of figures 6.7 and 6.8 by the effective target thickness which was taken here as constant and equal to one radiation length, i.e. 13.8 g cm^{-2}, and then

integrating with respect to the energy transfer (it was assumed, as in the previous case, that, on average, only one of the electrons from the direct pair-production and bremsstrahlung processes emerged). The lower limit of the energy transfer was taken as 24 MeV (critical energy for iron) for the knock-on process and 48 MeV for direct pair-production and bremsstrahlung processes, assuming equal energies for the two electrons in the produced pair. The upper limit of energy transfer was assumed of a value of 500 MeV. The results are shown in fig. 6.4, together with the experimental points. The contribution from bremsstrahlung, being very small compared with the other two processes, is not shown in these figures.

It can be seen that the total contribution curves shows a similar general behaviour as the experimental points and when it is normalised to the weighted mean of the experimental points (dotted curves) the fit to the experimental points seems to be good. The normalisation factor was 1.31. The difference is thought to be due to the contribution from the other parts of the magnet than the last radiation length which was not taken into account in the calculations. The conclusion, therefore, is that the experimental results can be explained in terms of muon interactions.

6.4.4 Probability of a muon producing cascade showers in the iron magnet

The observed showers are initiated by electrons produced in the

two main processes, knock-on and direct pair-production. The contribution from bremsstrahlung was considered as negligible and so not taken into account. Calling the number of electrons contained in a shower N_e, the effective target thickness as a function of energy of the incident electron was obtained, using the standard shower curves of fig. 6.9, for the two cases $N_e \geq 2$ and $2 \leq N_e \leq 9$ with the results shown in fig. 6.10. The second case was taken as representing the type of showers observed here, in view of the adopted selection criteria and, therefore, calculations are presented only for this case, although it was found the results from the other case are not much different. The contributions of the two processes to the probability in question were calculated as follows:

i) Contribution from knock-on process

This was found by multiplying the effective target thickness given in fig. 6.10 by the knock-on probability values given in figures 6.7 and 6.8 and integrating over the energy transfer.

ii) Contribution from direct pair production

This contribution is thought as coming from two origins:

Case (a):

Here it was assumed that the two electrons in the pair have equal energy and that both electrons from those pairs which are produced within the last two thirds of a radiation length will

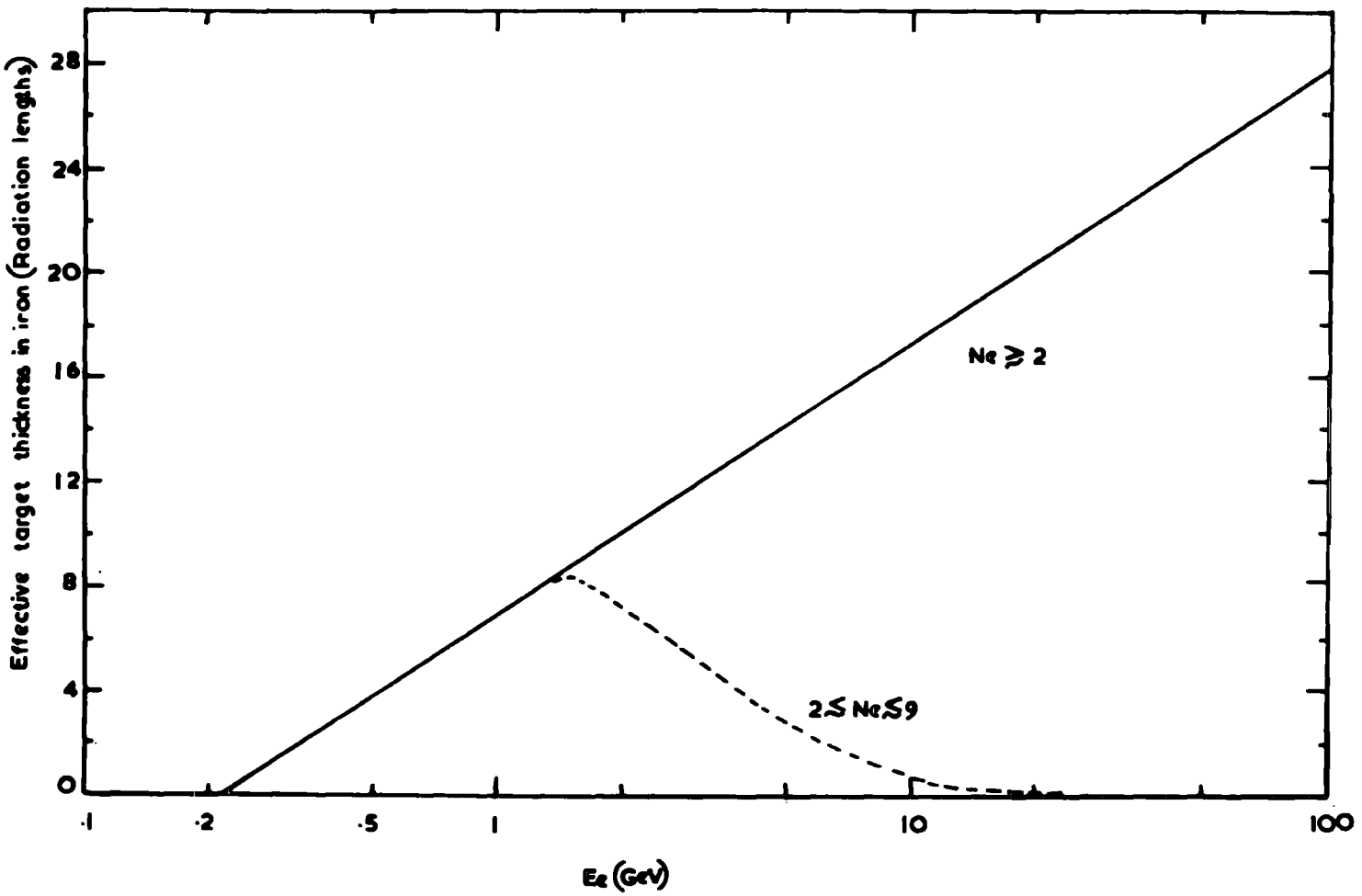

Fig. 6.10 Effective target thickness in iron as a function of energy of the incident electrons obtained via fig. 6.9.

emerge from the magnet and so contribute to the production of e showers since the minimum number of electrons in a shower was taken as two. The minimum energy (energy transfer) that the pair should have to traverse t g cm^{-2} of the target is given by $E_{min}(e^+ + \bar{e}) = 2t\,\varepsilon_o$, where ε_o is the rate of energy loss by an electron and was taken as constant and equals to 2 MeV g^{-1} cm^2. The above relation is plotted in fig 6.11 (dotted line) and is also shown displaced to a value of 10 MeV for pair energy because it was estimated that this value is that required, on average, by the pair to be seen in the flash tube tray succeeding the magnet. The contribution from this case to the probability in question was then obtained by multiplying the effective target thickness, given in fig. 6.11, by the probability values for direct pair-production given in figures 6.7 and 6.8 and integrating the result over the energy transfer.

Case (b)

In this case, the pairs are produced at any place in the magnet. This case can be thought as equivalent to the knock-on process case where we assume that one of the electrons takes half the pair energy and initiates a shower. It can be shown that the probability of producing these 'single' electrons in the pairs at a certain electron energy is equal to four times the probability of pair-production at the corresponding pair energy given in figures 6.7 and 6.8. After finding these probabilities the contribution of this case was calculated in the same way as that for the knock-on

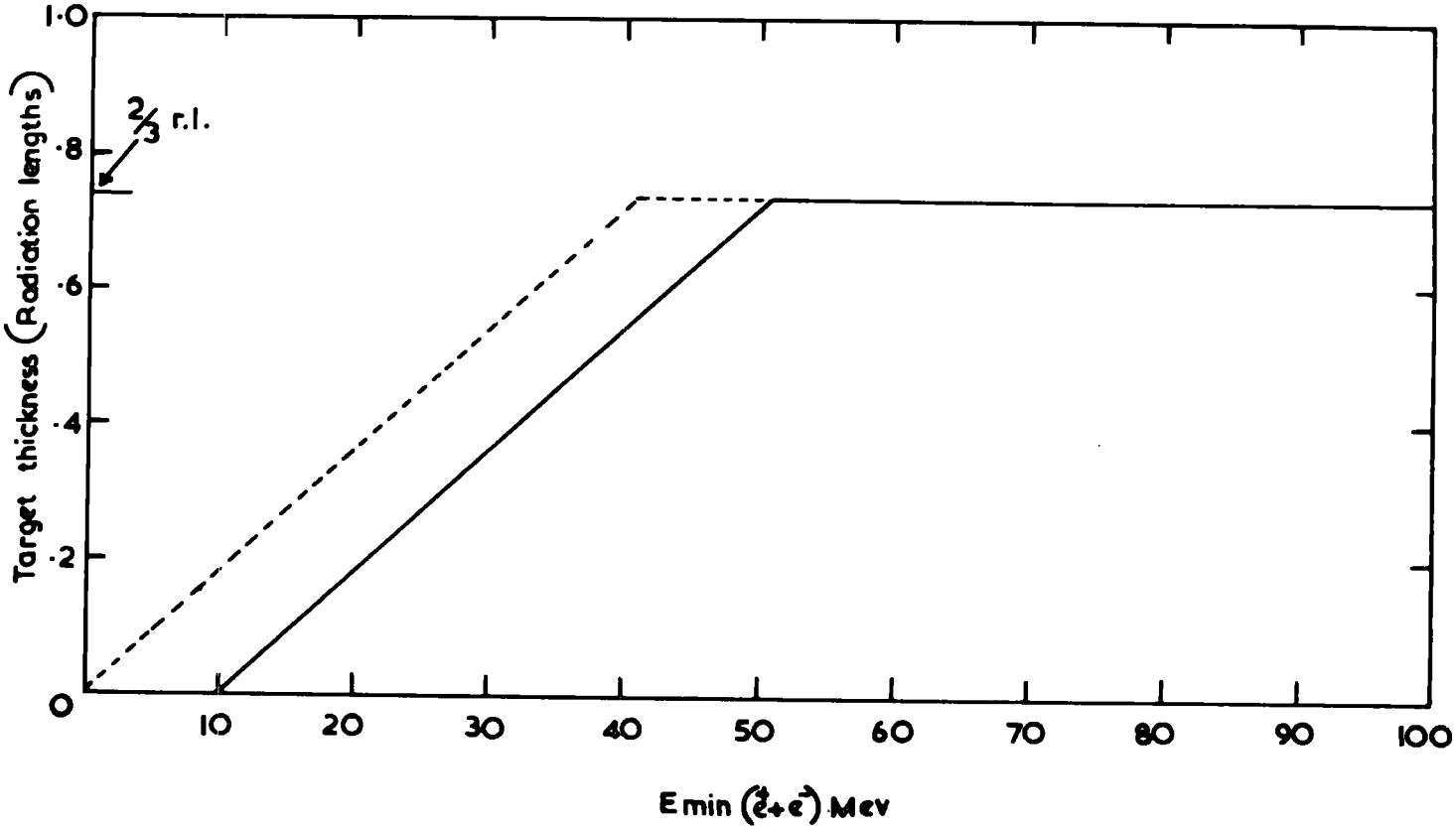

Fig. 6.11 Effective target thickness for pairs emerging from the magnet.

case, Case (i).

The contributions of all cases are shown in fig. 6.6 together with the total contribution. It is found that the total contribution curve accidentally passes through the weighted mean of the experimental pionts. It can be seen that this curve shows a good agreement with the experimental results indicating again that these results can be explained in terms of muon interactions.

6.4.5 Double electron cases

In the following the observed double electron cases are interpreted statistically in terms of their corresponding single electron cases. The idea behind this check was that if X - particles were present, having increased interaction, then the frequency of double electron cases would be excessive.

If the probability of producing single electrons by muons of certain energy in one object (in our case, in a flash tube tray or in a magnet) out of n ones is α_1, then the probability α_2 of producing double electrons in any two objects, one in each, out of the n ones is given by:

$$\alpha_2 = \alpha_1^{\,2} (1 - \alpha_1)^{n-2} \, C_n^2$$

where $C_n^2 = \frac{\lfloor n}{\lfloor n-2 \, \lfloor 2}$ is the number of ways of choosing 2 out of n. Using the above expressions, the expected probabilities of getting double electron for the two observed cases, namely, double electron in any two out of the five flash tube trays and double electron in

both magnets were calculated and are shown in figures 6.3 and 6.5 compared with the observed probabilities. It can be seen that the results agree within the statistical errors and that once more there is no evidence for an anomaly in these results indicating that here again there is no evidence for the existence of the so-called X - particle.

6.4.6 Conclusion

The overall conclusion from the interpretation of the observed results is clearly that these results could be explained in terms of the electromagnetic interactions of muons and there is no evidence from the present work for the existence of the so-called X - particles.

CHAPTER 7

Discussion and Conclusions

7.1 Properties of high energy nuclear interactions

Two studies reported in the present work, namely the muon momentum spectrum (Chapter 4) and the muon charge ratio (Chapter 5), both at large zenith angles, can give information on some of the properties of high energy interactions of the primary nucleons with air nuclei. By comparing the muon spectrum at large zenith angles with that at the vertical, some information can be obtained on the proportion of kaons to pions produced in these interactions, i.e. K/π ratio. Incidental to the momentum spectrum measurements is a determination of the charge ratio of the muon flux, a quantity much more sensitive to the properties of high energy interactions, which, if the charge composition of the primary radiation is known, can also shed light on the mechanisms of particle production at high energies.

It has been found in the present work (Chapter 4) that there is evidence of a contribution of kaons to the muon flux. For statistical reasons, the variation of the K/π ratio with energy could not be found and thus only an estimate of the average ratio has been made over a wide muon energy range at production 100-2000 GeV corresponding to the primary energy region of $\sim 3\ 10^3 - 10^5$ GeV. The estimate is $K/\pi = 0.42 \pm 0.20$ and this value is found to be

not inconsistent with previous ones obtained using the same method. The result has been included in the summary of all available results on the K/π ratio determined by other indirect and direct methods (see fig. 4.4). What can be said from the summary is that, if the mean energies of pions and kaons from individual interactions are in fact nearly the same, there is no evidence against a near-constant K/π ratio over a wide primary energy range, $10^2 - 10^6$ GeV and that the average value is 0.35 ± 0.20 over this energy range.

In the present work the determination of the muon charge ratio has been extended up to the highest energies yet attained, $E_\mu \sim$ 1000 GeV. The present result confirms the results of other authors (see fig. 5.2) on the existence of an appreciable charge excess up to energies of at least a few hundred GeV. The result suggests the existence of a maximum in the energy region 50-100 GeV, for muons at the largest zenith angles, a feature which is, apparently, not consistent with regard to the existence of a minimum in the same energy region reported by some other workers. When all available data on the charge ratio at large zenith angles have been combined into zenith angular cells, it is found that the maximum becomes more pronounced at extreme zenith angles (see fig. 5.4). The reason for the appearance of the maximum is not known despite strenuous efforts to explain it. At high energies, $E_\mu >$ 100 GeV, one cannot say, due to considerable errors in all the data, that there is disagreement

between the present result and other data and neither an increase or decrease in the ratio is ruled out. There is an indication from the present work that the ratio falls to unity above 1000 GeV, but again the statistics are poor in this region.

When all available data for the whole angular range (including the present result) on the charge ratio are combined into energy cells at production (fig. 5.5) the summary is not very suggestive of a pronounced minimum or a maximum in the ratio in the region 50-100 GeV; the summary shows that the ratio remains remarkably constant ($\sim$ 1.20 - 1.25) over a very wide energy region $\sim$ 3 - 500 GeV. The problem of interpreting this result has been examined in detail by MacKeown (1965). This author showed that pionization alone is insufficient but that models involving significant kaon or isobar production can provide the explanation. Kaon production (or isobar production in which kaon production is important in the ensuing de-excitation) appears to be slightly more probable. If, however, the ratio K^+ / K^- produced in high energy interactions remains at the value of 4 observed at machine energies, MacKeown has shown that a kaonisation process could give results in agreement with experimental results when the K/π is $\sim$ 0.50, a value which is consistent, at high energies, with the present result ($K/\pi = 0.42 \pm 0.20$ for $E_\mu > 100$ GeV). It is hoped that further information on the role of kaons will be obtained from a more detailed study of the zenith

angle dependence (§ 5.6.3), with good statistics at high energies, and from studies of the muon charge ratio in extensive air showers.

7.2 Presence of non-muons in the near-horizontal beam

In the present work (Chapter 6) the possibility of a contamination of the muon beam, incident in the near-horizontal direction, by other particles has been examined by studying the interaction of the incident beam. We had in mind the possibility of the contamination of the beam by the highly penetrating so-called 'X - particles' suggested by Vernov et al. (1965).

It was shown in Chapter 6 that the results on interactions could be interpreted in terms of the known electromagnetic interactions of muons and it was found that there was no anomaly in these results that could be attributed to the presence of appreciable flux of X - particles in the beam. The conclusion is, therefore, that one is really dealing with a pure beam of muons incident in the near-horizontal direction and there is no evidence from the present work (Chapter 6) for the existence of an appreciable flux of X - particles.

Confirmatory evidence against the presence of X - particles in the near-horizontal beam comes from the work of Ashton and Coats (1965 and private communications Sept. 1966) who studied burst

production in an iron absorber by high energy muons incident in the near-horizontal direction. These authors have found that their results do not indicate any deviation from the predicted behaviour of high energy muons up to muon energy of 600 GeV.

Another argument against the presence of a significant flux of X - particles is the agreement, reported in Chapter 4 of the present work, between the measured muon spectrum in the near-horizontal direction and that derived assuming that the particles in the vertical direction are almost entirely muons and that they come from pions and kaons (with $K/\pi \sim 20\%$).

7.3 Further studies

It has been shown in the present work (Chapter 4) that the effective use of the present method (i.e. studies of inclined muon spectra) for studying the K/π ratio need more accurate measurements of both the vertical and near-horizontal muon intensities in the muon energy region of 1000 GeV where the sensitivity to the K/π ratio is greatest (see fig. 4.3).

With the present Mark II spectrograph the rate of particles of high energies, $>$ 500 GeV is very low (1 per 35 hours, which is about two days running time) and, therefore, a similar instrument with larger accepting power is required for precise determination of the K/π ratio in a reasonable length time.

An increase in the rate of high energy muon will lead also to a

more accurate determination of the muon charge ratio at high energies in the near-horizontal direction. In order to gain information on the contribution of kaons to the observed charge ratio from a study of the zenith angle dependence on the ratio (§ 5.6.3) it is desirable also to have an accurate determination of the charge ratio up to 1000 GeV at the vertical, because the sensitivity of this method to the K/π ratio is greatest at these high energies (see fig. 5.7).

ACKNOWLEDGEMENTS

The author is greatly indebted to Professor G. D. Rochester, F.R.S., for the provision of the facilities for this work and also for his continuous support and interest. He is likewise extremely grateful to Professor A. W. Wolfendale, his supervisor, for his invaluable guidance and his constant co-operation, without which the work could not have been possible.

The author is very grateful to his colleagues, Mr. G. N. Kelly, Dr. P. K. MacKeown and Dr. J. Wdowczyk, who at various times by word and deed contributed to the final results. The author also appreciates the valuable discussions he has had with Dr. J. L. Osborne.

The technical staff of the Physics Department, notably Mr. W. Leslie, Mr. E. W. Lincoln, Mr. W. D. Threadgill and Mr. R. White, are thanked for their willing help, and particular thanks are expressed to Miss C. Guyll and Miss P. Wallace for their ready assistance in the measurements and in punching the data, and to Mr. P. Finley for his willing assistance in the day to day running of the spectrograph.

The staff of the University Computing Laboratory are thanked for their co-operation and assistance.

For her painstaking effort in typing this thesis Mrs. D.M.Willstrop is sincerely thanked.

Finally, the author wishes to thank the Iraqi Government for the award of a Scholarship during the period of the work.

REFERENCES

Allen, J. E., and Apostolakis, A. J., (1961), Proc. Roy. Soc., A265, 117.

Asatiani, T. L., Frishchyan, V. M., and Sharkatunyan, R.O., (1964) Sov. Phys. JETP, 19, 1299.

Ashton, F., and Wolfendale, A. W., (1963), Proc. Phys. Soc., 81, 593.

Ashton, F., MacKeown, P. K., Pattison, J.B.M., Ramana Murthy, P.V., and Wolfendale, A.W., (1963a), Proc. Int. Conf. on Cosmic Rays, Jaipur, 6, 72.

Ashton, F., MacKeown, P.K., Pattison, J.B.M., Ramana Murthy, P.V., and Wolfendale, A.W., (1963b), Phys. Lett., 6, 259.

Ashton, F., and Coats, R.B., (1965), Proc. Int. Conf. on Cosmic Rays, London, 2, 959.

Ashton, F., Kamiya, Y., MacKeown, P.K., Osborne, J.L., Pattison, J.B.M., Ramana Murthy, P.V., and Wolfendale, A.W., (1966), Proc. Phys. Soc., 87, 79.

* Aurela, A., (1965), Ph.D. Thesis, University of Durham.

Backenstoss, G., Hyams, B.D., Knop, G., and Stierlin, V., (1963), Nuclear Inst. and Methods, 21, 155.

* Bassi, P., Clemental, E., Filosofo, I., and Puppi, G., (1949), Nuovo Cim., 6, 484.

* Beretta, E., Filosofo, I., Sommacal, B., and Puppi, G., (1953), Nuovo Cim., 10, 1354.

Bhabha, H.J., (1938), Proc. Roy. Soc., A164, 257.

Borog, V.V., Kirillov-Ugryumov, V.G., Petrukhin, A.A., Rosental, I.L., and Shestakov, V.V., (1965), Proc. Int. Conf. on Cosmic Rays, London, 2, 962.

* Brode, R.B., (1949), Suppl. Nuovo Cim., 6, 465

* Brode, R.B., and Weber, M.J., (1955), Phys, Rev., 99, 610

* Brooke, G., Hayman, P.J., Taylor, F.E., and Wolfendale, A.W., (1962), unpublished.

Brooke, G., Hayman, P.J., Kamiya, Y., and Wolfendale, A.W., (1964a), Proc. Phys. Soc., 83, 853.

Brooke, G., Meyer, M.A., and Wolfendale, A.W., (1964b), Proc. Phys. Soc., 83, 871.

* Campbell, M.J., Murdoch, H.S., Ogilvie, K.W., and Rathgeber, H.D.,(1962), Nuovo Cim., 24, 37.

* Caro, D.E., Parry, J.K., and Rathgeber, H.D., (1951), Aust. J. Sci. Res., 4, 16.

Christy, R.F., and Kusaka, S., (1941), Phys. Rev., 59, 405.

Cocconi, G., Koester, L.J., and Perkins, D.H., (1961), Lawrence Radiation Laboratory Report, High Energy Physics Study Seminars No. 28 Part 2 (UCID) - 1444

Conversi, M., (1949), Phys. Rev., 76, 311.

Coxell, H., (1961), Ph.D. Thesis, University of Durham.

Crossland, A.D., and Fowler, G.N., (1965), Proc. Int. Conf. on Cosmic Rays, London, 2, 950

* Filosofo, I., Pohl, E., and Pohl-Ruhling, J., (1954) Nuovo Cim, 12,809.

Grigorov, N.L., and Shestoperov, V.Ya., (1963), Proc. Int. Conf. on Cosmic Rays, Jaipur, 5, 268.

Grigorov, N.L., and Shestoperov, V.Ya., (1964), Nucleonica, 9, 307.

Hayman, P.J., (1962), Ph.D. Thesis, University of Durham.

Hayman, P.J., and Wolfendale, A.W., (1962a), Proc. Phys. Soc., 80, 710.

* Hayman, P.J., and Wolfendale, A.W., (1962b), Nature, 195, 166.

Hayman, P.J., Palmer, N.S., and Wolfendale, A.W., (1963), Proc. Roy, Soc., A275, 391.

Higashi, S., Kitamura, T., Oda, M., Tanaka, Y., and Watase, Y., (1964), Nuovo Cim., 32, 1.

* Holmes, J.E.R., Owen, B.G., and Rodgers, A.L., (1961), Proc. Phys. Soc., 78, 505.

Jackeman, D., (1956), Canad. J. Phys., 34, 432.

Judge, R.J.R., and Nash, W.F., (1965), Nuovo Cim., 35, 1025.

Kamiya, Y., Sagisaka, S., Ueono, H., Kato, S., and Sekido, Y., (1961), Proc. Int. Conf. on Cosmic Rays, Kyoto (1962, J. Phys. Soc. Japan, (Suppl. A - III), 17, 315).

* Kamiya, Y., Ueno, H., Sagisaka, S., and Sekido, Y., (1963), Nuovo Cim., 30, 1.

* Kawaguchi, S., Sakai, T., Oda, H., Ueno, H., and Kamiya, Y., (1965), Proc. Int. Conf. on Cosmic Rays, London, 2, 941.

Kim, C.O., (1964), Phys. Rev., 136, B515

* MacKeown, P.K., (1965), Ph.D. Thesis, University of Durham.

MacKeown, P.K., Said, S.S., Wdowczyk, J., and Wolfendale, A.W. (1965a), Proc. Int. Conf. on Cosmic Rays, London, 2, 964.

MacKeown, P.K., Said, S.S., Wdowczyk, J., and Wolfendale, A.W., (1965b), Proc. Int. Conf. on Cosmic Rays, London, 2, 937.

MacKeown, P.K., and Wolfendale, A.W., (1966), in the Press.

Maeda, K., (1960), J. Atmosph. Terr. Phys., 19, 184.

Maeda, K., (1964), J. Geophys. Res., 69, 1725

Morewitz, H.A., and Shamos, M.H., (1953), Phys. Rev., 92, 134

* Moroney, J.R., and Parry, J.K., (1954), Aust. J. Phys., 7, 423.

Murota, T., Ueda, A., and Tanaka, H., (1956), Progr. Theor. Phys., (Kyoto), 16, 482.

Narayan, D.S., (1964), Nuovo Cim., 34, 981.

Nereson, N., (1948), Phys. Rev., 73, 565

O'Connor, P.V., and Wolfendale, A.W., (1960), Nuovo Cim., 15 (Suppl. 2), 202.

Okuda, H., (1963), Proc. Cosmic Ray Lab., Nagoya University, 10, 1.

Osborne, J.L., (1964), Nuovo Cim., 32, 816.

Osborne, J.L., and Wolfendale, A.W., (1964), Proc. Phys. Soc., 84, 901

Osborne, J.L., Wolfendale, A.W., and Palmer, N.S., (1964), Proc. Phys. Soc., 84, 911

Osborne, J.L., (1966), Ph.D.Thesis, University of Durham.

* Owen, B.G., and Wilson, J.G., (1951), Proc. Phys. Soc., 64, 417.

* Pak, W., Ozaki, S., Roe, B.P., and Greisen, K., (1961), Phys. Rev., 121, 905.

Pal, Yash, and Peters, B., (1964), Mat. Fys. Medd. Dan. Vid. Selsk. 33, No. 15.

Pattison, J.B.M., (1963), M.Sc. Thesis, University of Durham.

Pattison, J.B.M., (1965), Ph.D. Thesis, University of Durham.

Perkins, D.H., (1961), Proc. Int. Conf. on the Theoretical Aspects of Very High Energy Phenomena, CERN report 61-22, P99.

* Pine, J., Davisson, R.J., and Greisen, K., (1959), Nuovo Cim., 14, 1181.

Ramana Murthy, P.V., (1963), Nuovo Cim., 30, 762.

* Rastin, B.C., (1964), Ph.D. Thesis, University of Nottingham.

* Rastin, B.C. Baber, S.R., Bull, R.M., and Nash, W.F., (1965), Proc. Int. Conf. on Cosmic Rays, London, 2, 931.

* Rodgers, A.L., (1957), Ph.D. Thesis, University of Manchester.

Rogers, I.W., (1965), Ph.D.Thesis, University of Durham.

Sheldon, W.R., and Duller, N.M., (1962), Nuovo Cim., 23, 63.

Sitte, K., (1961), Handb. d. Phys., 46, 157.

Smith, J.A., and Duller, N.M., (1959), J. Geophys. Res., 64, 2297.

Vernov, S.N., Khristiansen, G.B., Netchin, Yu.A., Vedeneev, O.V., and Khrenov, B.A., (1965), Proc. Int. Conf. on Cosmic Rays, London, 2, 952.

Zatsepin, G.T., and Kuzmin, V.A., (1961), Zhurn, Eksper. Teur. Fiz., 39, 1677 (Sov. Phys. JETP, 12, 1171).

---

* References for the collection of results on the muon charge ratio presented in fig. 5.2 (see also § 5.4)